NASA CR-54560
PWA-FR-2433

DEVELOPMENT OF A SHORT-LENGTH TURBOJET COMBUSTOR

by
D. L. Klein

Prepared for

NATIONAL AERONAUTICS AND SPACE ADMINISTRATION

Contract NAS3-7905

Pratt & Whitney Aircraft
DIVISION OF UNITED AIRCRAFT CORPORATION
FLORIDA RESEARCH AND DEVELOPMENT CENTER
BOX 2691, WEST PALM BEACH, FLORIDA 33402

NASA CR-54560
PWA FR-2433

SUMMARY REPORT

DEVELOPMENT OF A SHORT-LENGTH TURBOJET COMBUSTOR

by
D. L. Kitts

Prepared for

NATIONAL AERONAUTICS AND SPACE ADMINISTRATION

18 March 1968

Contract NAS3-7905

Technical Management
NASA Lewis Research Center
Cleveland, Ohio
Air Breathing Engines Division

J. Grobman

Pratt & Whitney Aircraft DIVISION OF UNITED AIRCRAFT CORPORATION
FLORIDA RESEARCH AND DEVELOPMENT CENTER
BOX 2691, WEST PALM BEACH, FLORIDA 33402

FOREWORD

This summary report was prepared by the Pratt & Whitney Aircraft Division of United Aircraft Corporation under Contract NAS3-7905. The contract was administered by the Air-Breathing Engine Procurement Section of the National Aeronautics and Space Administration, Cleveland, Ohio. The report summarizes technical effort that was conducted during the period 3 June 1965 through 18 April 1967.

ABSTRACT

An experimental study was conducted using a quarter sector of a full-scale gas turbine combustor with an outer diameter of 40 inches and a combustion length of 12 inches. Two twin annulus combustor designs, providing either atomized or vaporized injection of ASTM-A1 fuel, were tested. Performance data were obtained for a range of operating conditions including simulated Mach 3 cruise at an altitude of 65,000 feet, with a combustor outlet temperature of 2200°F. Acceptable values for combustion efficiency and total pressure loss were measured in both combustors; however further improvements in combustor outlet temperature profile are required in both combustors.

CONTENTS

SECTION I
SUMMARY

The objective of this program was to develop a short-length-turbojet combustor (12-inch burning length with 40-inch external diameter) for use with ASTM A-1 fuel in advanced supersonic aircraft. The Pratt & Whitney Aircraft ram induction combustor concept was applied to the design of two combustors tested under this program at simulated sea level takeoff and Mach 3 cruise conditions.

Both combustors had a 12-inch burning length, an airflow compatible with a 260 lb_m/sec (at sea level takeoff) gas generator of a turbofan engine (bypass ratio of 1.3) and a design exit temperature of 2200°F. The overall length from compressor discharge to turbine inlet was 20 inches. Tests were conducted in a quarter sector of a full-scale combustor.

The most successful combustor tested, which had liquid fuel injection, achieved a combustion efficiency of 100% and a total pressure loss of 6.8% at a simulated supersonic cruise condition. The maximum exit temperature exceeded the mean exit temperature by about 240°F. At the end of the contract, this combustor was considered suitable for actual engine development, although some further temperature profile improvement at maximum temperature rise operation was required.

The second combustor, which incorporated a premixed air/fuel vapor injection system, also met the combustion efficiency and pressure loss goals. Additional cooling air required to achieve vaporizer tube durability prevented achieving the desired temperature profile during the contract period. Moderate additional development should achieve the desired performance for this combustor concept.

It is concluded that the two ram induction combustors demonstrated the potential of reducing the length of comparable state-of-the-art supersonic engine primary combustors by approximately 50 percent.

SECTION II
INTRODUCTION

A. CURRENT COMBUSTOR STATE OF THE ART

Two Pratt & Whitney Aircraft engines, the J58 turbojet engine for the SR-71/YF-12 and the JTF17 turbofan engine for the SST, have been designed for and operated at inlet conditions equivalent to flight speeds higher than Mach 2.5. These engines have gas generator airflows of approximately 300 lb/sec at sea level takeoff and outer combustor case diameters on the order of 44 inches. The combustor burning length for the J58 and JTF17 is 33.3 and 21.0 inches, respectively. The length from the compressor discharge to the turbine inlet for the J58 and JTF17 is 52.6 and 31.0 inches, respectively. Engines designed by other manufacturers for similar missions have comparable primary combustor dimensions.

B. ADVANCED COMBUSTOR STATE OF THE ART

To obtain high performance, minimum weight, and acceptable durability for even more advanced supersonic aircraft, combustor technology must be advanced. NASA Lewis Research Center Contract NAS 3-7905 was awarded for this purpose. The objective of the contract was to develop a primary combustor that would be approximately half the burning length of the present engine combustors. An outer combustor case diameter of 40 inches and a burning length of 12 inches were specified for this program.

To meet this objective, two short-length combustors were designed, based on the Pratt & Whitney Aircraft ram induction combustor concept. One combustor was designed with conventional liquid fuel injection, and one with vaporizing fuel injection. A double annulus combustor design rather than a single annulus was selected for both test combustors to provide a higher length to width ratio (L/D) for each combustor element, with resulting greater effective mixing length. The two combustors were built and tested in 90° sectors.

The contract performance goals were:

1. Combustor average exit temperature of 2200°F
2. Minimum combustion efficiency of 98%
3. Maximum isothermal combustor total pressure loss of 6%, measured between compressor discharge station and turbine inlet station

4. Design mean radial total temperature profile at the combustor outlet as specified in figure 1. At any radial position of the combustor outlet, the local peak temperature should not exceed the design mean total temperature at the radial position by more than 100°F.

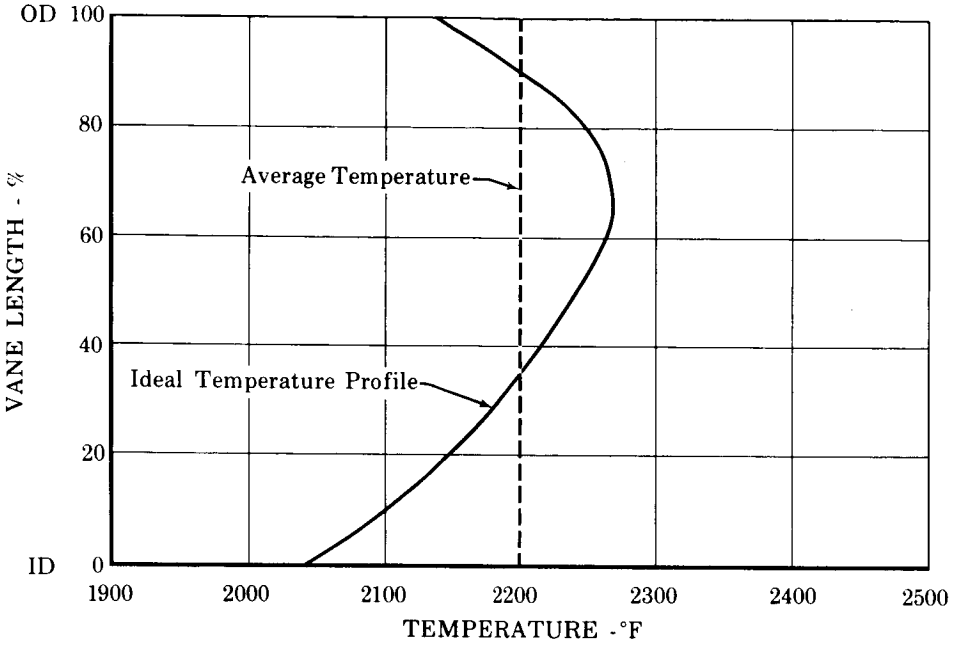

Figure 1. Desired Turbine Inlet Radial Temperature Profile FD 10707

Performance of each combustor design was determined at the following conditions:

1. Supersonic Cruise Simulation
   Diffuser inlet total pressure, p_{t3}*: 60 psia
   Diffuser inlet total temperature, t_{t3}: 1150°F
   Combustor reference velocity, V_{ref}: 150 ft/sec
   Combustor outlet temperature, t_{t4}: 2200°F
2. Sea Level Takeoff Simulation (SLTO)
   Diffuser inlet total pressure, p_{t3}: 60 psia
   Diffuser inlet total temperature, t_{t3}: 600°F
   Combustor reference velocity, V_{ref}: 100 ft/sec
   Combustor outlet total temperature, t_{t4}: 2200°F

*Nomenclature is listed in Appendix A

A planned 50-hour endurance test of the best combustor configuration was deleted from the program as a result of warpage problems encountered in both the combustor casing and liner. The warpage problem was diminished by incorporating structural supports and stiffeners, and by reducing the diffuser inlet total pressure requirement from 90 to 60 psia. In place of the endurance test, more emphasis was placed on improving the combustor outlet temperature profile. Nineteen modifications of the liquid fuel injection combustor and seven modifications of the vaporizing fuel injection combustor were tested.

SECTION III
APPARATUS AND PROCEDURES

A. APPARATUS

1. Test Facilities

All combustion tests during this program were conducted on test stand B-2 at the Florida Research and Development Center. The combustor rig air supply was provided by compressor discharge air bleed from a JT4 turbojet engine. The engine bleed system had the capability of delivering air to the test rig at conditions slightly higher than the original maximum program requirements (24 lb/sec at 90 psia). An altitude test capability was also provided by a two stage ejector system driven by the JT4 exhaust. This system had the capability of aspirating throttled ambient temperature air at sub-atmospheric pressure levels in sufficient quantity to simulate combustor altitude relight conditions (4 lb/sec at 5 psia).

2. Combustor Test Rig

A cross section of the 90 degree sector combustor test rig is shown in figure 2. Figure 3 shows the rig installed in the B-2 test facility. Stainless steel (AISI type 347) construction was used throughout the rig. The major sections of the rig and a brief description of each component are described in the following paragraphs.

a. Flow Straightener

This section straightened the rig inlet airflow and provided a near-stagnation region where accurate total pressure and temperature measurements were made for use in calculating the venturi airflow. The bleed air supply from the JT4 slave engine entered the flow straightener through a 10-inch hand valve. The flow straightener was fabricated from a 12-inch diameter cylinder, 24 inches in length. The inlet flow was straightened by a bank of 1.5 inch diameter tubes, 12 inches in length.

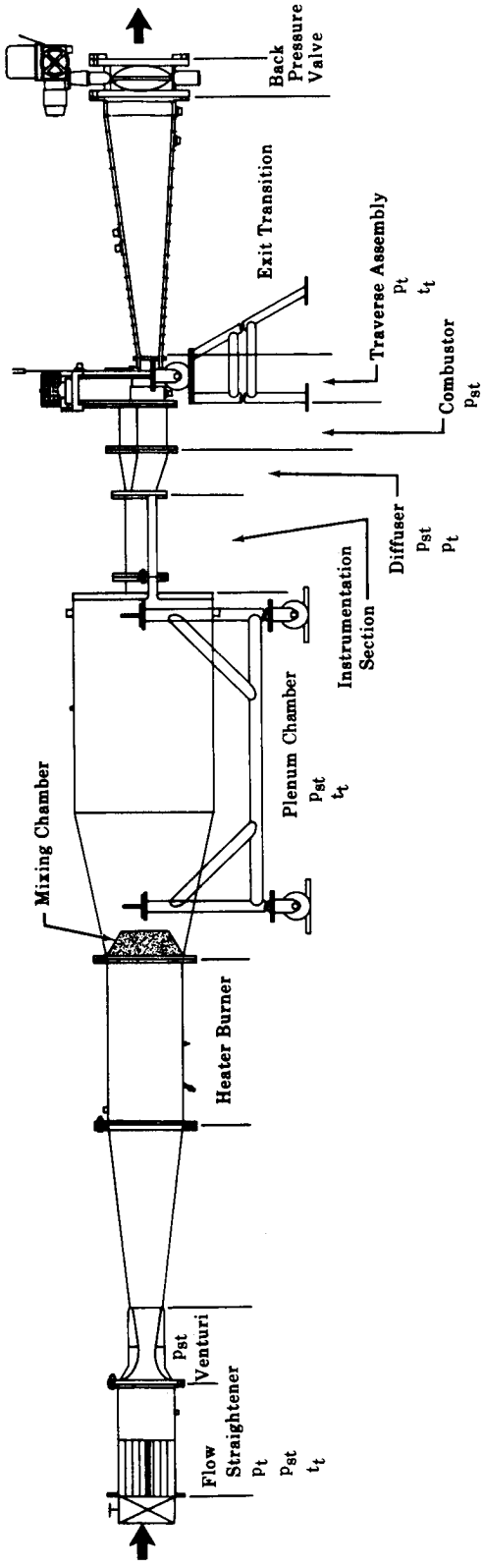

FD 13874B

Figure 2. Short-Length Turbojet Combustor Rig

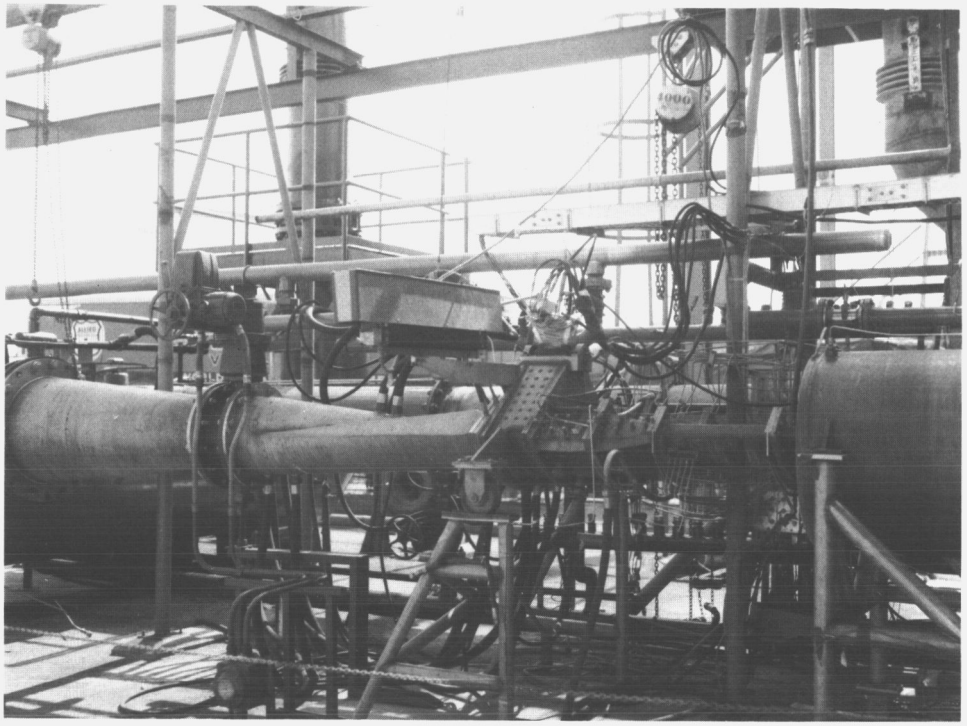

Figure 3. Combustor Rig Installed in B-2 Stand FE 58678

b. Venturi

The venturi, providing accurate airflow measurement with minimum pressure loss, was fabricated in two sections consisting of:

1. A 4.7485-inch diameter throat with a constant radius flow nozzle inlet. The throat diameter was measured at 71°F. A coefficient of linear expansion of 12×10^{-6} in./in.-°F was used to correct the throat diameter for higher temperature airflows.
2. A 12° 30' included angle, 40.840 inches long, transition to the heater burner inlet.

c. Heater Burner

This section provided a heating capability for raising the inlet air from the JT4 bleed temperature to the desired levels of 600°F or 1150°F, over the test program airflow range. Approximate JT4 bleed temperatures were 425°F at the sea level takeoff test condition and 450°F at the cruise test condition. The heater burner consisted of a cylindrical housing and a modified J58 burner can. Various flow-range fuel nozzles were utilized to maintain high fuel pressure drop for maximum efficiency operation.

d. Plenum Chamber

The plenum chamber consisted of a cylinder 29 1/4 inches in diameter and 48 inches long with an inlet transition from 15 3/4 to 29 1/4 inch diameter. The plenum chamber volume was approximately 23.3 ft^3. Temperature and velocity uniformity of the preheated air was provided by a multiholed mixing chamber in the forward section of the plenum. The cross-sectional area of the plenum was reduced from 672.1 in^2 to 43.4 in^2 at the inlet to the instrumentation section. This area transition was made by a bellmouth flange to provide a uniform airflow profile.

e. Instrumentation Section

The instrumentation section provided for measurement of static and total pressures to determine the diffuser inlet velocity profile. The instrumentation section was 18 inches long and corresponded to a 90-degree sector of the design engine compressor discharge area. Typical diffuser inlet velocity profiles are shown in figure 4. The measured maximum deviation in velocity was ± 4% for the average radial profile and ± 2% for the average circumferential profile.

f. Combustor Case Section

The combustor case section provided support and housing for both combustor designs. This section formed the diffuser and combustor shroud flow path. The diffuser and combustor casings were constructed of type 347 stainless steel of 1/8 and 1/4 inch thickness, respectively.

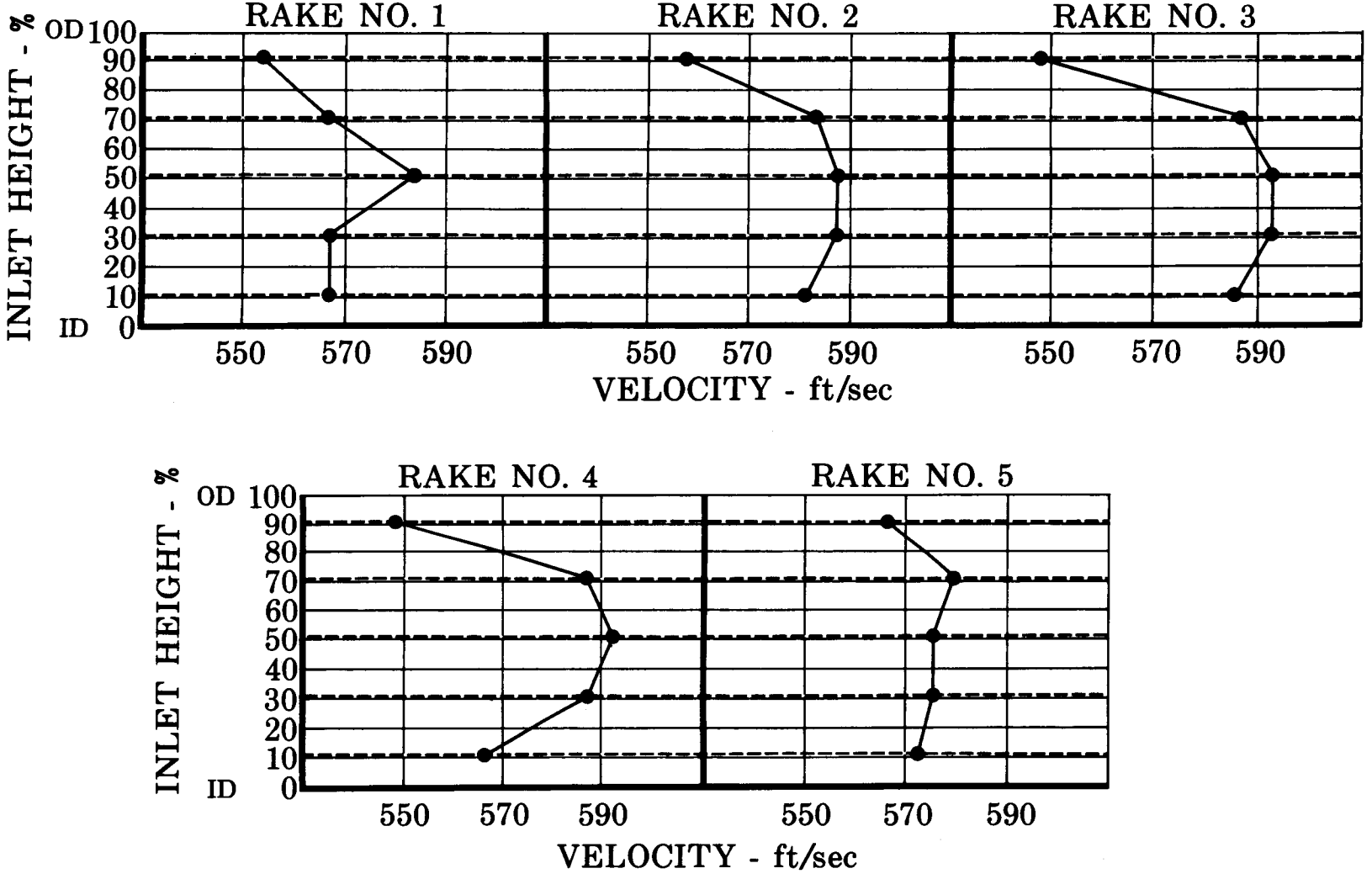

Figure 4. Typical Diffuser Inlet Velocity Profile at Cruise Conditions (Taken from Test No. 109)

FD 21846 A

g. Traverse Section

The traverse section supported and enclosed a five-point total pressure-total temperature combustor exit traversing rake and contained the choke plate assemblies. The rake was traversed across the combustor exit plane to measure total pressure and temperature within equal area regions.

h. Choke Plate Assembly

The rig exit choke plate assembly simulated the presence of choked turbine inlet guide vanes. It consisted of a 90 degree arc segment water-jacketed frame including 14 water-cooled tubes positioned radially across the gas flow area. This plate assembly was installed in the traverse case immediately downstream of the total temperature and pressure rake. The choke plate provided the area restriction required to choke the combustor exit plane at simulated cruise combustor inlet conditions and 2200°F combustor discharge temperature.

i. Combustor Exit Transition Section

The exit transition section diffused the exhaust gas stream and included spray water nozzles to quench the hot gas stream to the temperature limits of the downstream back pressure valve.

j. Back Pressure Valve

The back pressure valve controlled the rig pressure-flow relationship when the exit choke plate was not used.

k. Tailpipe

The tailpipe connected the rig to the facility exhaust system.

The calculations made to size the venturi throat area and the heater burner effective flow area are presented in Appendix B. These calculations were made for the originally specified 90 psia diffuser inlet pressure test condition. This was reduced to 60 psia because of insufficient strength of the segment combustor case and liners at the higher pressure condition.

3. Instrumentation

Rig instrumentation was provided to measure diffuser inlet pressure, temperature, and airflow; combustor exit pressure and temperature; and

fuel flow. Additionally, combustor metal temperatures were measured with thermocouples in some of the tests.

a. Airflow Measurement

Airflow was determined by a venturi as stated in the previous test rig description. Venturi inlet total temperature and pressure and throat static pressure were measured and the data used to compute airflow using standard compressible flow relationships, as presented in Appendix C. The venturi throat area was corrected for thermal expansion.

b. Inlet Condition Measurement

Diffuser inlet conditions were measured in the instrumentation section. Figure 5 presents the location of total pressure rakes and static pressure taps in this section. Four static pressure taps were equally spaced in line near the exit plane; and five total pressure rakes, each with 5 radially spaced pressure ports, were equally spaced in the same plane. The combustor inlet Mach number was calculated using an average of the 25 total pressure values taken at this station, the cross-sectional area at this section, the total temperature measured at the exit of the plenum chamber, the airflow measured by the venturi, and the heater burner fuel flow.

c. Exit Condition Measurement

Combustor exit conditions were measured in the traverse section with the five-point total pressure-total temperature exit traverse rake. Thirty circumferential traverse positions were set sequentially at each test point. Five radial pressure and temperature measurements were taken at each position. Figure 5 shows the location of the rake probe heads in the traverse plane.

The combustor exit total temperature and pressure traverse rake assembly was positioned to swing across the combustor exit as it pivoted on the combustor annulus centerline. Sealing between the traverse case and the rake journal was accomplished with Teflon sheet. The rake total temperature and pressure head assembly, located directly in the combustor discharge stream, was made entirely of 70/30 platinum-rhodium alloy. The aspirating, radiation shielded, thermocouple elements were junctions of platinum and 90/10 platinum-rhodium alloy. The probe housing assembly

was machined from AISI type 347 stainless steel and was water cooled internally. Figure 6 shows the exit rake assembly with the water-cooled journal assembly removed.

The rake assembly, when mounted in the rig exit traverse case, as shown in figure 7, had all temperature and pressure connections, aspirated gas discharge, and water cooling port connections external to the traverse case.

d. Fuel Flow Measurement

Fuel flow was measured with rotameters. The data were corrected for (1) fuel temperature and (2) the difference in specific gravity between the fuel tested and the calibrating fluid.

Data was reduced as presented in Appendix C, Performance Analysis, to establish the operating condition and determine the combustion efficiency, exit temperature pattern, and pressure loss characteristics of the test combustors.

4. Fuel

The fuel used during this program was ASTM Jet A-1 type. The specifications for this fuel are described in Reference 1, Appendix F. The fuel had an average measured net heat of combustion of 18,505 Btu/lb and a hydrogen/carbon ratio of 0.16.

5. Combustor Design

a. The Ram Induction Principle

The ram induction combustor concept is based on efficient use of the air velocity head to create a turbulent combustion zone. Figure 8 compares a conventional combustor with a ram induction combustor. In the conventional, static-pressure-fed combustor, the air is diffused to low velocities, then reaccelerated through the combustor liner holes by the static pressure differential. In the ram induction combustor, the air discharged from the compressor is only partly diffused (to a Mach number of 0.2, compared to 0.1 in a conventional combustor), and then turned into the combustion zone through a series of efficient elbows or vanes. This is termed "ram induction" because the air is induced to enter the combustor by the ram effect, rather than by the static pressure differential across the wall.

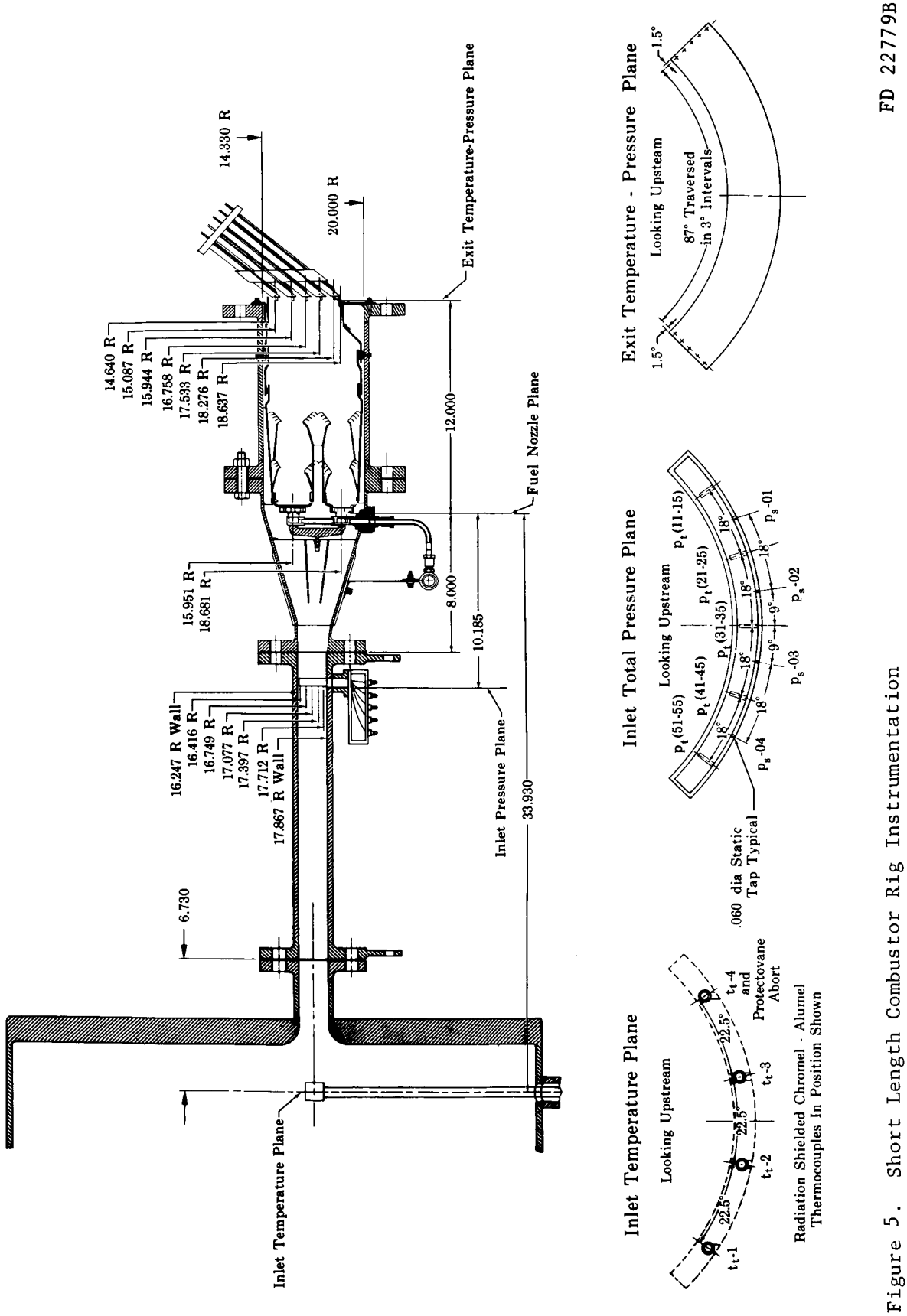

FD 22779B

Figure 5. Short Length Combustor Rig Instrumentation

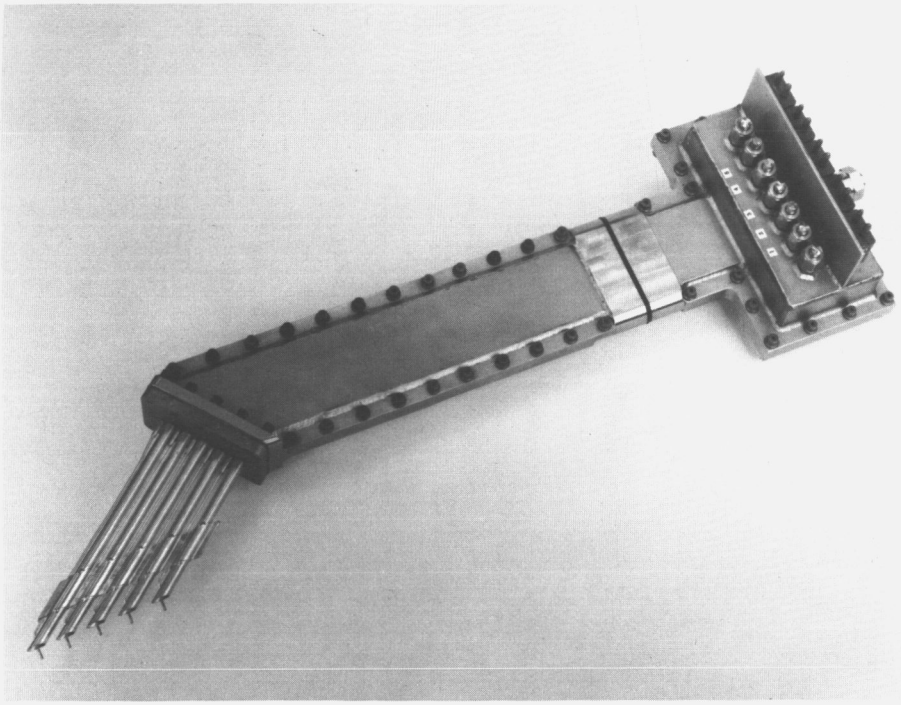

Figure 6. Exit Temperature and Pressure Rake Assembly FE 55370

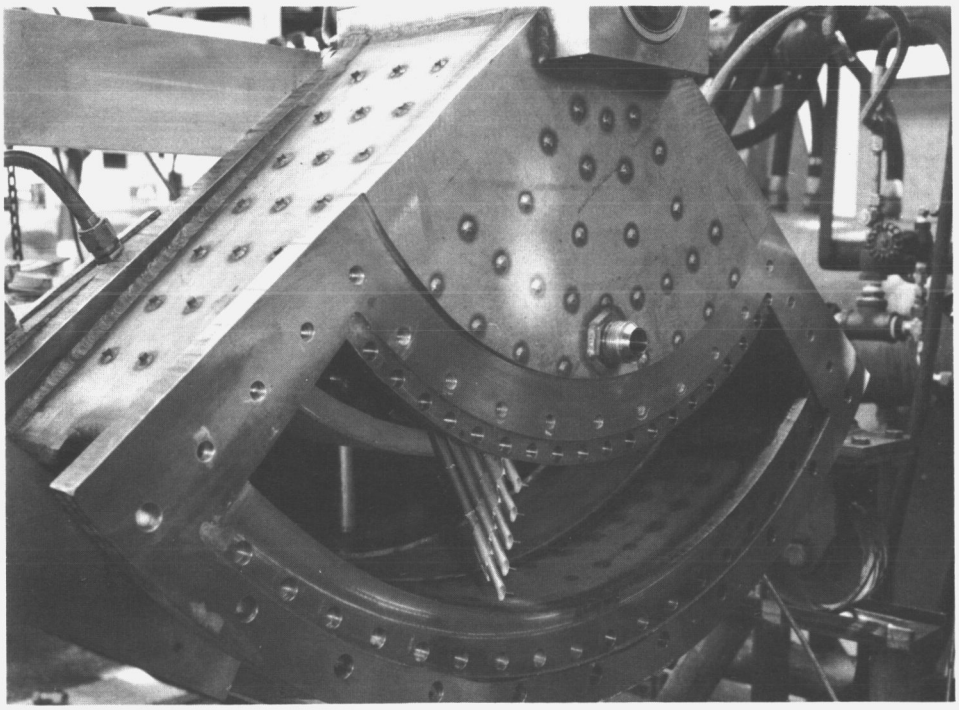

Figure 7. Rig Exit Traverse Case and Rake FAE 55727

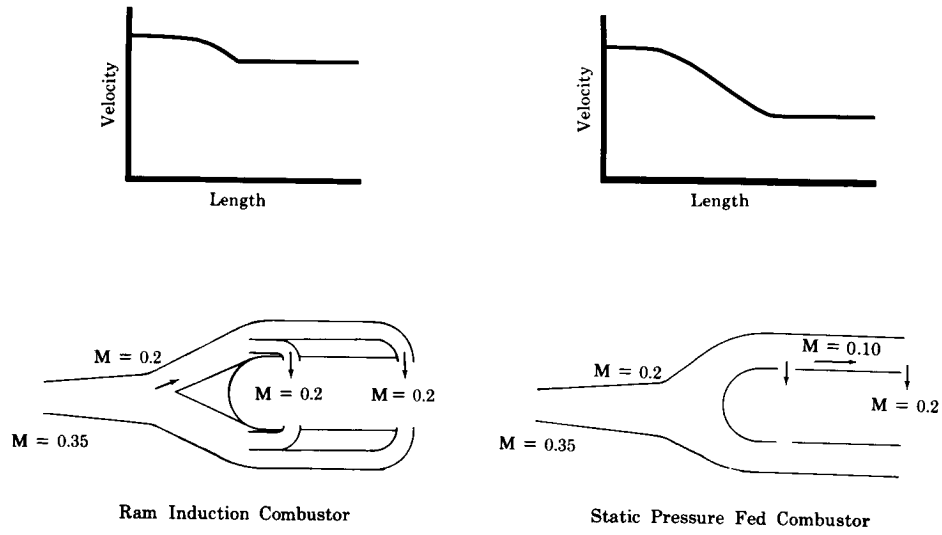

Figure 8. Comparison of Combustor Using Air Entry Scoops vs a Combustor with Air Entry Openings Flush with the Liner Surface

FD 10792B

The advantages provided by this concept include:

1. Overall compressor-exit to turbine-inlet length is substantially reduced, because a large part of the diffuser is eliminated and because the high degree of turbulence attainable permits thorough mixing in a short length.

2. Pressure loss can be reduced as much as 3% primarily because of the potential 2% lower loss associated with the lower diffusion required.

3. Flow stability is greatly increased because the usual compromise between amount of diffusion and diffuser length (which frequently leads to flow separation) is not necessary, and because the driving force producing airflow into each scoop is kept high and does not vary along the length of the combustor as in conventional designs. This effect (figure 8) is especially critical in high temperature rise combustors where higher front end airflow is required, but where the front end pressure is also higher due to increased pressure loss from heat addition. The improved flow stability of the ram induction combustor provides the turbine

inlet temperature profile stability and uniformity required for higher turbine inlet temperature operation.

4. The increased jet velocity tends to improve mixing and thus makes the turbine inlet temperature more uniform.

5. The use of scoops improves penetration, by providing a high turning angle, and controls air direction, making it easier to develop the desired temperature profile.

6. The high velocity of cool air along the sides of the combustor, and through the scoops, provides a substantial level of convective cooling to these parts, which greatly reduces the requirements for film cooling. This also is more important in high-temperature-rise combustors where combustion gas temperatures are higher and less air is available for cooling.

These advantages are gained at the expense of a higher fabrication cost and more difficult modification during the development period.

b. Combustor Configurations

The combustor designs tested under NASA Contract NAS3-7905 were based on scaling of a research ram induction combustor design concept that had previously demonstrated excellent performance at the desired operating conditions.

The first configuration, shown in figure 9, was a single liquid injection ram induction combustor scaled down until two units could be installed side-by-side. Hence this configuration was called a Twin Ram Induction Combustor. This twin annulus combustor design was chosen to provide a higher length to width ratio (L/D) for each combustor element with resulting greater effective mixing length. The twelve-inch burning length of this combustor was somewhat longer than the scaled burning length of the basic combustor. This was considered to be advisable to provide margin for factors, such as fuel atomization, which cannot be geometrically scaled.

The second configuration, shown in figure 10, used the same external liners as the Twin Ram Induction Combustor but a different method of fuel injection. The fuel was injected into a very small amount of the combustor

air, near the middle of the combustor. This extremely over-rich mixture (fuel-air ratio of 0.2) passed through a series of tubes that formed the inner combustor walls, evaporating the fuel and cooling these walls. The vaporized, or partially vaporized, mixture was discharged into the front end of the combustor, where it mixed with the primary air and burned. This design combined the "vaporizing centertube" principle developed at the Florida Research and Development Center under Navy Contract NOw63-0489-d (Reference 2), with the concept of ram induction air admission. The design was termed Vaporizing Ram Induction Combustor. Although this design did not contain the center ram induction scoops of the Twin Ram Induction Combustor configuration, vapor fuel injection characteristics were not significantly affected by scaling, and combustion chamber length required for atomization/vaporization was eliminated. Therefore, the slight loss in mixing effectiveness due to elimination of the centertube scoops was compensated by the greater effective burning length with vaporized fuel.

The design calculations for these two combustors are contained in Appendix B. The combustors were fabricated of Hastelloy X material with nicrobrazed and riveted construction.

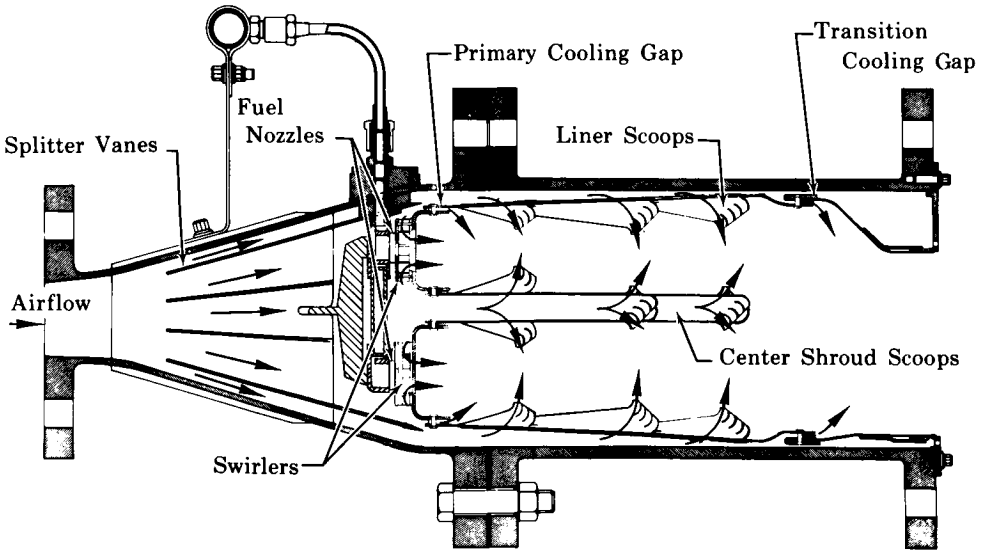

Figure 9. Twin Ram Induction Combustor, Model 1 FD 22566

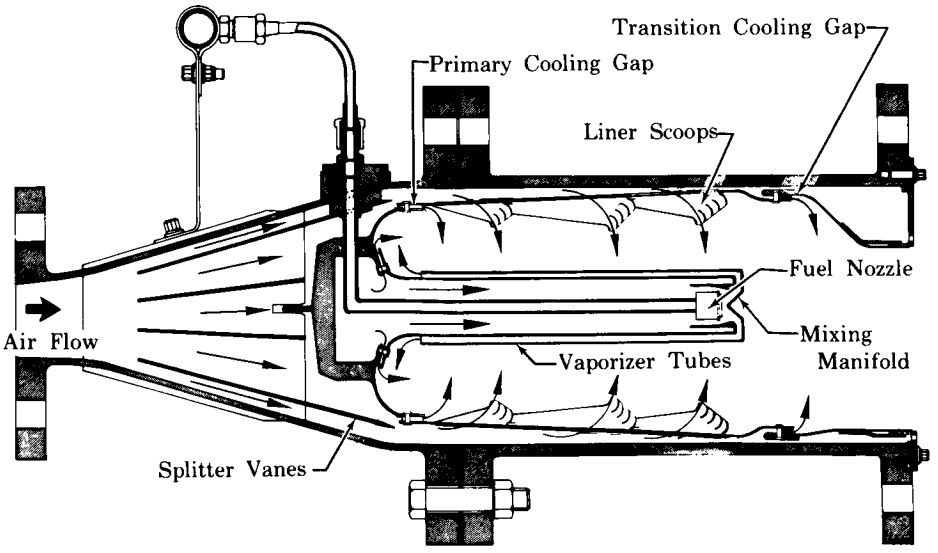

Figure 10. Vaporizing Ram Induction Combustor, Model 1 FD 22565

B. PROCEDURES

1. Test Procedure

a. Test Conditions

Tests of most combustor models were conducted at the simulated supersonic cruise and sea level conditions.

1. Supersonic Cruise Simulation

Diffuser Inlet Total Pressure	60 psia
Diffuser Inlet Total Temperature	1150°F
Combustor Reference Velocity*	150 ft/sec
Diffuser Inlet Velocity	541 ft/sec
Rig Airflow	15.36 lb/sec
Combustor Outlet Total Temperature	2200°F

2. Sea Level Takeoff Simulation

Diffuser Inlet Total Pressure	60 psia
Diffuser Inlet Total Temperature	600°F
Combustor Reference Velocity*	100 ft/sec
Diffuser Inlet Velocity	359 ft/sec

*See Appendix C for a definition of combustor reference velocity

Rig Airflow	15.88 lb/sec
Combustor Outlet Total Temperature	2200°F

The Model 14 Twin Ram Induction Combustor and the Model 6 Vaporizing Ram Induction Combustor were tested over a range of reference velocities and outlet temperatures to determine the effect of these variables on combustor performance. Some models were not tested at every specified condition, as during initial tests, when exit temperature pattern hot spots exceeded thermocouple limits, or when performance was unsatisfactory.

The following ranges of conditions were covered during the test program:

Diffuser Inlet Total Pressure	14.7-91.9 psia
Diffuser Inlet Total Temperature	240-1255°F
Combustor Outlet Total Temperature	847-2338°F

Limited ignition testing was conducted at pressures below 1 atmosphere.

Test data were obtained with the instrumentation described in the Apparatus section. These data were reduced by a digital computer program and converted to the following performance parameters. The performance analysis procedure is presented in detail in Appendix C.

b. Combustion System Performance Measurements

(1) Combustion Efficiency

Combustion efficiency was computed as the ratio of actual temperature rise to ideal temperature rise. Actual temperature rise was determined from measured diffuser inlet temperature and mass weighted average combustor exit temperature. Ideal temperature rise was determined from measured airflow, fuel flow, diffuser inlet pressure and temperature, and the fuel heating value. Corrections were made for the presence of water vapor in the inlet air and for vitiation when the heater burner was used. The estimated degree of accuracy of combustion efficiency measurement was ±5%.

(2) Combustion System Pressure Loss

Combustion system pressure loss was computed as the ratio of total pressure drop between the diffuser inlet and combustor exit to the diffuser inlet total pressure. An alternative method of presentation was as a total pressure loss coefficient (ratio of the total pressure drop to the diffuser inlet dynamic pressure head). Estimated accuracy of pressure loss measurement was ±1%.

(3) Combustor Exit Temperature Pattern

The combustor exit temperature pattern was measured with a five-point traversing thermocouple rake as discussed in the preceding Apparatus section. The data are presented in Appendices D and F as exit annulus plots with isotherms, as average radial temperature profile plots compared with the desired profile, and as average circumferential temperature profile plots. The overall temperature pattern uniformity factor was computed as ΔTVR^*, or the ratio of the maximum local temperature rise to the overall average temperature rise. The deviation of the measured average radial profile from the desired profile was presented as $D_{R\ max}^*$ and the maximum deviation of a local radial temperature profile from the desired profile was presented D_{max}^* The accuracy in measuring these factors was estimated as ±2%.

*See Appendix C for complete definition

SECTION IV
RESULTS AND DISCUSSION

A. TWIN RAM INDUCTION COMBUSTOR

1. Development Procedure

The Twin Ram Induction Combustor was developed through testing of 19 designated configurations. A new model designation was assigned to identify each change, including changes in the fuel flow split between the inner and outer annulus fuel nozzles. The general development procedures which were applied to the burner are summarized below:

a. Combustor Exit Radial Temperature Profile

The fuel/air ratios of the outer and inner annular chambers were varied to obtain the required general profile shape. Although this effect could have been achieved by adjusting relative airflow, aerodynamic complexity and diffuser flow disturbances were avoided by simply adjusting relative chamber fuel flows.

Reduction in overall centershroud airflow (achieved by reducing the centertube scoops from three rows to two rows) and increased crossflow penetration of centershroud discharge, (achieved by scoop staggering and increased scoop discharge L/D) eliminated a cold midspan in the exit profile.

Excessively cold or hot borders of the exit temperature profile were controlled by varying the intermediate and transition liner cooling gaps, while maintaining adequate cooling.

b. Durability Improvement

Durability of the liners and firewall required attention during the development program. The centershroud assembly showed no durability problems. In general, liner hot spots were eliminated by incorporating "thumbnail" cooling scoops in the affected locations.

Sufficient overall liner cooling was provided by incorporating an intermediate liner cooling gap immediately behind the second row of liner ram scoops, combined with the original primary and transition cooling gaps.

Firewall overheating and coke formation in early combustor configurations were eliminated by adding an airflow louver arrangement around each nozzle and small cooling and scrubbing air holes around the nozzles and along the firewall lips.

The diffuser and combustor casings and liners experienced warpage at inlet conditions of 1150°F and 90 psia. Further warpage was diminished by incorporating structural supports and stiffeners and by limiting the inlet operating pressure to 60 psia. The diffuser and combustor cases were constructed of 1/8 and 1/4 inch thick type 347 stainless steel, respectively. It is expected that the structural warpage problems that occurred in the 90-degree sector would not be present in a full annulus.

c. Combustor Exit Circumferential Temperature Pattern

The combustor circumferential exit temperature patterns for Models No. 1 through 14 showed a periodic characteristic related to the longest (No. 3) external liner scoops. The number of rows of scoops in the external liners was then reduced from three to two in the Model 15 and subsequent models. Both the liner and centertube ram scoop patterns were made symmetrical with respect to each fuel nozzle, with the circumferential scoop pattern repeating twice per nozzle spacing.

Re-indexing of the centertube provided circumferential staggering of the centertube ram scoop discharge with respect to the corresponding liner scoops and resulted in a satisfactory circumferential temperature pattern.

d. Diffuser Discharge Variations

The inner and outer diffuser flow splitters were removed because they became warped during testing. This change to the diffuser resulted in a peaked exit temperature profile on the ID of the combustor. It was inferred that this change to the exit temperature profile was caused by an alteration to the diffuser exit velocity profile. The shift in the diffuser exit velocity may have been caused by flow separation on the inner wall of the diffuser. No attempt was made at replacing the inner and outer flow splitters because the inner and outermost diffuser flow passages that were formed by replacing the splitters would have had substantial circumferential-area variations due to case wall warpage.

The percent variation in flow passage area was reduced by omitting the inner and outer flow splitters. For final performance evaluation, these flow variations were reduced slightly by incorporating a coarse wire mesh screen at the diffuser exit plane during tests of the Models No. 18 and 19 combustors.

e. Ignition

Initial attempts to ignite the combustor with spark igniters were unsuccessful. Early in the program, it was decided to pass over the ignition problem by using pyrophoric ignition with the injection of triethylborane. Limited data were obtained with spark igniters. Unless indicated otherwise, the tests described herein were run using pyrophoric ignition.

The results of comprehensive performance tests of the Model No. 14 combustor are presented in this section. Also presented is a discussion of the development of the Twin Ram Induction Combustor from the Model No. 1 through the final Model No. 19. Model No. 19 incorporated all of the design modifications intended to meet the program goals.

2. Development Chronology

Table I summarizes modifications to the Twin Ram Induction Combustor by model number. The locations of these modifications are shown in figure 11. Table II lists for all combustor models the effective open area and percent of total effective open area for each air entry station shown in figure 11. A sequential summary of test results for each of the Twin Ram Induction Combustor models is presented in Appendix D, which includes a complete test result summary, exit temperature patterns, radial temperature profiles, and circumferential temperature profiles. Figure 12 presents representative exit radial temperature profiles for each of the models.

a. Models No. 1 through 4

The initial design Twin Ram Induction Combustor, Model No. 1, is snown in figure 13. The design analysis for this combustor is presented in Appendix B. Initial atmospheric pressure testing of this configuration indicated both a hot OD profile as shown in figure 12 and a total pressure loss higher than that specified for the cruise inlet conditions. Since

slight liner warpage was also apparent, design modifications in Models No. 2 through 4 dealt primarily with eliminating the liner hot spots while decreasing the combustor total pressure loss. As can be seen from figure 12 the hot OD profile was reduced considerably for Model No. 2 by adding 1/4-inch cooling holes on the OD liner and increasing the primary and transition cooling gaps. However, the hot profile began to shi over to the ID.

To prevent further warpage, eliminate coke formation, and to better distribute the necessary cooling air on the OD and ID liners, the combustor was modified to the Model No. 3 configuration. In addition to rearranging the liner cooling holes and adding OD liner thumbnail scoops, firewall holes with deflectors were incorporated. The deflectors directed a scrubbing gas film around each nozzle. A typical Model No. 3 temperature profile is shown in figure 12.

All testing of Models No. 1 through 3 was conducted at 1 atm pressure. Prior to high pressure testing, the Twin Ram Induction Combustor was modified to Model No. 4 (table I).

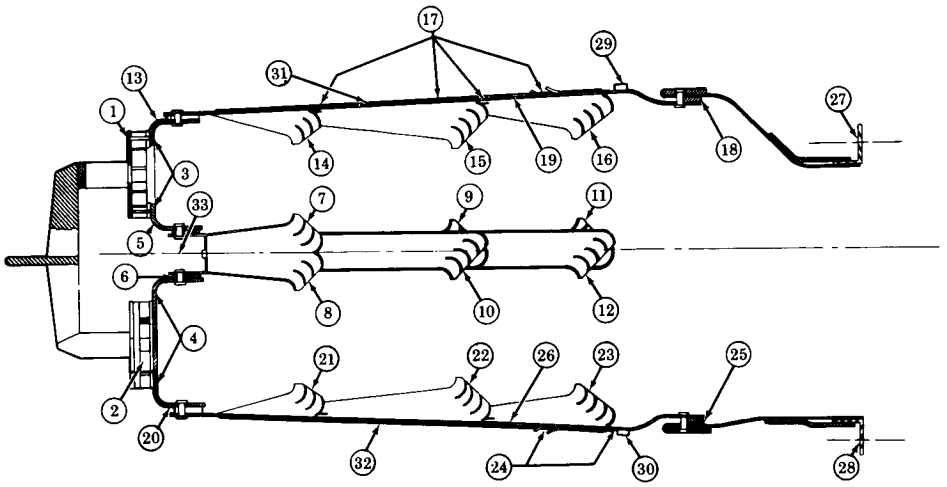

Figure 11. Location of Features of Twin Ram Induction Combustor FD 22784

Table I. Modification Summary of the Twin Ram Induction Combustor

Model Number		OD to ID Fuel Nozzle Flow Ratio	Firewall			Outer L			
			Dome Cooling and Sweep Holes	Deflectors	Swirler Restrictor	Primary OD Cooling Gap, in.	O/L Cooling Holes	O/L Cooling Thumbnail Scoops	O/L- Sp
	Location (Figure 28)		3,4	3,4	1,2	13	17	17	
1		1 to 1	None	None	None	0.052	None	None	None
2						0.071	1/4 in. Dia Behind Every Ram Scoop		0.1
3			8 0.116 in. Dia at Each Nozzle	Beside Each Nozzle Position				3 Behind Each 2nd Ram Scoop	Adde at T
4							Added 1/4 in. Dia at Trans Behind 1st and 2nd Ram Scoops	Added 1 Behind 2nd Ram Scoop	
5						0.092	Removed All	Removed 1 Behind 2nd Ram Scoop. Added Flap Behind 2nd Ram Scoop	
6		1.1 to 1	Added 16 0.092 in. Holes at Each Nozzle Location						
7			Added 6 0.093 in. Holes Along C/S Between Nozzle Locations						
8		2 to 1			Added 40% Restrictors to ID and OD			Added 2 Behind 2nd Scoops, 1 Between, and Ram Scoops	
9					Removed OD Restrictor		Added 7 1/8 in. Dia Around 3rd Ram Scoop	Added 2 Behind 2nd Ram Scoops	
10			Added 4 0.093 Holes at OD at Each Nozzle Location						
11									
12			Added 4 0.093 Holes at OD Between Nozzles			0.117			
13		1 to 1							
14		2 to 1				0.071			
15							Removed All	Removed All Behind 2nd Scoops	Remo 0.1C
16		1 to 1							
17		1.6 to 1							
18		1.23 to 1							
19									

Notes: Inner Liner - I/L Outer Liner - O/L Center Shroud - C/S

FOLDOUT FRAME

Table I. Modification Summary of the Twin Ram Induction Combustor

			Inner Liner							Center Shroud		
OD Transition ooling Gap, in.	O/L Support Devices	O/L Ram Scoop Blockage	Primary ID Gap, in.	I/L Cooling Holes	I/L Cooling Thumbnail Scoops	I/L-to-Case Spacers	ID Transition Gap	I/L Support Devices	I/L Ram-Scoop Blockage	OD/ID Cooling Gap	Restrictor	
18	31	15	20	24	24	30	25	32	22	5,6	33	
.052	None	None	0.071	None	None	None	0.071	None	None	0.066/0.66	None	Unreinfo 4 Split
.071						0.10						
				1/8 in. Dia Behind Every Ram Scoop		Added 0.060 at Trans.						
				1/4 in. Dia Behind 2nd Ram Scoops								
.092	Bolts at Trans. Gap		0.119	Removed All	Added 3 Behind 2nd Scoop and Flap Behind 2nd Ram Scoop		0.119	Bolts at Trans/Gap				
066					Added 2 Behind 2nd Scoops and Ram Scoops		0.071					
	Added Liner Beams							Added Liner Beams				1.) Adde Brac 2.) Remo OD V
	Added Retaining "Hooks"							Added Re-taining Hooks			Added 4% Restrictor at Entrance	
19												Replaced Vanes Us Expansio
		25% Block. of Ram Scoops	0.071						25% Block. of 2nd Ram Scoops			
er/Trans. 14/0.114	Removed Hooks	Removed 25% Block.			Removed All Behind 2nd Ram Scoop	Removed 0.010	Inter/Trans. 0.092/0.092	Removed "Hooks"	Removed 25% Block.		Removed Restrictor	
96/0.096												Added No

FOLDOUT FRAME

FOLDOUT FRAME

Model Number	Location (Figure 28)	Dome						
		OD Swirler	ID Swirler	OD Cooling	ID Cooling	OD Gap	ID Gap	OD No. 1 Scoo
		1	2	3	4	5	6	7
1	A_{eff}	11.784	11.784	0	0	7.361	7.062	11.926
1	%	5.837	5.837	0	0	3.646	3.498	5.907
2	A_{eff}	11.784	11.784	0	0	7.361	7.062	11.926
2	%	5.616	5.616	0	0	3.508	3.366	5.686
3	A_{eff}	11.784	11.784	1.677	1.677	7.361	7.062	11.926
3	%	5.493	5.493	0.782	0.782	3.431	3.292	5.560
4	A_{eff}	11.784	11.784	1.677	1.677	7.361	7.062	11.926
4	%	5.373	5.373	0.764	0.764	3.357	3.220	5.439
5	A_{eff}	11.784	11.784	1.677	1.677	7.361	7.062	11.926
5	%	5.612	5.612	0.798	0.798	3.500	3.362	5.680
6	A_{eff}	11.784	11.784	4.150	4.150	7.361	7.062	11.926
6	%	5.484	5.484	1.921	1.921	3.425	3.285	5.550
7	A_{eff}	11.784	11.784	4.967	4.967	7.361	7.062	11.926
7	%	5.442	5.442	2.284	2.284	3.399	3.261	5.508
8	A_{eff}	9.936	9.936	4.967	4.967	7.361	7.062	11.926
8	%	4.654	4.654	2.316	2.316	3.448	3.308	5.587
9	A_{eff}	11.784	9.936	4.967	4.967	7.361	7.062	11.926
9	%	5.390	4.545	2.263	2.263	3.367	3.230	5.456
10	A_{eff}	11.784	9.936	5.473	4.967	7.361	7.062	9.650
10	%	5.599	4.721	2.601	2.360	3.498	3.356	4.585
11	A_{eff}	11.784	9.936	5.473	4.967	7.361	7.062	9.650
11	%	5.421	4.571	2.518	2.285	3.386	3.249	4.439
12	A_{eff}	11.784	9.936	5.691	4.967	7.361	7.062	9.650
12	%	5.337	4.502	2.579	2.250	3.336	3.200	4.373
13	A_{eff}	11.784	9.936	5.691	4.967	7.361	7.062	9.650
13	%	5.337	4.502	2.579	2.250	3.336	3.200	4.373
14	A_{eff}	11.784	9.936	5.691	4.967	7.361	7.062	9.650
14	%	5.552	4.681	2.681	2.340	3.468	3.327	4.546
15	A_{eff}	11.784	9.936	5.691	4.967	7.361	7.062	11.926
15	%	5.089	4.291	2.458	2.145	3.179	3.050	5.150
16	A_{eff}	11.784	9.936	5.691	4.967	7.361	7.062	11.926
16	%	5.089	4.291	2.458	2.145	3.179	3.050	5.150
17	A_{eff}	11.784	9.936	5.691	4.967	7.361	7.062	11.926
17	%	5.089	4.291	2.458	2.145	3.179	3.050	5.150
18	A_{eff}	11.784	9.936	5.691	4.967	7.361	7.062	11.926
18	%	5.089	4.291	2.458	2.145	3.179	3.050	5.150
19	A_{eff}	11.784	9.936	5.691	4.967	7.361	7.062	11.926
19	%	5.189	4.375	2.506	2.187	3.241	3.110	5.252

FOLDOUT FRAME

Table II. Combustor Flow Areas and Percent Areas for Liquid Injection, Twin Ram Induction Combustor Schemes

Center Shroud					Outer Liner									
Scoop	OD No. 2 Scoop	ID No. 2 Scoop	OD No. 3 Scoop	ID No. 3 Scoop	Primary Cooling Gap	OD No. 1 Scoop	OD No. 2 Scoop	OD No. 3 Scoop	OD Cooling	Transition Gap	Intermediate Gap	Primary Cooling	ID No. 1 Scoop	ID No. 2 Scoop
	9	10	11	12	13	14	15	16	17	18	19	20	21	22
26 07	10.735 5.317	10.735 5.317	10.735 5.317	10.735 5.317	6.427 3.173	11.926 5.907	10.735 5.317	10.735 5.317	0 0	7.155 3.544	-- --	6.427 3.173	11.926 5.907	10.735 5.317
26 86	10.735 5.116	10.735 5.116	10.735 5.116	10.735 5.116	8.749 4.170	11.926 5.686	10.735 5.116	10.735 5.116	3.905 1.861	8.818 4.203	-- --	6.427 3.053	11.926 5.686	10.735 5.116
26 60	10.735 5.003	10.735 5.003	10.735 5.003	10.735 5.003	8.749 4.078	11.926 5.560	10.735 5.003	10.735 5.003	4.310 2.009	8.818 4.110	-- --	6.427 2.986	11.926 5.560	10.735 5.003
26 39	10.735 4.895	10.735 4.895	10.735 4.895	10.735 4.895	8.749 3.989	11.926 5.439	10.735 4.895	10.735 4.895	8.342 3.804	8.818 4.021	-- --	6.427 2.921	11.926 5.439	10.735 4.895
26 80	10.735 5.112	10.735 5.112	-- --	-- --	11.300 5.381	11.926 5.680	10.735 5.112	10.735 5.112	4.448 2.118	10.926 5.203	-- --	11.300 5.381	11.926 5.680	10.735 5.112
26 50	10.735 4.995	10.735 4.995	-- --	-- --	11.300 5.258	11.926 5.550	10.735 4.995	10.735 4.995	4.448 2.069	10.926 5.084	-- --	11.300 5.258	11.926 5.550	10.735 4.995
26 08	10.735 4.957	10.735 4.957	-- --	-- --	11.300 5.219	11.926 5.508	10.735 4.957	10.735 4.957	4.448 2.054	10.926 5.046	-- --	11.300 5.219	11.926 5.508	10.735 4.957
6 7	10.735 5.027	10.735 5.027	-- --	-- --	11.300 5.292	11.926 5.587	10.735 5.027	10.735 5.027	8.937 4.186	8.196 3.839	-- --	11.300 5.292	11.926 5.587	10.735 5.027
6 6	10.735 4.912	10.735 4.912	-- --	-- --	11.300 5.169	11.926 5.456	10.735 4.912	10.735 4.912	18.998 8.691	8.196 3.749	-- --	11.300 5.169	11.926 5.456	10.735 4.912
0 5	8.685 4.127	8.685 4.127	-- --	-- --	11.300 5.369	11.926 5.667	10.735 5.101	10.735 5.101	18.998 9.027	8.196 3.894	-- --	11.300 5.369	11.926 5.667	10.735 5.101
0 9	8.685 3.995	8.685 3.995	-- --	-- --	11.300 5.200	11.926 5.490	10.735 4.938	10.735 4.938	18.998 8.739	15.090 6.942	-- --	11.300 5.200	11.926 5.490	10.735 4.938
0 3	8.685 3.936	8.685 3.936	-- --	-- --	14.371 6.512	11.926 5.404	10.735 4.865	10.735 4.865	18.998 8.609	15.090 6.838	-- --	11.300 5.121	11.926 5.404	10.735 4.865
0 3	8.685 3.936	8.685 3.936	-- --	-- --	14.371 6.512	11.926 5.404	10.735 4.865	10.735 4.865	18.998 8.609	15.090 6.838	-- --	11.300 5.121	11.926 5.404	10.735 4.865
0 6	8.685 4.092	8.685 4.092	-- --	-- --	8.200 3.863	11.926 5.619	8.051 3.793	10.735 5.058	18.998 8.950	15.090 7.109	-- --	8.721 4.109	11.926 5.619	8.051 3.793
6 0	10.735 4.636	10.735 4.636	-- --	-- --	8.200 3.541	11.926 5.150	21.470 9.272	-- --	6.738 2.910	14.144 6.108	14.144 6.108	8.721 3.766	11.926 5.150	21.470 9.272
6 0	10.735 4.636	10.735 4.636	-- --	-- --	8.200 3.541	11.926 5.150	21.470 9.272	-- --	6.738 2.910	14.144 6.108	14.144 6.108	8.721 3.766	11.926 5.150	21.470 9.272
6 0	10.735 4.636	10.735 4.636	-- --	-- --	8.200 3.541	11.926 5.150	21.470 9.272	-- --	6.738 2.910	14.144 6.108	14.144 6.108	8.721 3.766	11.926 5.150	21.470 9.272
6 0	10.735 4.636	10.735 4.636	-- --	-- --	8.200 3.541	11.926 5.150	21.470 9.272	-- --	6.738 2.910	14.144 6.108	14.144 6.108	8.721 3.766	11.926 5.150	21.470 9.272
6 2	10.735 4.727	10.735 4.727	-- --	-- --	8.200 3.611	11.926 5.252	21.470 9.454	-- --	6.738 2.967	11.911 5.245	11.911 5.245	8.721 3.840	11.326 5.252	21.470 9.454

FOLDOUT FRAME

Liner Loop	ID Cooling	Transition Gap	Intermediate Gap	OD T/D Bleed	ID T/D Bleed	Total
	24	25	26	27	28	
	0	7.155	--	1.599	1.599	201.901
	0	3.544	--	0.792	0.792	100.00
	0	7.155	--	1.599	1.599	209.812
	0	3.411	--	0.762	0.762	100.00
	0.974	7.155	--	1.599	1.599	214.542
	0.454	3.336	--	0.745	0.745	100.00
	1.704	7.155	--	1.599	1.599	219.305
	0.777	3.263	--	0.729	0.729	100.00
	4.448	10.926	--	1.599	1.599	209.994
	2.118	5.203	--	0.761	0.761	100.00
	4.448	10.926	--	1.599	1.599	214.898
	2.069	5.084	--	0.744	0.744	100.00
	4.448	10.926	--	1.599	1.599	216.532
	2.054	5.046	--	0.738	0.738	100.00
	7.786	6.495	--	1.599	1.599	213.500
	3.647	3.042	--	0.748	0.748	100.00
	7.292	6.495	--	1.599	1.599	218.598
	3.336	2.971	--	0.733	0.733	100.00
	7.292	6.495	--	1.599	1.599	210.452
	3.465	3.086	--	0.760	0.760	100.00
	7.292	6.495	--	1.599	1.599	217.387
	3.354	2.988	--	0.736	0.736	100.00
	7.292	6.495	--	1.599	1.599	220.676
	3.304	2.943	--	0.725	0.725	100.00
	7.292	6.495	--	1.599	1.599	220.676
	3.304	2.943	--	0.725	0.725	100.00
	7.292	6.495	--	1.599	1.599	212.259
	3.435	3.060	--	0.753	0.753	100.00
	4.507	6.495	6.495	1.599	1.599	231.557
	1.946	2.805	2.805	0.691	0.691	100.00
	4.507	6.495	6.495	1.599	1.599	231.557
	1.946	2.805	2.805	0.691	0.691	100.00
	4.057	6.495	6.495	1.599	1.599	231.557
	1.946	2.805	2.805	0.691	0.691	100.00
	4.507	6.495	6.495	1.599	1.599	231.557
	1.946	2.805	2.805	0.691	0.691	100.00
	4.507	6.495	6.495	1.599	1.599	227.091
	1.985	2.860	2.860	0.704	0.704	100.00

Note:
1. C_d swirlers = 0.50
2. C_d holes = 0.62
3. C_d scoops and slots = 1.00
4. A_{eff} ~ $in.^2$
5. All areas based on full 360-degree annulus.

FOLDOUT FRAME

FOLDOUT FRAME

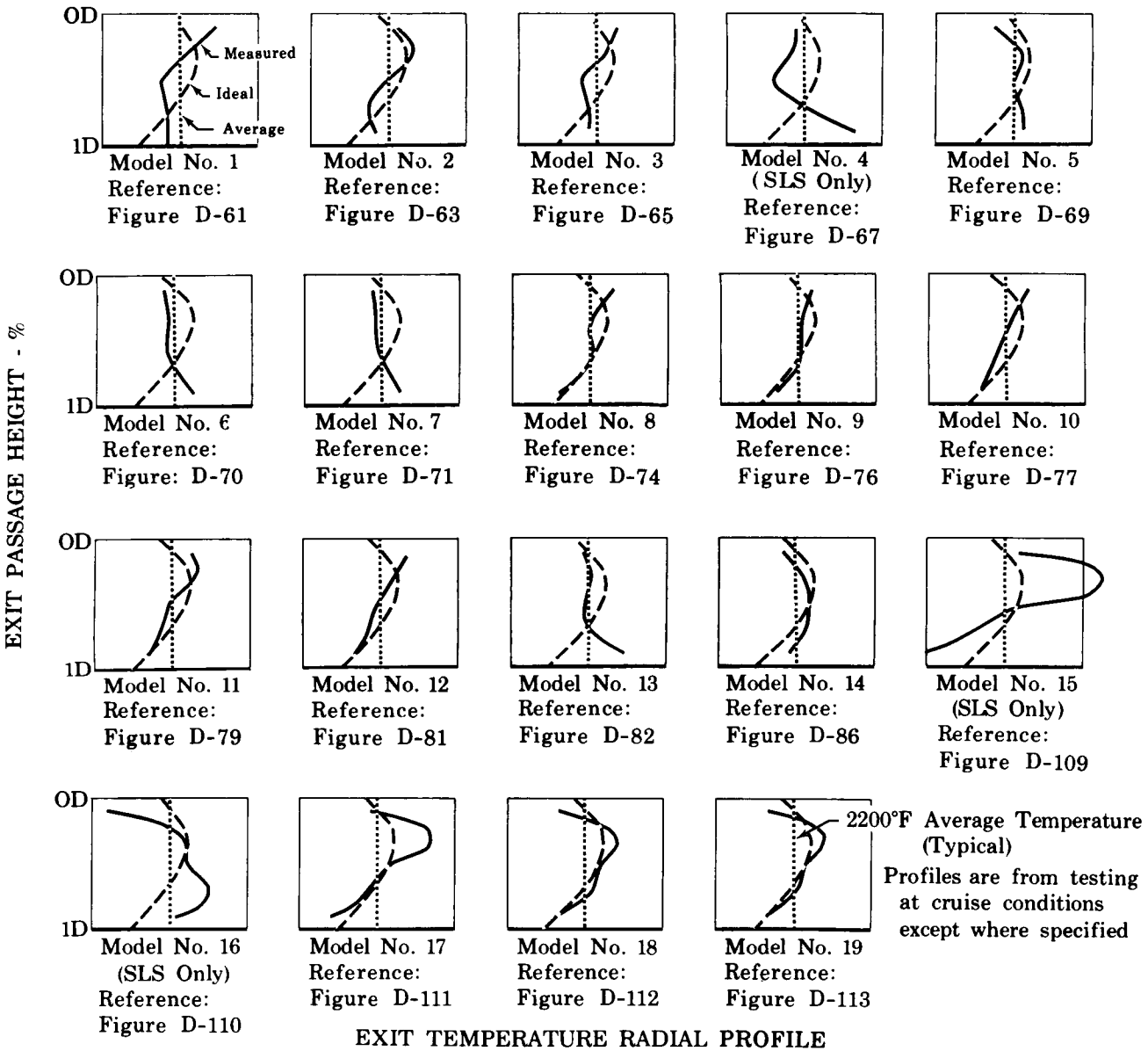

Figure 12. Exit Temperature Radial Profile Development - Twin Ram Induction Combustor

FD 21790A

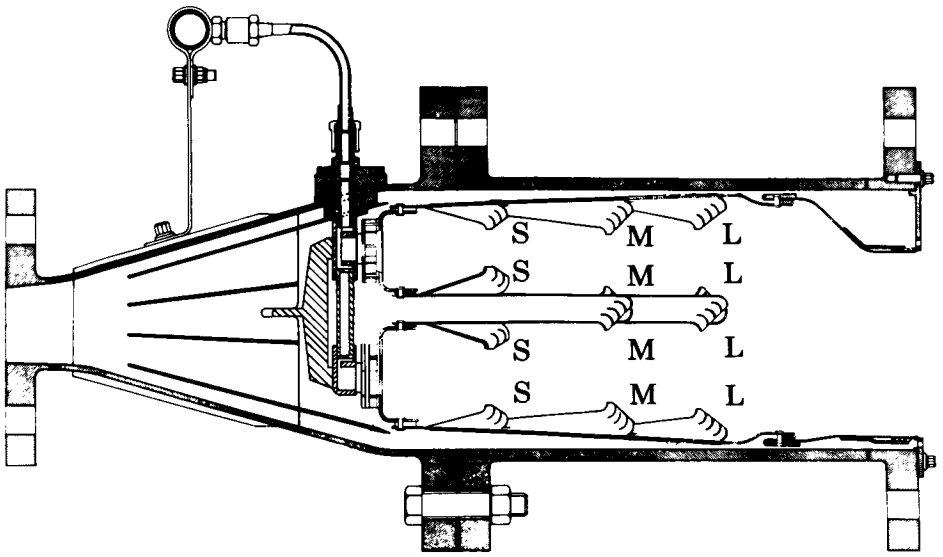

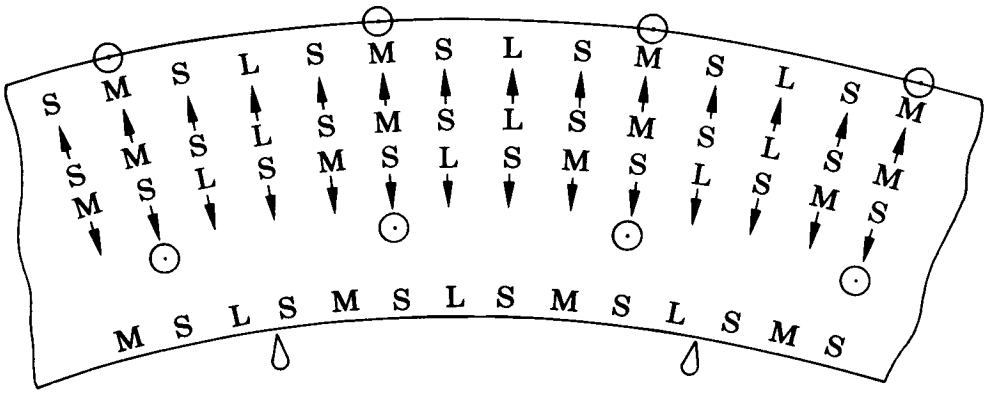

Scoop Discharge Pattern

⊙ Fuel Nozzle Locations

Arrows Indicate Direction of Centertube Scoop Discharge
Looking Upstream

Figure 13. Twin Ram Induction Combustor, Model No. 1 FD 12870H

A series of tests was planned on the Model No. 4, at 90 psia and increasing temperature levels, to determine performance and structural integrity. Two tests were completed with no visible combustor deterioration. During the third test, an operating error resulted in a large decrease in rig airflow prior to reducing fuel flow. The ensuing high fuel/air ratio and high temperatures caused combustor failure. Inspection of the rig revealed extensive damage to the combustor and the outlet thermocouple rake. Melting of the thermocouple rake indicated that exit temperatures exceeded 3200°F.

A safety abort system was installed to avoid a similar incident in the future. This system automatically shut off rig fuel and airflow, providing a decreasing fuel/air ratio, when any of the following parameters reached a marginal condition:

1. Rig inlet pressure above 95 psia
2. Tailpipe spray water pressure below 95 psia
3. Combustor inlet temperature above 1300°F
4. Combustor outlet temperature above 2800°F.

b. Models No. 5 Through 14

The design of the Model No. 5 Twin Ram Induction Combustor, shown in figure 14, incorporated experience gained with Models No. 1 through 4. Modifications included removal of the third row of ram induction scoops from the centertube and an increase in OD and ID shroud passage height to provide additional liner flow. A photograph of the Model No. 5 combustor is shown in figure 15. A design analysis of the Model No. 5 combustor is presented in Appendix B.

The Model No. 5 combustor configuration exhibited the temperature profile shown in figure 12, which showed a substantial reduction of the previously cold midspan region of the exit radial temperature profile. The ID region of the exit profile was still hot compared to the design goal, despite increased primary and transition liner cooling gaps. The ΔTVR value at simulated cruise conditions was reduced to 1.20, but elimination of local liner cooling holes and scoops raised the combustor system pressure loss above the design goal.

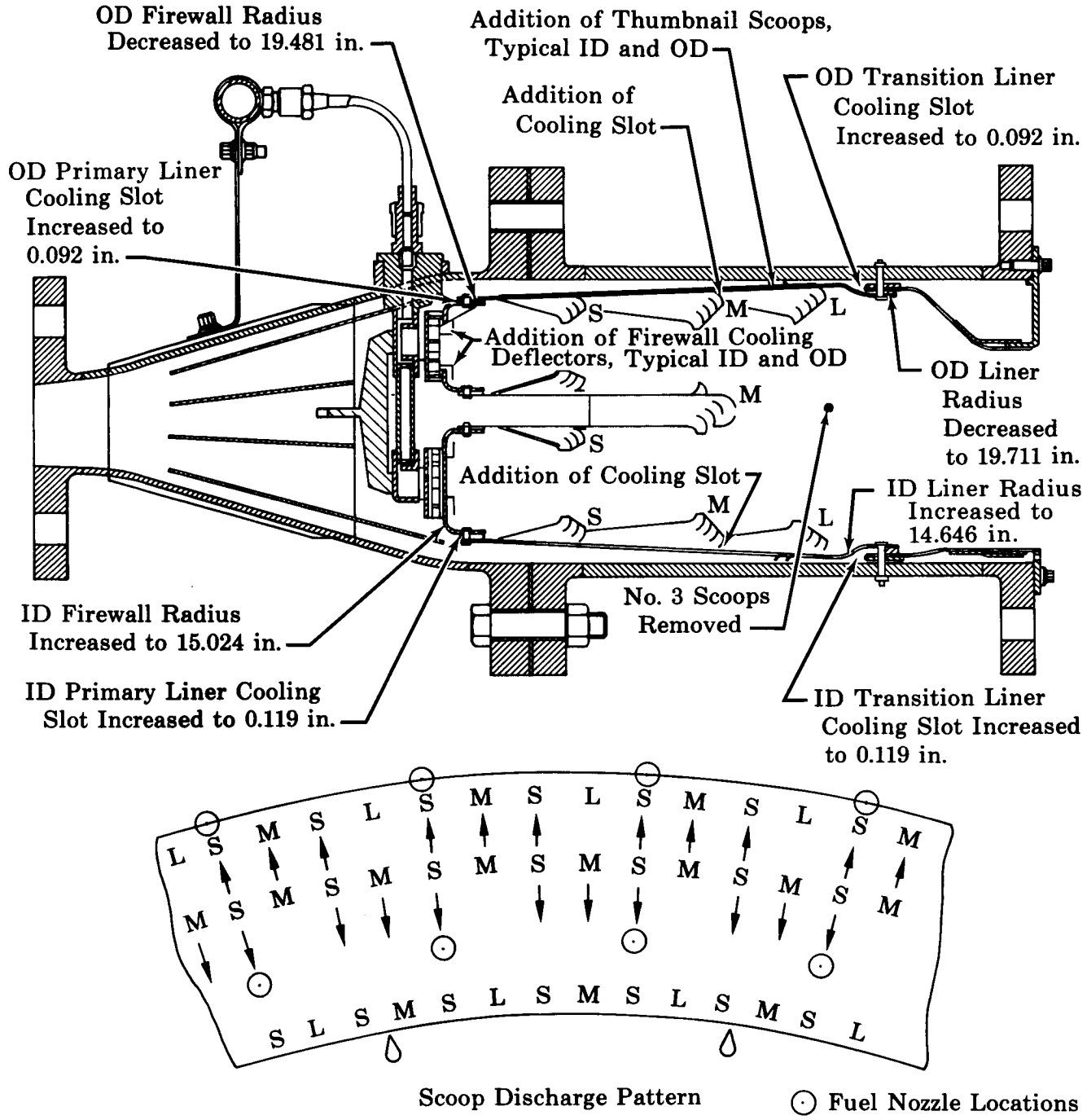

Arrows Indicate Direction of Centertube Scoop Discharge
Looking Upstream

Figure 14. Twin Ram Induction Combustor, Model No. 5

FD 15133D

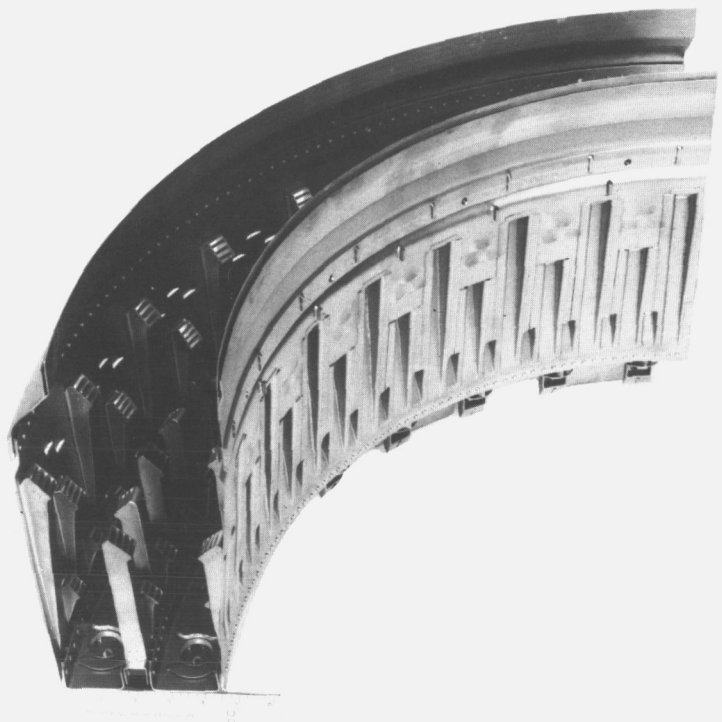

Figure 15. Twin Ram Induction Combustor, Model No. 5 FE 57839

The Models No. 6 and 7 combustors incorporated successive additions of firewall cooling and sweep holes around each nozzle location in both the inner and outer chambers to eliminate firewall soot deposits and reduce combustor pressure loss. These modifications are illustrated in figure 16. Testing at simulated cruise temperature conditions to an inlet pressure level of 76 psia showed that the firewall modifications were successful in preventing soot deposits and associated temperature distress while reducing the system total pressure loss to slightly below the design goal. Combustor Models No. 6 and 7 exhibited a flattened cruise exit temperature profile, even though an OD chamber to ID chamber fuel nozzle flow ratio of 1.1 to 1 had been incorporated to minimize this effect.

To reduce the persistently hot ID region of the exit radial profile, the Model No. 8 combustor provided increased fuel flow to the outer combustor chamber. An OD chamber to ID chamber fuel nozzle flow ratio of 2 to 1 was incorporated. Also the transition cooling gaps were

reduced and rings providing 40% swirler inlet blockage were added as shown in figure 17 to increase combustor system pressure loss without reducing firewall cooling. Test results showed that the previously hot ID exit profile region was near the design goal, but that some improvement was needed in the OD region. The effectiveness of differential nozzle flows was demonstrated as a useful tool in tailoring the exit temperature profile. However, the high fuel flow in the outer chamber resulted in metal discoloration indicated outer liner skin temperatures of 1500 to 1700°F with a corresponding decrease in liner strength as indicated by inward bowing of 0.150 inch.

Modifications to combustor Models No. 9 through 12 were intended to provide increased outer liner cooling and supporting strength while improving the combustor cruise discharge temperature profile by varying the transition liner cooling gaps. This had been shown to be an effective means of changing the profile near the liner walls.

To improve airflow distribution the diffuser was modified during testing of combustor Models No. 9 through 12. Prior to testing the Model No. 9 configuration, the warped No. 1 and No. 4 diffuser flow splitter vanes were removed. The warpage was due to lack of provision for differential thermal expansion between the splitter vanes and the diffuser case. Warpage of up to 0.300-inch radial displacement occurred locally with the outer splitter contacting the outer wall and the inner splitter distorting toward the OD. In the Model No. 12 diffuser section, the remaining No. 2 and No. 3 splitter vanes were replaced. A slip joint construction was used adjacent to the struts to minimize the splitter vane bowing caused by differential thermal expansion between the diffuser case walls and the splitter vanes. These modifications to Models No. 9 and 12 diffusers are shown in figure 18.

Testing of the Model No. 12 combustor indicated inadequate cooling of the liners immediately downstream of the second row of liner ram scoops. This effect was most prominent on the OD liner. The scrubbing gas cooling effect from the primary cooling gap was dissipated due to ram scoop blockage within four inches after entry, but it did provide adequate skin cooling to that distance. Previous results had indicated the primary cooling gap height should be minimized to prevent restriction of the shroud area supplying the liner ram scoops and transition cooling gaps.

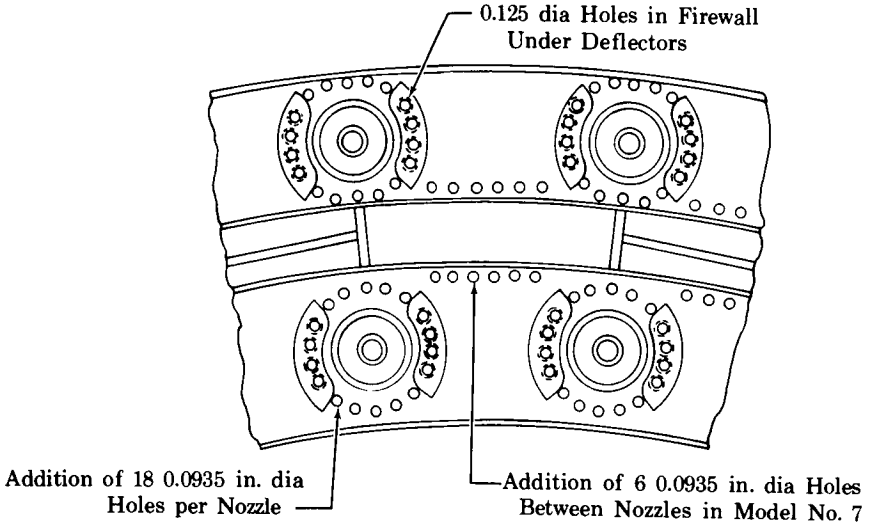

Figure 16. Twin Ram Induction Combustor Firewall Modifications - Model No. 6 and 7 FD 16013B

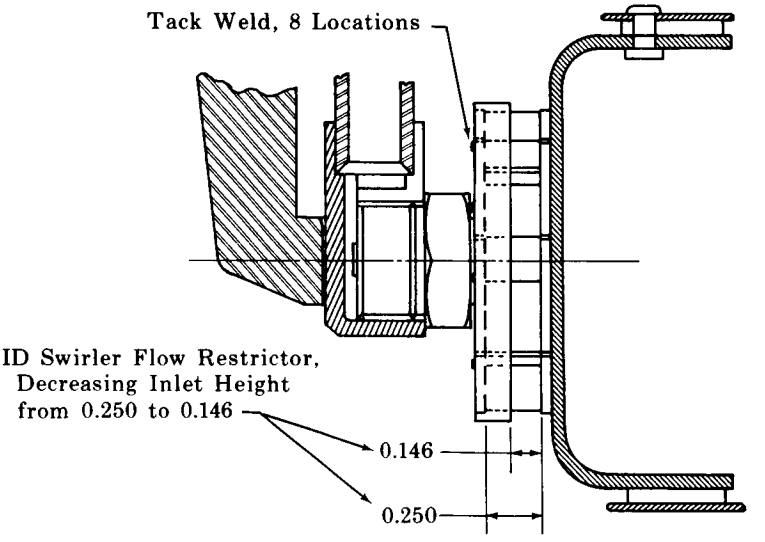

Figure 17. Twin Ram Induction Combustor Model No. 8 Through 19 - ID Swirler Blockage

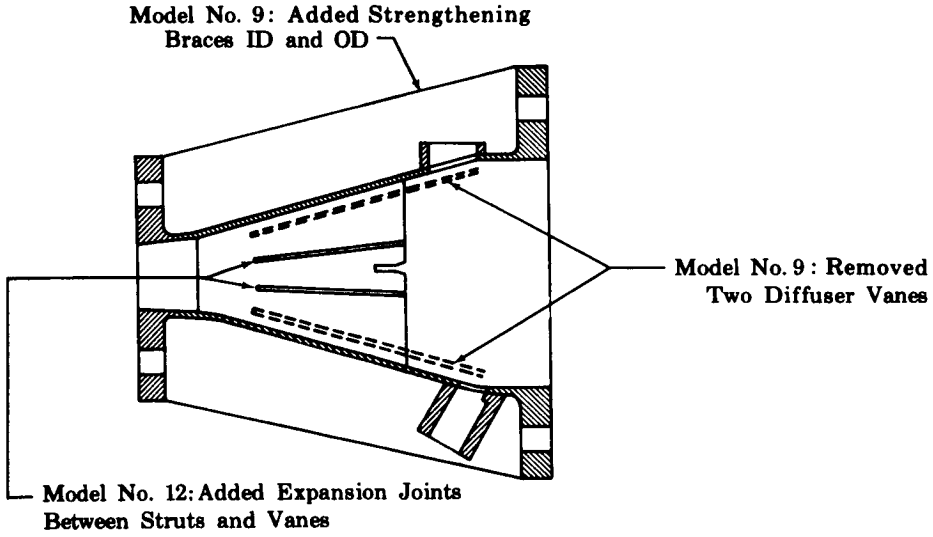

Figure 18. Diffuser Modifications - Model No. 9 and 12 FD 18091B

The Model No. 13 combustor incorporated nozzles of equal flow rates in the OD and ID chambers. Tests of this combustor indicated that the previous combustor modifications plus the equal chamber fuel flow ratio still did not provide the required exit temperature profile.

Therefore, the Model No. 14 combustor included reinstallation of the 2 to 1 fuel nozzle flow split. Reduced primary liner cooling gaps and 25% discharge blockage of the second row of liner ram scoops were incorporated to provide a system pressure loss near the design goal.

Subsequent testing showed the Model No. 14 combustor exit temperature profile to be cool near the walls, and both the SLTO and cruise temperature profiles to be close to that desired, as shown in figure 12. Having achieved an improved temperature profile, a test program was conducted to more extensively investigate the performance characteristics of the Model No. 14 Twin Ram Induction Combustor. This program was discussed in paragraph 3 of this section.

c. Models No. 15 Through 19

Development of the liquid-injection Twin Ram Induction Combustor through Model No. 14 was directed toward improvement of combustor durability and discharge profile, while limiting the combustion system

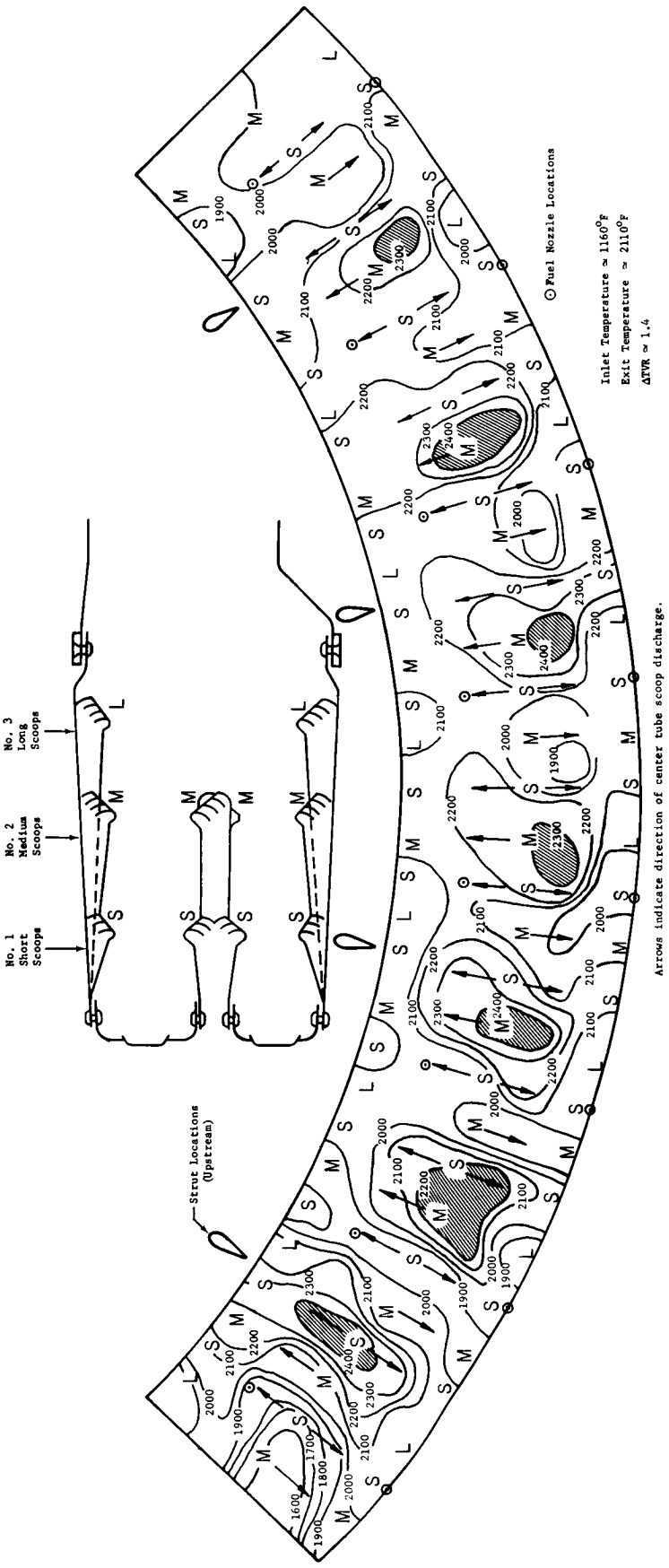

FD 19933A

Figure 19. Model No. 14 Combustor Outlet Temperature Distribution

isothermal total pressure loss to the design goal of 6% at cruise. Tests of successive modifications to both the combustor and diffuser indicated a pattern of circumferential hot spots that coincided with the angular placement of the third row of liner ram induction scoops.

A review of the test data indicated that as early as the Model No. 7 configuration (which incorporated an OD-to-ID fuel nozzle flow ratio of 1 to 1) the exit temperature pattern had a relation to liner scoop arrangement. Incorporating a 2-to-1 nozzle flow ratio in the Model No. 8 configuration, which improved the radial temperature profile, also increased the magnitude of these high temperature areas. However, these areas were not obviously periodic, probably because of airflow distribution variation associated with splitter vane warpage in the diffuser section. With the successive diffuser modifications in Model No. 9 through 12, intended to provide airflow uniformity, the periodic frequency of hot spots emerged uniformly over the entire exit plane. The increase in the outer liner transition gap, for exit temperature radial profile improvement, increased the magnitude of these periodic hot spots.

The repetitive high temperature regions in the Model No. 14 combustor, coincident with the long (No. 3) scoops, presented a hindrance to further temperature pattern improvement. Figure 19 presents a typical temperature distribution pattern obtained with the Model No. 14 combustor, and shows the location of the short, medium, and long scoops.

The Model No. 15 combustor design was intended to reduce the periodic circumferential hot spots while providing an improved degree of exit radial temperature profile control. As shown in figure 19, the Model No. 14 combustor had exhibited hot spots toward the OD of the exit temperature traverse plane, directly behind the long (No. 3) scoops. Analysis also indicated that insufficient flow was passing through the long scoops.

Figure 20 is a plot of the OD shroud Mach number (based on design calculations) vs axial distance along the shroud for the Model No. 14 combustor. Also plotted in figure 20 is the actual shroud Mach number that was calculated from dimension measurements from the Model No. 14 combustor. Note that the actual Mach number is steadily decreasing and has a value of 0.152 at the exit of the long scoops, compared to 0.190 for the medium-length scoops. The design and actual shroud Mach numbers differed significantly due to the liner warpage evident in figure 21.

limiting flow area. The combustor design calculations assumed that the discharge coefficients and pressure drops for all scoops were equal. Therefore, airflow was assumed to be proportional to the scoop exit area.

The shroud Mach number decrease from 0.190 to 0.152 between the medium and long scoops resulted in an approximately 15% lower C_d in the long scoop, with a corresponding reduction in airflow. Further evidence indicating insufficient airflow through the long scoops was seen from the metal discoloration temperature pattern on each scoop. Figure 23 shows the ideal temperatures of the combustion gases based on complete mixing of fuel air between consecutive sets of scoops. If the mass flows of air through both the medium and long scoops were equal, as designed, the wall temperature at the exit of the long scoop would have been cooler than the medium scoops, but this was not the case. The wall temperature at the exit of the long scoop was consistently 300 to 400°F higher than at the exit of the medium scoops, a further indication that the long scoop was not flowing full. Because the long scoop was not passing the required mass flow, the penetration of the diluting air was also reduced. This reduced airflow and penetration resulted in the hot spots found in the exit traverse behind the long scoops.

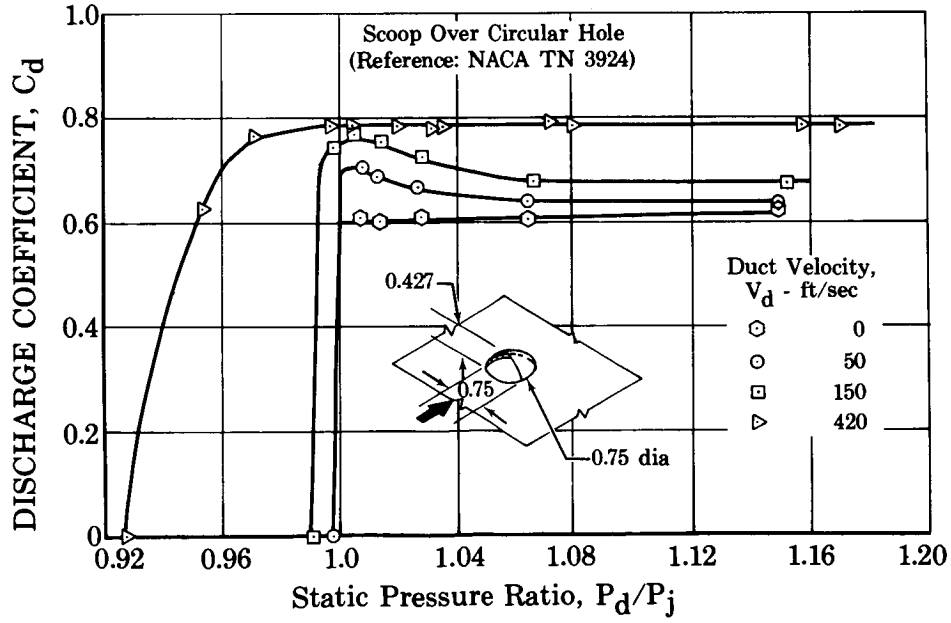

Figure 22. Discharge Coefficient vs Static Pressure Ratio FD 22774

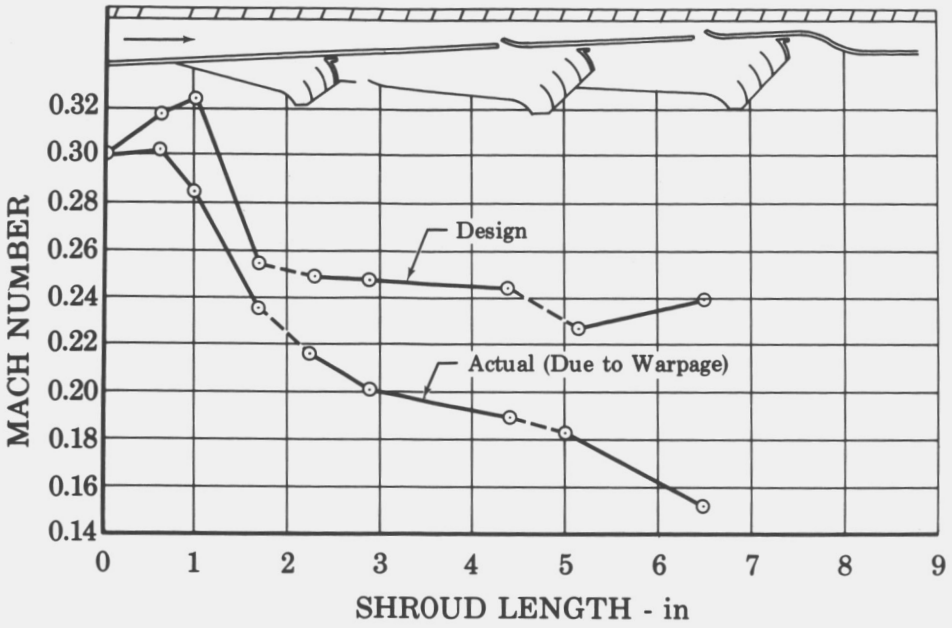

Figure 20. Mach Number vs Shroud Length FD 23036

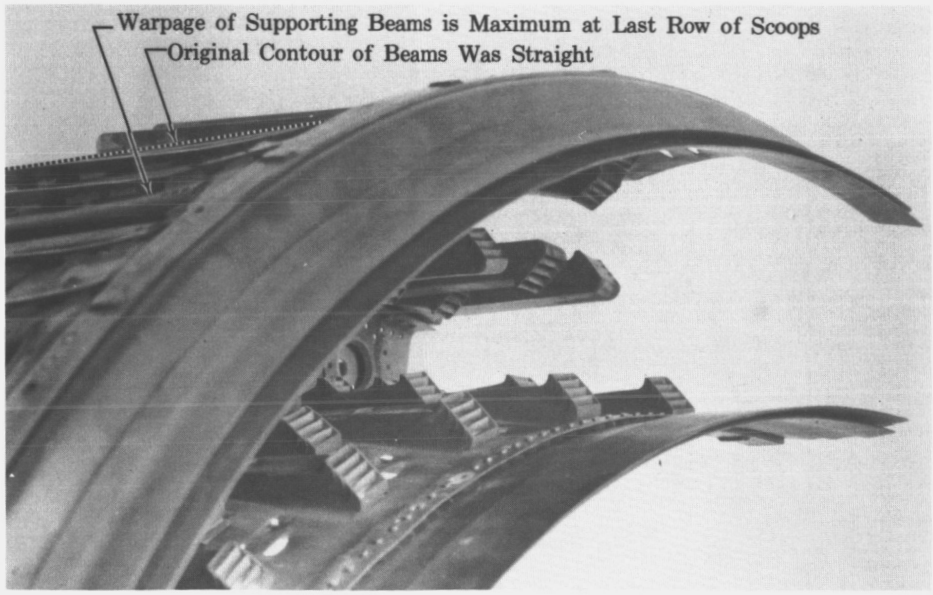

Figure 21. Warpage of Model No. 14 Combustor Liner FD 19920A

Figure 22, which is replotted from Reference 3, shows that the scoop discharge coefficient decreases as the shroud Mach number decreases. In the ram induction burner, this discharge coefficient was applied to the scoop exit area normal to the scoop flow direction, as this was the

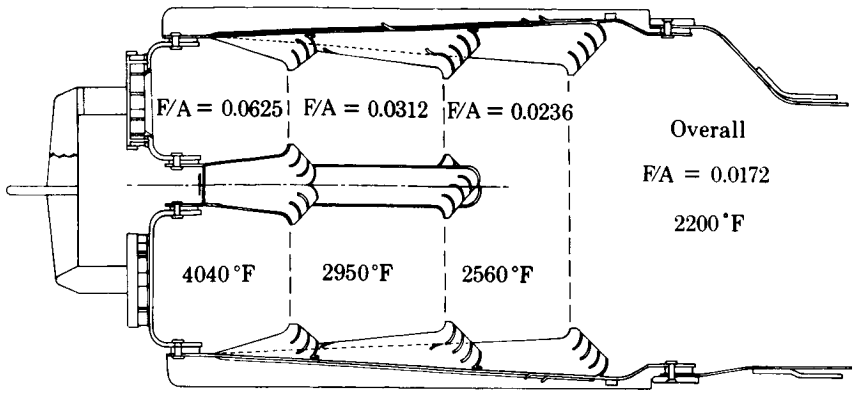

Figure 23. Temperature Gradient in Model No. 14 Combustor FD 18079E

Observation of atmospheric pressure tests showed flame in the first 4 to 5 inches of the combustor. This indicated that the combustor could be shortened if a more effective scoop pattern was installed for temperature pattern control. Since the purpose of this program was to develop a short-length turbojet combustor, the Model No. 15 was designed with an option for shortening the combustor an additional 2.2 inches. For testing the shortened combustor a reduction in case length would also have been required.

The Model No. 15 design changes consisted of the following items:

1. Eliminating the long (No. 3) scoops on both the OD and ID liners and replacing them by medium scoops in line with the existing second row of scoops.
2. Redesigning the center shroud to include the same number of center shroud rear scoops as OD and ID liner rear scoops; this required the fabrication of back-to-back or double center shroud scoops. This feature essentially doubled the number of scoop discharge jets into each annulus from the rear center shroud scoops without increasing center shroud airflow. To help promote penetration of these individually smaller jets, the scoop discharge length/width ratio was increased from a value of 1 to 2.
3. Indexing the center shroud assembly so that both the front and rear scoops were circumferentially staggered relative to the OD and ID liner scoops.
4. Incorporating additional liner sections to join the shortened primary liners to the existing transition liners.

5. Increasing the material thickness of the OD and ID intermediate liners from 0.037 to 0.060 in. The additional strength of the liner segments was required to prevent inward bowing during the combustion testing. Liner bowing on previous models had affected the scoop airflow distribution and hindered exit profile control.

These design changes are shown in figure 24.

The increased flow of dilution air from the medium scoops that replaced the long scoops was intended to provide more complete mixing in the front of the combustor, which would reduce the existing hot spots. The scoop frequency, defined as the number of identical scoops in a given angular distance, was doubled. This more uniform circumferential air injection was also intended to provide a more uniform exit temperature pattern. Experience with other ram induction combustor systems had indicated that improved scoop discharge mixing resulted from circumferential staggering of ram scoops with respect to the scoops in the opposite liner. This was incorporated in the Twin Ram Induction Combustor by indexing the center shroud assembly to stagger all center scoops with respect to the scoops of each opposing liner.

Removal of the long scoops required the addition of an intermediate liner section to maintain the original combustor length. This intermediate liner provided an additional circumferential cooling gap just downstream of the rear scoops. The air provided by this gap cooled the liner section immediately downstream of the gap, an area that had shown distress on earlier models. This air was also usable as a controlling device for the exit radial profile. On previous models the transition cooling air was useful as a profile control tool, at the expense of liner durability. With the addition of the extra liner cooling gap, it was considered that both profile control and liner durability could be achieved. Figure 25 shows the calculated combustor airflow distribution for the Model No. 15 configuration.

Figure 26 is a photograph of the Model No. 15 combustor. Testing of the Model No. 15 combustor at SLTO conditions showed that although the exit radial temperature profile was sharply peaked at the OD, the exit gas temperatures near the liners were quite cool. The exit temperature hot spots, previously associated with the long liner scoops, had virtually disappeared.

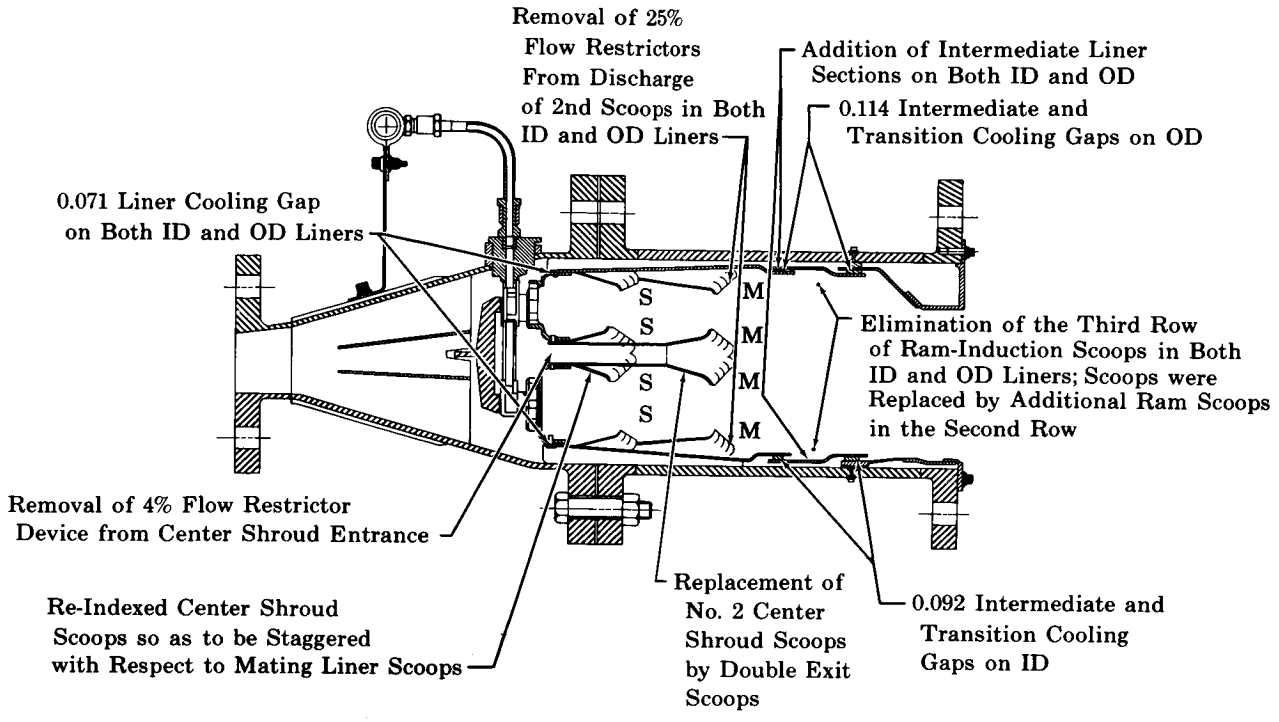

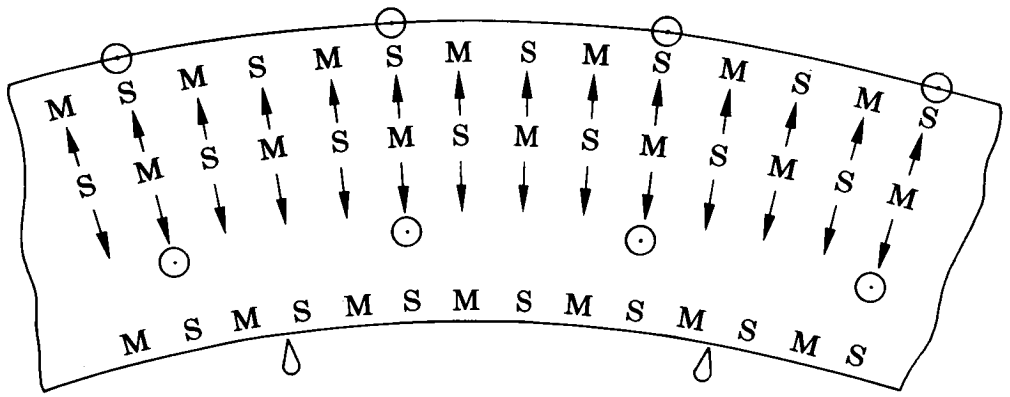

Scoop Discharge Pattern

Arrows Indicate Direction of Centertube Scoop Discharge Looking Upstream

⊙ Fuel Nozzle Locations

Figure 24. Model No. 15 Twin Ram Induction Combustor Configuration

FD 20575B

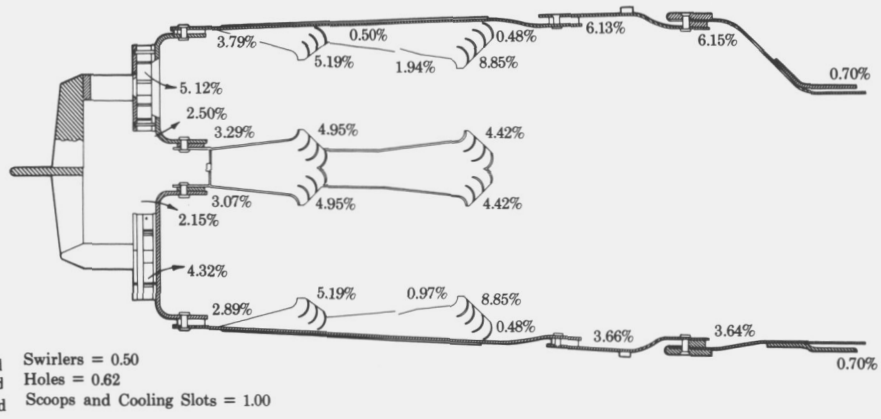

Figure 25. Calculated Effective Flow Distribution - Twin Ram Annular Combustor, Model No. 15 FD 21841A

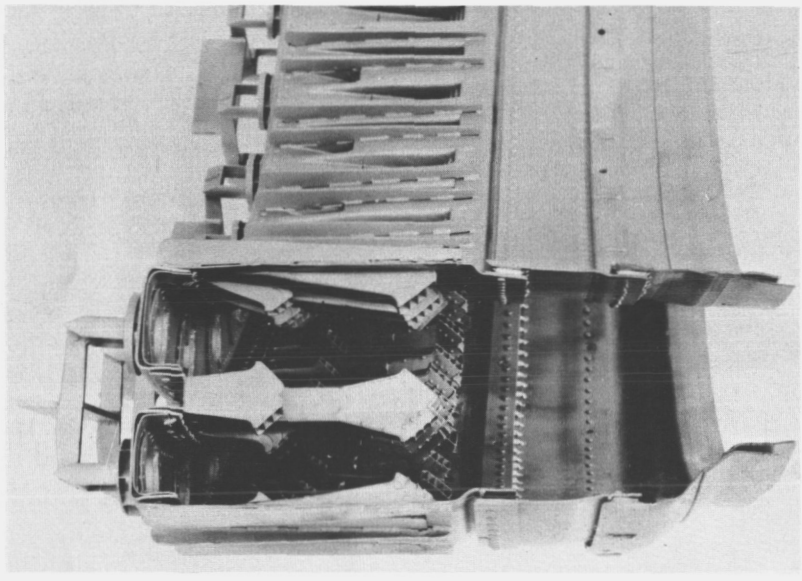

Figure 26. Twin Ram Induction Combustor, Model No. 15 FE 68638

Tests of the Model No. 8 combustor and subsequent configurations had indicated the combustor airflow was directed predominantly toward the outer shroud. This required a higher fuel flow from the OD chamber fuel nozzles to achieve the desired exit radial temperature profile. The Model No. 14 combustor achieved an exit profile near the design goal with an OD to ID chamber fuel flow ratio of 2 to 1. This split was retained in the Model No. 15 combustor. However, Model No. 15 test results indicated that the air distribution to the combustor had improved,

probably due to a shift from radial diffuser separation to circumferential separation, thus eliminating the need for the high OD to ID fuel split. The shift in diffuser flow pattern may have been influenced by the combustor liner scoop rearrangement.

The Model No. 16 and 17 combustors incorporated 1 to 1 and 1.6 to 1 nozzle flow ratios, respectively, and provided test data to bracket the fuel flow split required to achieve the desired exit temperature radial profile. The test results indicated that hot areas of the circumferential exit temperature distribution were located between diffuser strut locations, not periodic with any scoop arrangement, and were therefore due primarily to circumferential diffuser flow variations. The Model No. 18 combustor incorporated a 1.23 to 1 nozzle flow ratio, as bracketed from Model No. 16 and 17 testing. A coarse screen, No. 4 stainless steel mesh with 0.067-inch diameter wire providing 52% area blockage, was installed at the diffuser exit to improve the circumferential airflow distribution. The diffuser with the screen installed is shown in figure 27. Test results showed the cruise exit temperature radial profile to be near the design goal. The screen provided little if any reduction in circumferential variations in the combustor inlet airflow pattern and caused an increase in measured cruise pressure loss of 0.4%.

In the Model No. 19 combustor, the outer liner intermediate and transition cooling gaps were reduced slightly to further tailor the exit temperature profile. The Model No. 19 combustor is shown in figure 28. Testing at cruise inlet conditions showed the Model No. 19 combustor to have an exit radial temperature profile very near that desired with a $D_{R\ max}$ value of less than 6% (local average temperature 63°F higher than desired profile) and a ΔTVR value of 1.19. The combustion system isothermal pressure loss, corrected to the cruise inlet Mach number of 0.281, was 6.5%, including the pressure loss of the diffuser screen.

Testing at sea level takeoff conditions showed the exit radial temperature profile to have a $D_{R\ max}$ value of 8.7% with a ΔTVR value of 1.25 and a SLTO corrected system isothermal total pressure loss of 3.4%.

This concluded Twin Ram Induction Combustor testing. Tests were not conducted with the 2.2 inch liner extensions removed.

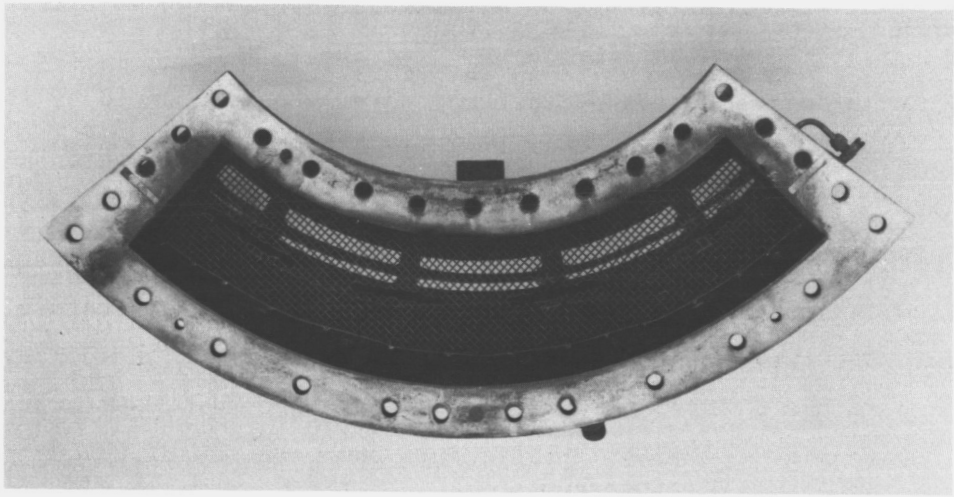

Figure 27. Diffuser With Screen Installed FE 68500

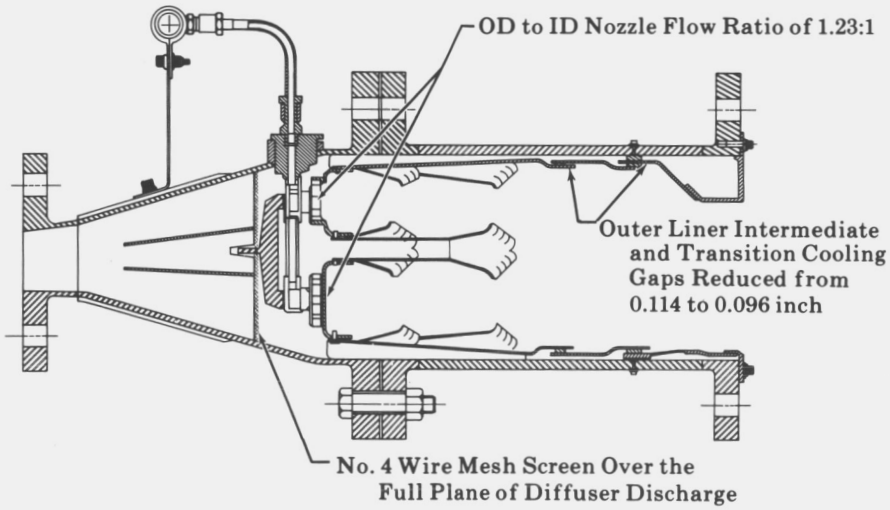

Figure 28. Twin Ram Induction Combustor, Model No. 19 FD 20567A

3. Performance of Models 14 and 19

The Model No. 14 combustor was considered to have combustor durability and an exit temperature profile close enough to the program goals so that further modifications to improve these areas would not affect fundamental combustor operating characteristics.

Having achieved this level of performance, a test program was conducted with the Model No. 14 combustor to determine the combustion efficiency, pressure loss, and temperature pattern characteristics over a range of

reference velocities and fuel/air ratios at 60 psia rig inlet pressure and inlet temperatures of 600°F and 1150°F.

Tests were also conducted to evaluate combustor lean blowout and ignition capabilities at low pressures and to determine the effect of the rig exit choke plate used to simulate the presence of turbine inlet nozzle vanes.

a. Combustion Efficiency

Figures 29 and 30 show the results of combustion efficiency tests conducted at 600°F inlet temperature and 60 psia inlet pressure. Data were obtained at fuel/air ratios of 0.0060, 0.00124, and 0.0187 at combustor reference velocities of 78, 102, and 162 ft/sec.

The test results indicated that reference velocity and fuel/air ratio had little effect on combustion efficiency for fuel/air ratios above about 0.012. These tests indicated that the degree of fuel atomization and dispersion determined a minimum fuel pressure below which combustor efficiency decreased rapidly. As the fuel nozzle pressure differential decreased with decreasing fuel flow, the fuel was injected in larger droplets, and a point was reached where incompletely vaporized fuel passed through the combustor. The combustion efficiency then decreased as an apparent function of nozzle pressure drop. This minimum effective fuel nozzle pressure drop was found to vary with combustor reference velocity. Increased combustor through-velocities resulted in decreased residence time and required more complete fuel atomization to achieve high combustion efficiency.

Figures 31 and 32 show the results of tests conducted to determine combustion efficiency at fuel/air ratios of 0.0056, 0.0114, and 0.0178 and combustor reference velocities of 107, 152, and 189 ft/sec at an inlet pressure of 60 psia and an inlet temperature of 1150°F. These tests showed the same high combustion efficiency and insensitivity to reference velocity and fuel/air ratio as at 600°F. In addition, the test results indicated that at the higher rig inlet temperature, combustion efficiency was less affected by poor fuel atomization and dispersion resulting from low fuel nozzle pressure drop.

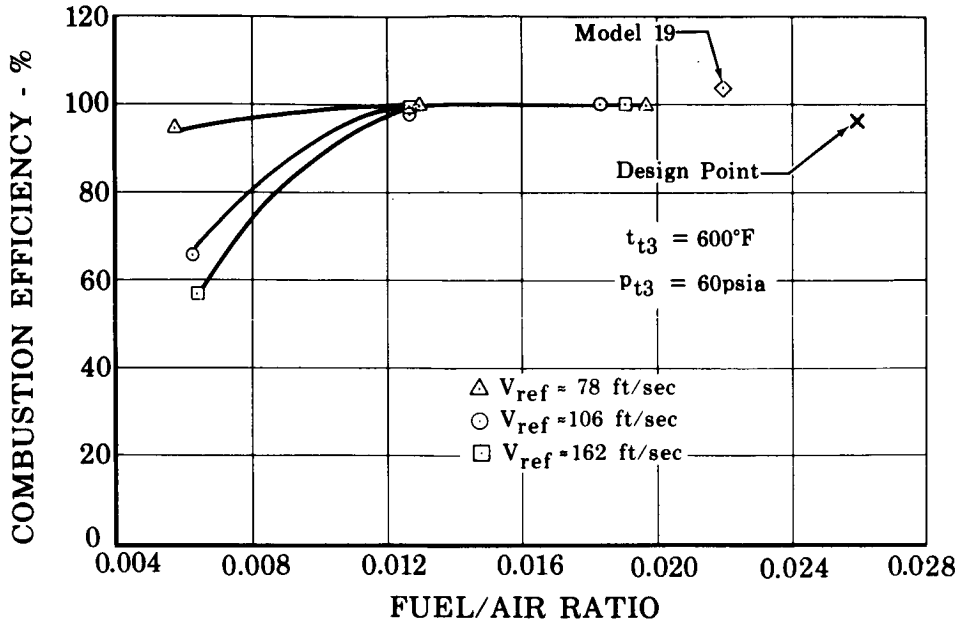

Figure 29. Twin Ram Induction Combustor, Model No. 14 - Combustion Efficiency vs Fuel/Air Ratio, Takeoff FD 22767

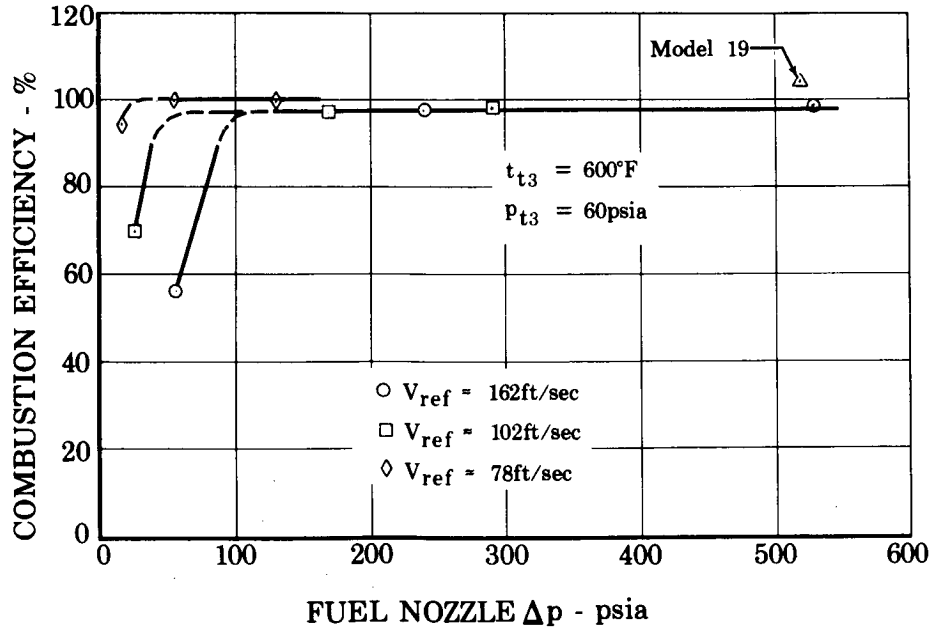

Figure 30. Twin Ram Induction Combustor, Model No. 14 - Combustion Efficiency vs Fuel Nozzle ΔP, Takeoff FD 22768

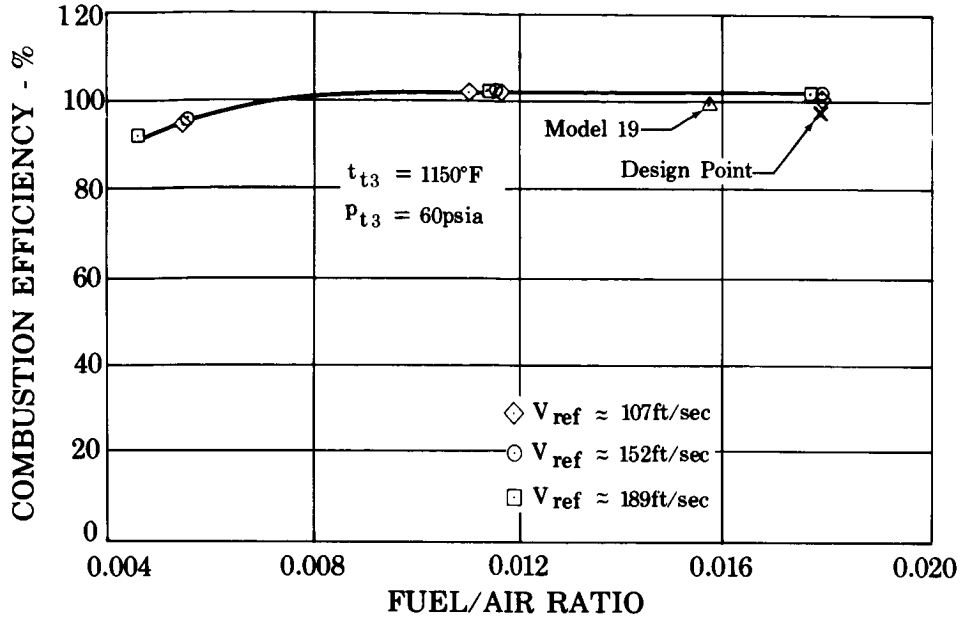

Figure 31. Twin Ram Induction Combustor, Model No. 14 - Combustion Efficiency vs Fuel/Air Ratio, Cruise FD 22769

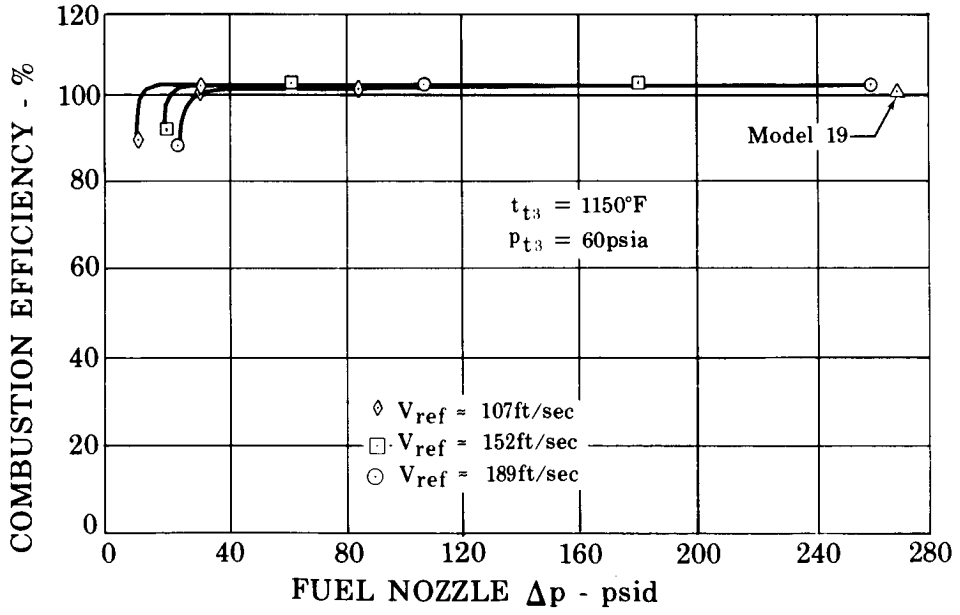

Figure 32. Twin Ram Induction Combustor, Model No. 14 - Combustion Efficiency vs Fuel Nozzle ΔP, Cruise FD 22770

Efficiency results for the Model No. 19 combustor are also shown on the preceding curves. There was no significant difference between the Models No. 14 and 19 in measured combustion efficiency.

In summary, the combustor operated at high efficiency levels over the full range of conditions tested. The efficiency level was relatively insensitive to fuel nozzle performance at the elevated inlet temperature condition.

b. Combustor System Pressure Loss

Model No. 14 combustor system pressure loss was determined over a range of air velocities. Figures 33 and 34 present pressure loss as a percentage of inlet total pressure, $\Delta P_t/P_t$, as a function of diffuser inlet Mach number at the takeoff and cruise conditions. Figures 35 through 38 present pressure loss as a percentage of inlet dynamic pressure, $\Delta P_t/q$, as functions of diffuser inlet Mach number and combustor total temperature ratio at the takeoff and cruise conditions. The $\Delta P_t/q$ curves appear to vary in trend due to the expanded scale and the sensitivity of this parameter to data scatter. By utilizing the isothermal combustor system total pressure loss at the test cruise conditions from figure 34, the Model No. 14 combustor effective entry hole area from table II, and the method of determining liner pressure loss as presented in Appendix B, the estimated diffuser pressure loss at cruise conditions was 3%.

Model No. 19 combustor pressure loss data are also presented in figures 33 and 34. This configuration had overall system isothermal total pressure losses, corrected to the design diffuser inlet Mach numbers, of 6.5% and 3.4% at the simulated cruise and sea level static conditions, respectively, including the pressure loss caused by the installation of the coarse screen in the diffuser.

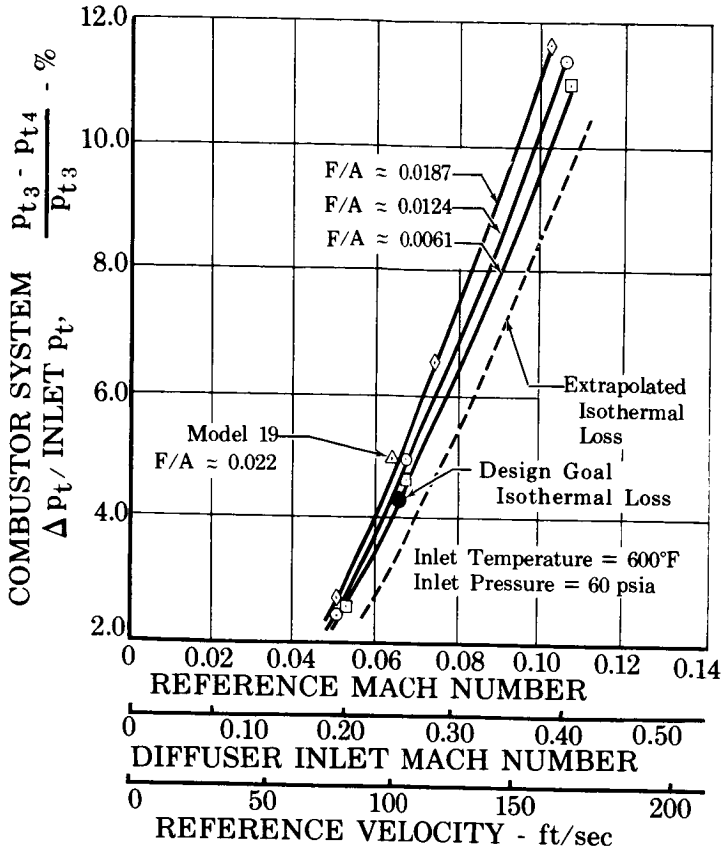

Figure 33. Twin Ram Induction Combustor, Pressure Loss at Takeoff FD 22771A

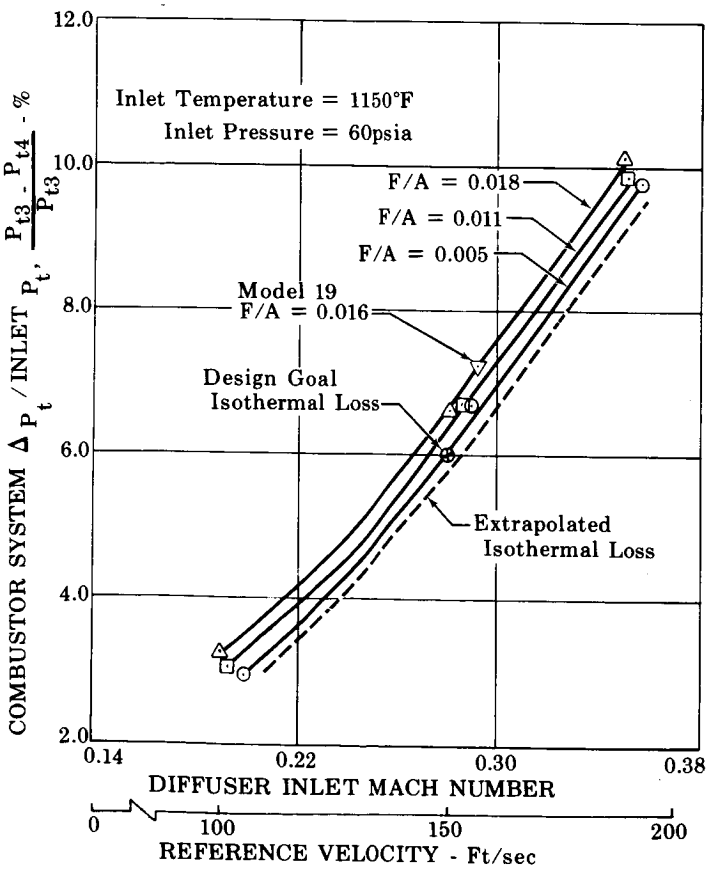

Figure 34. Twin Ram Induction Combustor, Pressure Loss at Cruise FD 22976A

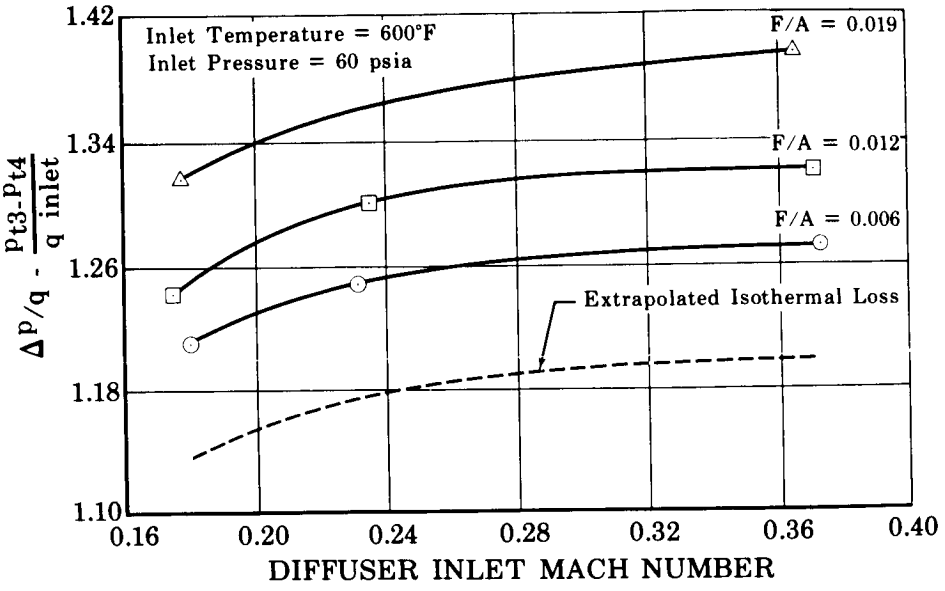

Figure 35. Twin Ram Induction Combustor Pressure Loss Coefficient at Takeoff FD 22780

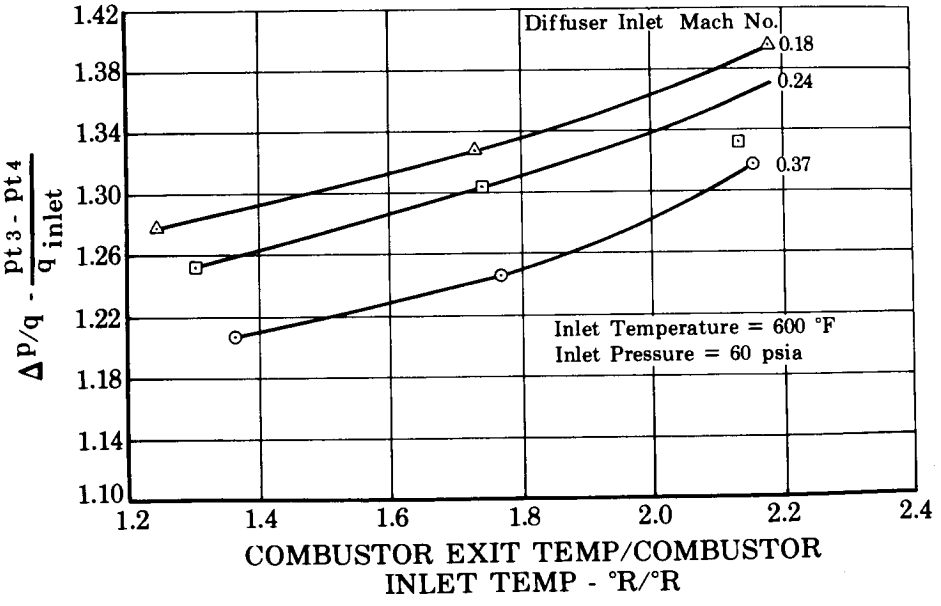

Figure 36. Twin Ram Induction Combustor Pressure Loss Coefficient at Takeoff FD 22781

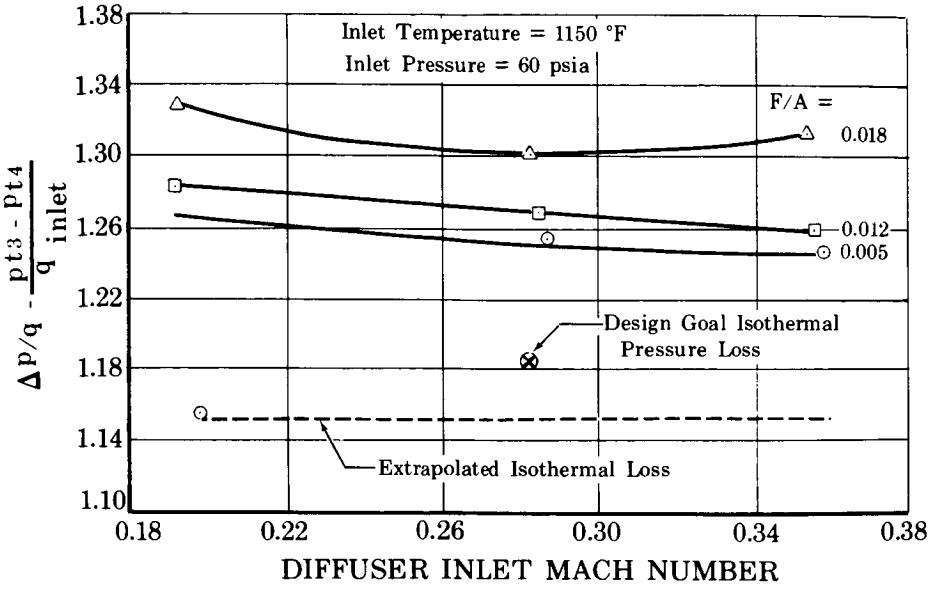

Figure 37. Twin Ram Induction Combustor Pressure Loss Coefficient at Cruise FD 22782

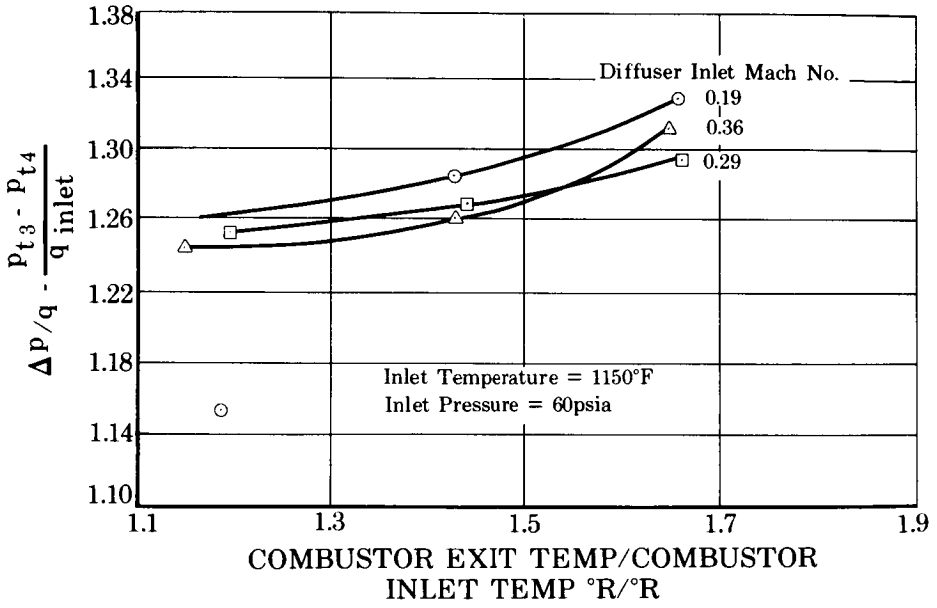

Figure 38. Twin Ram Induction Combustor Pressure Loss Coefficient at Cruise FD 22783

c. Combustor Outlet Temperature Profile

Figures 39 and 40 present Model No. 14 combustor outlet radial temperature profiles at cruise and takeoff test conditions. This combustor demonstrated an exit temperature pattern ΔTVR* value of 1.33 with D_{max}

*Definitions of ΔTVR, D_{max}, and $D_{R_{max}}$ are presented in Appendix C.

of 24.7% and $D_{R_{max}}$ of 7.33% at cruise conditions. At takeoff conditions (except average exit temperature was 1801°F) the values were: ΔTVR of 1.54, D_{max} of 38.1% and $D_{R_{max}}$ of 4.0%. The performance goals for ΔTVR, D_{max}, and $D_{R_{max}}$ at cruise conditions are 1.16, 9.52%, and 9.52%, respectively, for the radial temperature profile shown in figure 1. The corresponding performance goals for ΔTVR, D_{max}, and $D_{R_{max}}$ at takeoff conditions are 1.11, 6.25%, and 6.25%, respectively.

The Model No. 19 combustor outlet radial temperature profiles are presented in figures 41 and 42 for cruise and takeoff conditions, respectively. This combustor demonstrated a cruise exit temperature ΔTVR value of 1.19 with D_{max} of 15.6%. The corresponding exit radial temperature profile was very near the design target with a $D_{R_{max}}$ = 5.9%. At the simulated sea level takeoff condition, the Model No. 19 combustor had a ΔTVR value of 1.25, a D_{max} value of 22.4%, and a $D_{R_{max}}$ value of 8.7%.

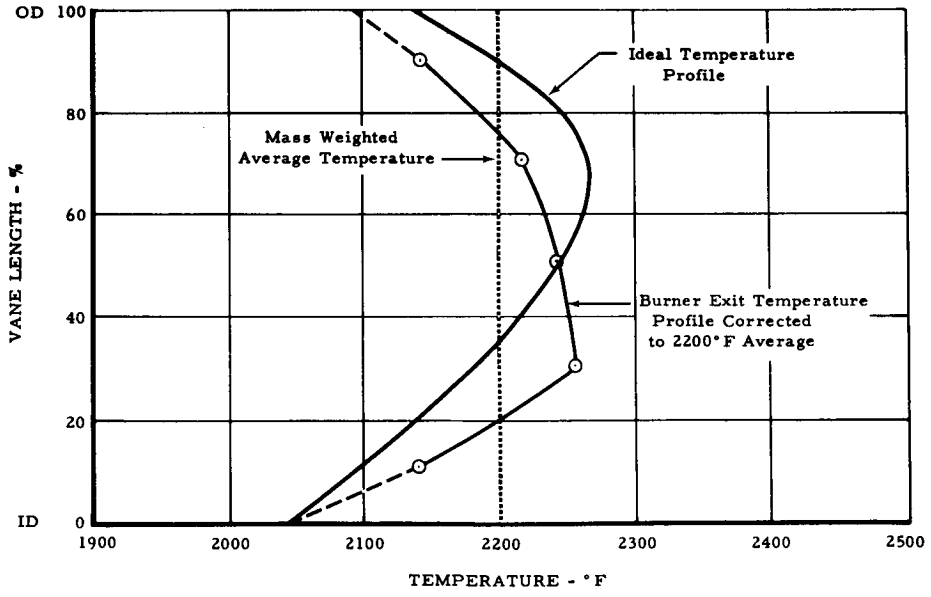

Figure 39. Cruise Radial Temperature Profile - Twin Ram Induction Combustor - Model No. 14 FD 18919

Diffuser Inlet Total Pressure	60.69 psia
Diffuser Inlet Total Temperature	1149.7°F
Diffuser Inlet Mach Number	0.265
Combustor Exit Total Temperature	1959°F

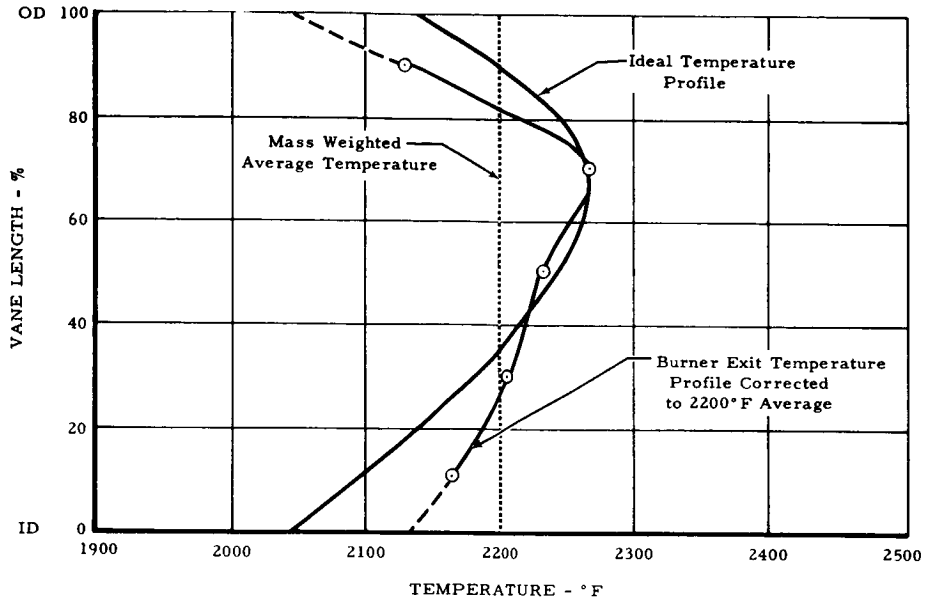

Figure 40. Takeoff Radial Temperature Profile - Twin Ram Induction Combustor - Model No. 14 FD 19127

Diffuser Inlet Total Pressure	61.42 psia
Diffuser Inlet Total Temperature	599.4°F
Diffuser Inlet Mach Number	0.262
Combustor Exit Total Temperature	1801°F

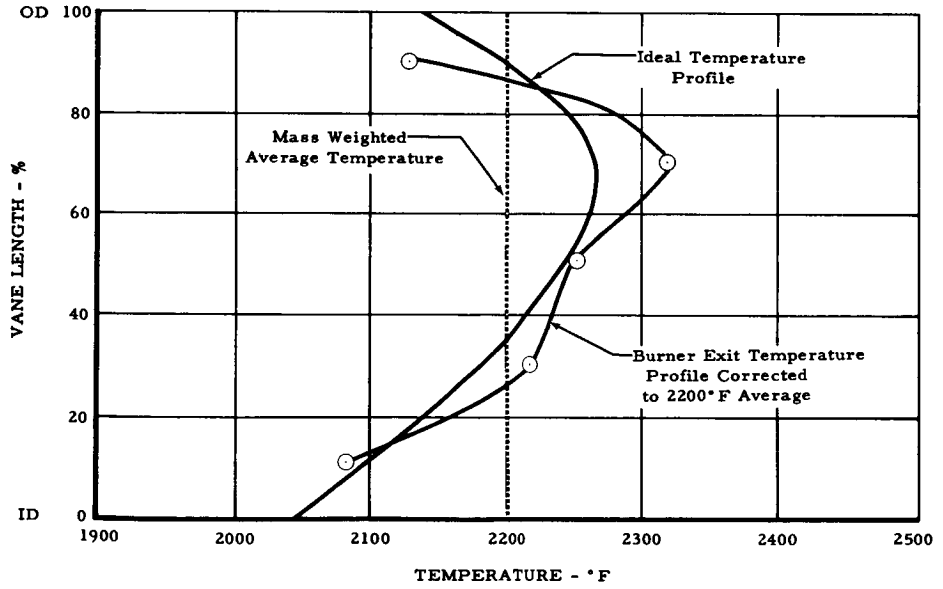

Figure 41. Cruise Radial Temperature Profile - Twin Ram Induction Combustor - Model No. 19 FD 21821

Diffuser Inlet Total Pressure	60.77 psia
Diffuser Inlet Total Temperature	1163.3°F
Diffuser Inlet Mach Number	0.290
Combustor Exit Total Temperature	2126°F

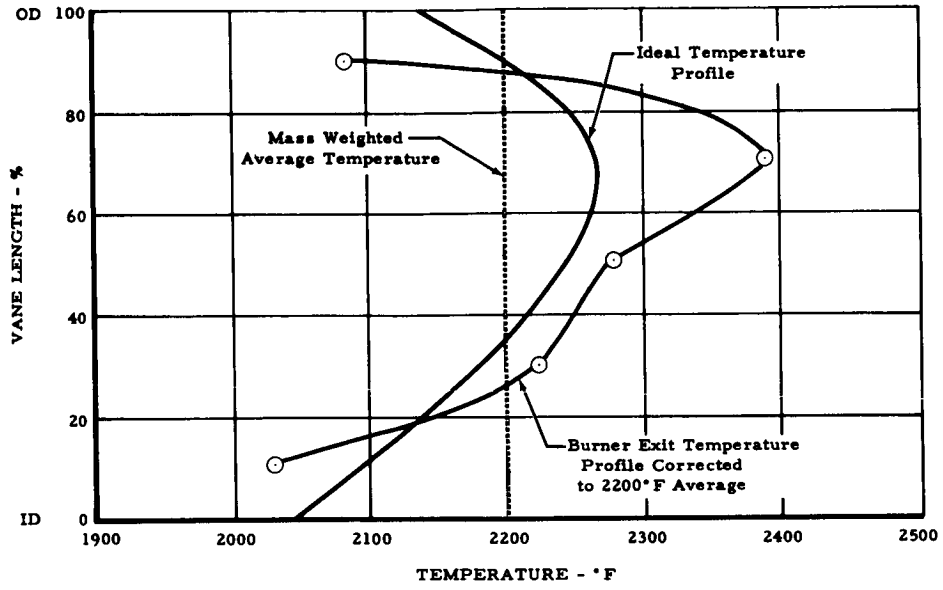

Figure 42. Takeoff Radial Temperature Profile - Twin Ram Induction Combustor - Model No. 19 FD 21822

Diffuser Inlet Total Pressure	59.63 psia
Diffuser Inlet Total Temperature	600.5°F
Diffuser Inlet Mach Number	0.232
Combustor Exit Total Temperature	2051°F

d. Combustor Durability

Neither the Model No. 14 or No. 19 combustors exhibited durability problems over the length of time they were tested. Since endurance tests were not run, no indication of potential combustor life was attained.

e. Lean Blowout Investigation

Figure 43 shows the results of tests conducted to determine the Model No. 14 combustor lean blowout limits over a range of reference velocities at inlet temperatures of 600°F and 1150°F and 60 psia rig inlet pressure. These values are considered satisfactory. However, blowout data were not obtained at low inlet pressure and temperature operating conditions where lean blowout problems may be encountered.

To provide a maximum degree of fuel nozzle atomization, the lean blowout tests were conducted with high pressure drop nozzles installed. To determine precisely when combustor lean blowout occurred, a bare wire thermocouple was inserted into the combustor through the outer combustor

case and liner. The position of the thermocouple was 45 degrees from the rig side wall, axially in line with the transition cooling gap, and protruding one inch into the combustor through the ID liner.

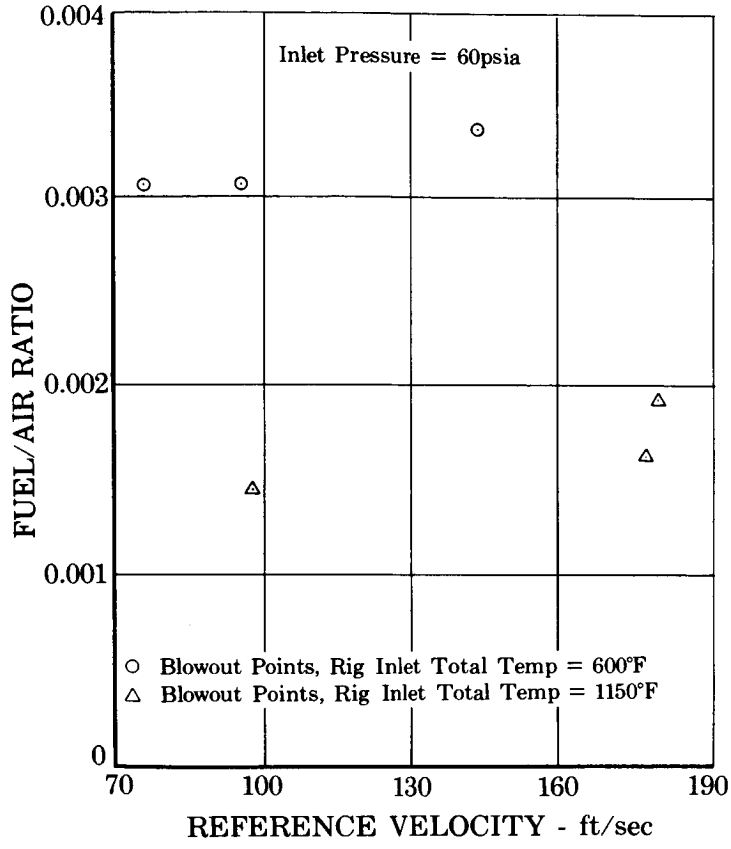

Figure 43. Twin Ram Induction Combustor Lean Blowout Tests, Model No. 14 FD 22772

It was noted that blowouts at an inlet temperature of 600°F were quite definite, with little flame-flickering indicated by the bare wire thermocouple. However, at 1150°F inlet temperature, the exact point of blowout was much less definite. The monitor thermocouple indicated erratic flame strength and position at fuel/air ratios near blowout.

f. Combustor Low Pressure Ignition Evaluation

A brief investigation was conducted to determine the Model No. 14 combustor ignition characteristics at relatively low pressure levels. Ignition at all points tested was attempted with both a 20-joule surface discharge spark ignition system and the injection of a pyrophoric fluid, triethylborane (TEB). The igniter and TEB injection locations are shown in figure 44.

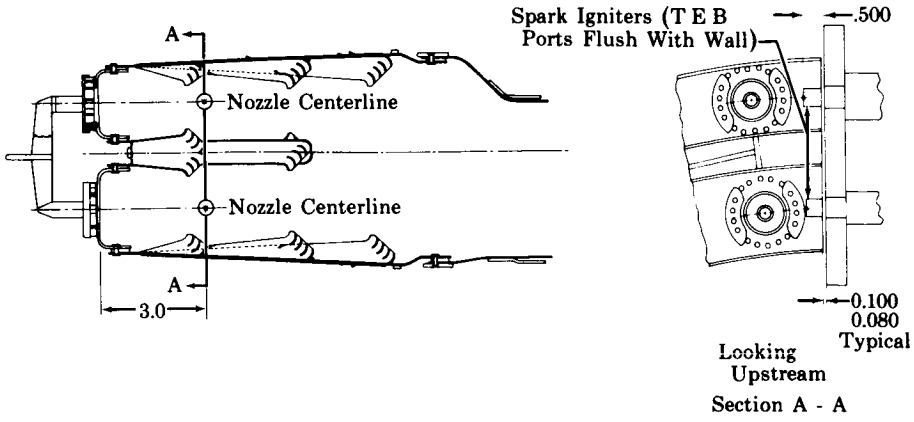

Figure 44. Location of Spark Igniters and TEB Injection Ports of Twin Ram Induction Combustor, Model No. 14 FD 22794

The ignition capability of the Model No. 14 combustor was found to be poor, but this was partly due to a nonideal igniter location. Ignition was not achieved at fuel/air ratios below 0.0185 at 20 psia, and not at all below 16.6 psia. Ignition was not attempted at fuel/air ratios above 0.022 or at pressures above 20 psia during this investigation. Although no development effort was directed toward ignition, the following factors are believed to influence the ignition performance.

1. Lean Fuel/Air Ratios in the Dome Region of the Combustor - At 20 psia rig inlet pressure, ignition could only be attained at high overall fuel/air ratios. In a small effective diameter combustor such as the twin ram configuration, a front end fuel/air ratio near stoichiometric is required for ignition. Since this requirement was apparently satisfied only at high overall fuel/air ratios, the fuel/air ratio in the front of the combustor must have been relatively lean.

2. Poor Fuel Nozzle Atomization and Droplet Dispersion - The limited selection of fixed orifice nozzles used in this program, which had characteristically narrow turndown capability, resulted in nozzle pressure drops as low as 10 psid at the flows required for the majority of the ignition conditions tested. The spray angle and atomization were

less than would be desired for an engine combustor and did not provide the necessary fuel/air mixture at the ignition location.

3. Location of Spark Igniter Tip and TEB Injection Port - Ignition tests of the Model No. 14 combustors were conducted with both the spark igniter tips and TEB injection ports located, as shown in figure 44, in the segment end wall of the test rig where lean boundary regions exist. If high fuel/air ratio gradients exist, the location of the ignition source becomes increasingly important. The wall location was far from ideal and also not representative of a possible engine installation. Separate ignition was provided for each combustor annulus. This would probably not be practical for an actual engine installation and a cross fire tube from one annulus to the other might be required.

g. Choke Plate Investigation - Model No. 14 Combustor

To determine the effect of the presence of choked turbine nozzle vanes on combustor discharge temperature pattern, tests were conducted with and without the rig exit choke plate installed. This plate, positioned immediately downstream of the combustor exit traverse rake, provided the required uniform area restriction to simulate the presence of turbine inlet nozzle vanes.

Tests 046 and 047 (Table D-1) were conducted with the plate installed. Those test conditions were repeated in tests 056 and 057 (Table D-1) with the plate removed. Tests 046 and 056 were conducted at 60 psia inlet pressure, 1150°F inlet temperature, and 2100°F exit temperature; tests 047 and 057 were conducted at 60 psia inlet pressure, 600°F inlet temperature, and 1800°F exit temperature.

Test results indicated that the choke plate had a minor flattening effect on the exit radial temperature profile. This effect was most prominent at the takeoff conditions where the combustor temperature rise was highest, and was barely discernible at cruise temperature conditions.

A comparison of the radial temperature profiles and temperature distributions indicated a reduction in combustor ΔTVR value at cruise conditions and a reduction in discharge temperatures near the OD transition liner with the choke plate installed. Both of these effects occurred in regions of highest temperature gradients where slight aerodynamic changes or probe position differences would be greatly magnified. Slight alignment differences may have been introduced when the exit traverse rake was removed and disassembled to replace a thermocouple element between comparative tests.

B. VAPORIZING RAM INDUCTION COMBUSTOR

1. Development Procedure

Development effort on the Vaporizing Ram Induction Combustor was directed primarily to the achievement of a durable and effective vaporizer tube design. Since this combustor had the same outer liner design, changes to the liner developed in the Twin Ram Induction Combustor investigation were applied to the Vaporizing Ram Induction Combustor. These changes included alterations in the cooling gaps, the addition of thumbnail scoops, and finally, the reduction in the number of rows of scoops from three to two.

In the initial design of the Vaporizing Ram Induction Combustor, a primary objective was to achieve a high degree of heat transfer to the vaporizing tubes to ensure that the fuel was fully vaporized before injection into the front of the burner. Satisfactory first tests on the burner were conducted at low temperature and pressure conditions. Pyrophoric ignition with triethylborane, containment of visible flame within the combustor, and efficiency, posed no problems and liner durability was achieved with the cooling procedures applied to the Twin Ram Induction Combustor. However, when the inlet temperature and pressure were raised to the levels of the program goals, the vaporizer tubes experienced burning. Analysis of the burned tubes and the temperature of other metal surfaces in the affected area indicated the possibility of chemical reaction (spontaneous combustion) occurring inside the vaporizing passages. An attempt to eliminate this problem by shortening the vaporizing tubes was ineffective. Therefore, the vaporizing centertube was redesigned.

Most of the remaining program was spent in this redesign and construction of a vaporizing centertube which incorporated film cooling over the vaporizer tubes and decreased hot surface area. This was achieved in the Model No. 4 combustor. Since the hot side of the redesigned vaporizing passages operated at a lower temperature than the inlet air temperature during high heat flux combustion testing, it was indicated that the original problem was overcorrected. The exit temperature profile had a relatively cold mid-section, and reduction of the vaporizing tube film cooling flow was required to improve the profile while reducing the excess margin of cooling. Time and funding limitations did not permit this final development.

The following two sections discuss the development of the Vaporizing Ram Induction Combustor from Models No. 1 through the final Model No. 7 and present the results of comprehensive performance testing of the Model No. 6 combustor.

2. Development Chronology

Vaporizing Ram Induction Combustor modifications are listed in table III. The locations of these modifications are shown in figure 45. Table IV lists the effective open area and percent of total effective open area for each air entry station shown in figure 45, for all combustor models. Appendix E contains the test results for the vaporizer combustor, including a test results summary, exit temperature pattern, radial temperature profile, and circumferential temperature profile for each model tested. Figure 46 presents representative exit temperature radial profiles for each model tested.

a. Models No. 1 through 3

The Model No. 1 Vaporizing Ram Induction Combustor is illustrated in figures 47 and 48. A detailed design analysis is presented in Appendix B. Testing of Model No. 1 was conducted entirely at atmospheric pressure. Wall temperatures and fuel/air mixture temperatures along four of the vaporizer tubes were recorded. The vaporizer tubes showed local signs of overheating, as indicated by the values in figure 49 from test No. 018 conducted at cruise inlet temperature. Figure 50 shows a crack that developed in two of the vaporizer tubes due to flameholding and high local temperature gradients behind the center thermocouple. All thermocouples were then removed to avoid similar thermal stress concentrations.

Model Number		Firewall		Outer Liner				
		Dome Cooling Holes	Deflectors	Primary OD Gap	Intermediate OD Gap	Transition OD Gap	O/L Support Devices	Thu
	Location (Figure 59)	10	11	14		19	30	
1		None	None	0.052	None	0.052	None	
2				0.071		0.071	4 Bolts at Transition Gap	
3				0.104				1 A 2nd Sco Ram Add 2nd
4				0.092		0.092		Rem Beh Sco Fla 2nd
5		6 0.093 Dia Holes Between Nozzle Positions	6 Deflector Plates Added to Center Firewall	0.092			15 Support Beams Added	2 A Dil Sco Add Dil
6		2 0.093 Dia Holes Outside Tube Film Cooling Slots		0.071				
7		Plugged 6 0.093 Dia Holes	6 Deflector Plates Removed		0.096	0.096		

Model Number		Center Shroud						
		Vapor Tube OD	Vapor Tube ID	No. 1 Hole OD	No. 1 Hole ID	No. 2 Hole OD	No. 2 Hole ID	No. 3 Hole OD
	Location (Figure 59)	1	2	3	4	5	6	7
1	A_{eff}	8.256	8.256	15.321	15.321	7.816	7.816	7.572
	%	4.126	4.126	7.656	7.656	3.906	3.906	3.784
2	A_{eff}	8.256	8.256	26.376	15.321	7.816	7.816	7.572
	%	3.825	3.825	12.210	7.098	3.621	3.621	3.508
3	A_{eff}	8.256	8.256	18.121	15.321	--	--	--
	%	4.119	4.119	9.040	7.643	--	--	--
4	A_{eff}	8.267	8.267	6.480	6.480	--	--	--
	%	4.146	4.146	3.250	3.250	--	--	--
5	A_{eff}	8.267	8.267	6.480	6.480	--	--	--
	%	3.427	3.427	2.686	2.686	--	--	--
6	A_{eff}	8.267	8.267	6.480	6.480	--	--	--
	%	3.306	3.306	2.591	2.591	--	--	--
7	A_{eff}	8.267	8.267	6.480	6.480	--	--	--
	%	3.809	3.809	2.986	2.986	--	--	--

FOLDOUT FRAME

2

Table III. Modification Summary of the Vaporizing Ram Induction Combustor

		Inner Liner							Center Shroud		
ps	Inboard Scoop Tips	Liner Cooling Slots	Primary ID Gap	Intermediate ID Gap	Transition ID Gap	I/L Support Devices	Thumbnail Scoops	Inboard Scoop Tips	Liner Cooling Slots	Primary Air Slots	Vaporizing Tube Film Cooling Slot	OD Cooling Hole Area
	15	18	21		26	31	25	22	25	12,13	10	10
			0.071	None	0.071	None	None				None	
						4 Bolts at Transition Gap				Increased 15%		0.4567 $in.^2$
	Cut Back to First Vane		0.119				1 Added to 2nd Row of Scoops on Ramp. 0.3 Added Behind 2nd Scoop	Cut Back to First Vane				0.3860 $in.^2$
					0.119		Added 3 Behind 2nd Scoop and Flap Behind 2nd Ram Scoop				0.2 x 0.8	
f		0.500 x 0.625 in. Slots Added Behind 2nd and 3rd Ram Scoops					2 Added Between Dilution Ram Scoops. Scoops Added to Ramp of Dilution Scoops		0.500 x 0.625 in. Slots Added Behind 2nd and 3rd Ram Scoops			
			0.071									
				0.092	0.092						0.075 x 0.8	

le IV. Combustor Flow Areas and Percent Areas for Vaporizing Ram Induction Combustor Models

					Outer Liner							Inner Liner				
Center Liner Cooling	Tube Film Cooling	Bulkhead Cooling	Dome Slot OD	Dome Slot ID	Primary Cooling	OD No. 1 Scoop	OD No. 2 Scoop	OD No. 3 Scoop	OD Cooling	OD Trans Cooling	Intermediate Gap	Primary Cooling	ID No. 1 Scoop	ID No. 2 Scoop	ID No. 3 Scoop	Co
9	10	11	12	13	14	15	16	17	18	19	20	21	22	23	24	
--	--	--	13.097	13.097	6.405	11.927	10.735	10.735	--	6.459	--	6.631	11.927	10.735	10.735	
--	--	--	6.545	6.545	3.201	5.960	5.365	5.365	--	3.228	--	3.314	5.960	5.365	5.365	
--	--	--	13.097	13.097	8.748	11.927	10.735	10.735	--	8.817	--	6.631	11.927	10.735	10.735	
--	--	--	6.068	6.068	4.053	5.526	4.974	4.974	--	4.085	--	3.072	5.526	4.974	4.974	
6.286	--	--	13.097	13.097	12.793	11.927	10.735	10.735	4.446	8.817	--	11.039	11.927	10.735	10.735	
3.136	--	--	6.534	6.534	6.382	5.950	5.355	5.355	2.216	4.399	--	5.507	5.950	5.355	5.355	
7.974	11.932	--	13.097	13.097	11.300	11.927	10.735	10.735	4.446	11.419	--	11.300	11.927	10.735	10.735	
3.999	5.984	--	6.569	6.569	5.668	5.982	5.384	5.384	2.230	5.727	--	5.668	5.982	5.384	5.384	
7.974	11.932	10.435	13.097	13.097	11.300	11.927	10.735	10.735	20.158	11.419	--	11.300	11.927	10.735	10.735	2
3.305	4.946	4.326	5.429	5.429	4.684	4.944	4.450	4.450	8.356	4.733	--	4.684	4.944	4.450	4.450	
21.888	11.932	10.435	13.097	13.097	8.748	11.927	10.735	10.735	20.158	11.419	--	6.631	11.927	10.735	10.735	2
8.753	4.772	4.173	5.238	5.238	3.499	4.770	4.293	4.293	8.062	4.567	--	2.652	4.770	4.293	4.293	
21.888	4.475	--	13.097	13.097	8.200	11.927	21.470	--	6.738	11.911	11.911	8.721	11.927	21.470	--	
10.086	2.062	--	6.035	6.035	3.778	5.496	9.893	--	3.105	5.488	5.488	4.016	5.496	9.893	--	

2

FOLDOUT FRAME

r	Vaporizing Tube	Film Cooling Slot Flow Area	Diffuser	Major Modifications
	1,2	10		
				(1) Scoops Opposing
	1/4 in. Hole Added at Exit of Tube			(1) Distance Between Fuel Nozzle Exit and Flow Spreader Decreased From 0.250 to 0.156 in. (2) Shortened Center Tube by 2.10 in. Eliminated 3rd Row Air Slots
				(1) Inner Liner From Twin Ram Induction Combustor Model No. 5 (2) Outer Liner From Twin Ram Induction Combustor Model No. 5
		Reduced by 62.5%	Add No. 4 Wire Mesh	(1) Incorporated OD, ID Liners From Twin Ram Induction Combustor Model No. 19

ID Cooling	Intermediate Gap	OD T/D Bleed	ID T/D Bleed	Total
6	27	28	29	
96	--	1.598	1.598	200.105
47	--	0.798	0.798	100.00
96	--	1.598	1.598	215.841
10	--	0.740	0.740	100.00
96	--	1.598	1.598	200.459
41	--	0.797	0.797	100.00
07	--	1.598	1.598	199.380
71	--	0.802	0.802	100.00
07	--	1.598	1.598	241.239
21	--	0.662	0.662	100.00
07	--	1.598	1.598	250.049
62	--	0.639	0.639	100.00
95	6.495	1.598	1.598	217.019
93	2.993	0.736	0.736	100.00

Note:
1. C_d holes = 0.620
2. C_d scoops and slots = 1.00
3. A_{eff} ~ $in.^2$
4. All areas based on full 360-degree annulus.

FOLDOUT FRAME

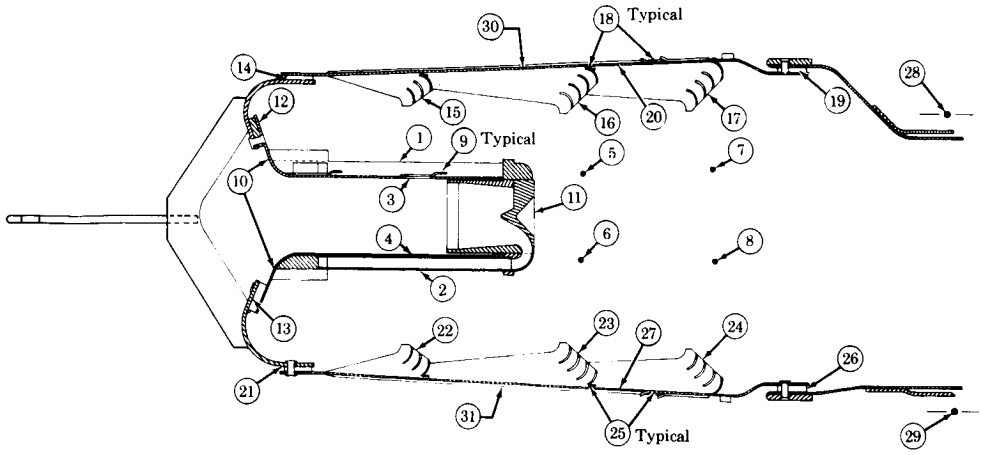

Figure 45. Location of Features of Vaporizing Ram Induction Combustor FD 22791

Exit temperature patterns (Appendix E) indicated local hot spots along the Model No. 1 OD liner, as the radial temperature profile in figure 46 substantiates. The centertube primary air slots and OD primary cooling gap were enlarged in the Model No. 2 combustor as listed in table III. The OD liner was also reindexed to oppose the scoops on the ID liner since the Model No. 1 had the scoops staggered due to an assembly misalignment.

Model No. 2 was tested at 2 and 6 atmospheres pressure. After 18 minutes of testing at cruise conditions the combustor OD vaporizer tubes were burned off 1-3/4 inches at their exit. Figures 51 and 52 show the vaporizer centertubes after test No. 24. Two factors contributed to the failure of the OD vaporizing tubes:

1. The increased quantity of centertube OD primary air caused combustion to be initiated very near the dome and increased the heat release in this area.

2. The decreased combustor pressure loss (4.95% at cruise) caused a reduction in cooling airflow through the vaporizer tubes.

Local burning of the ID vaporizer tubes was explained in a similar manner. Leakage at the 90-degree combustor segment end walls provided a combustible mixture in these regions causing damage to the ID vaporizer tubes at each end of the 90-degree sector.

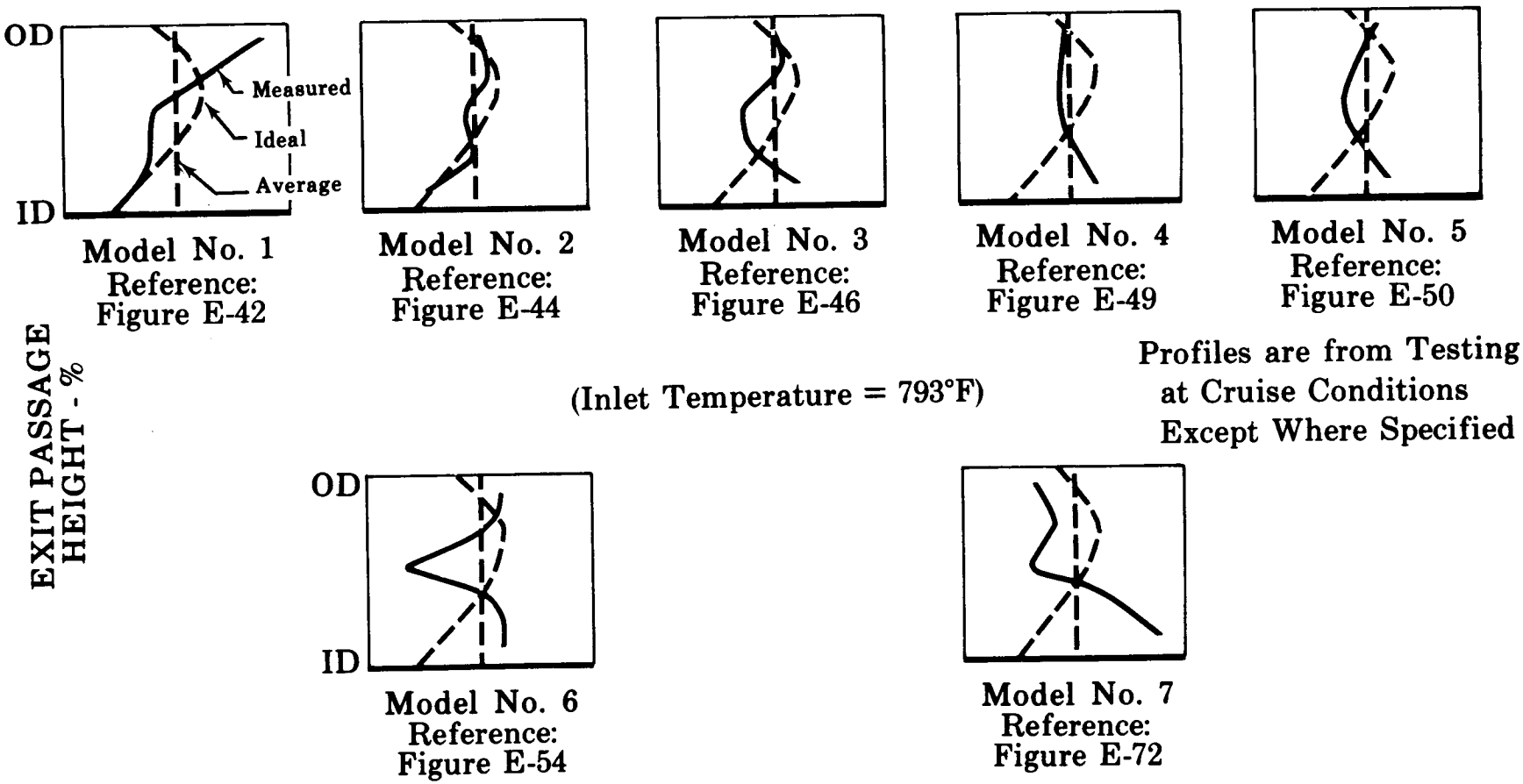

Figure 46. Exit Temperature Radial Profiles, Vaporizing Ram Induction Combustor

FD 21791 A

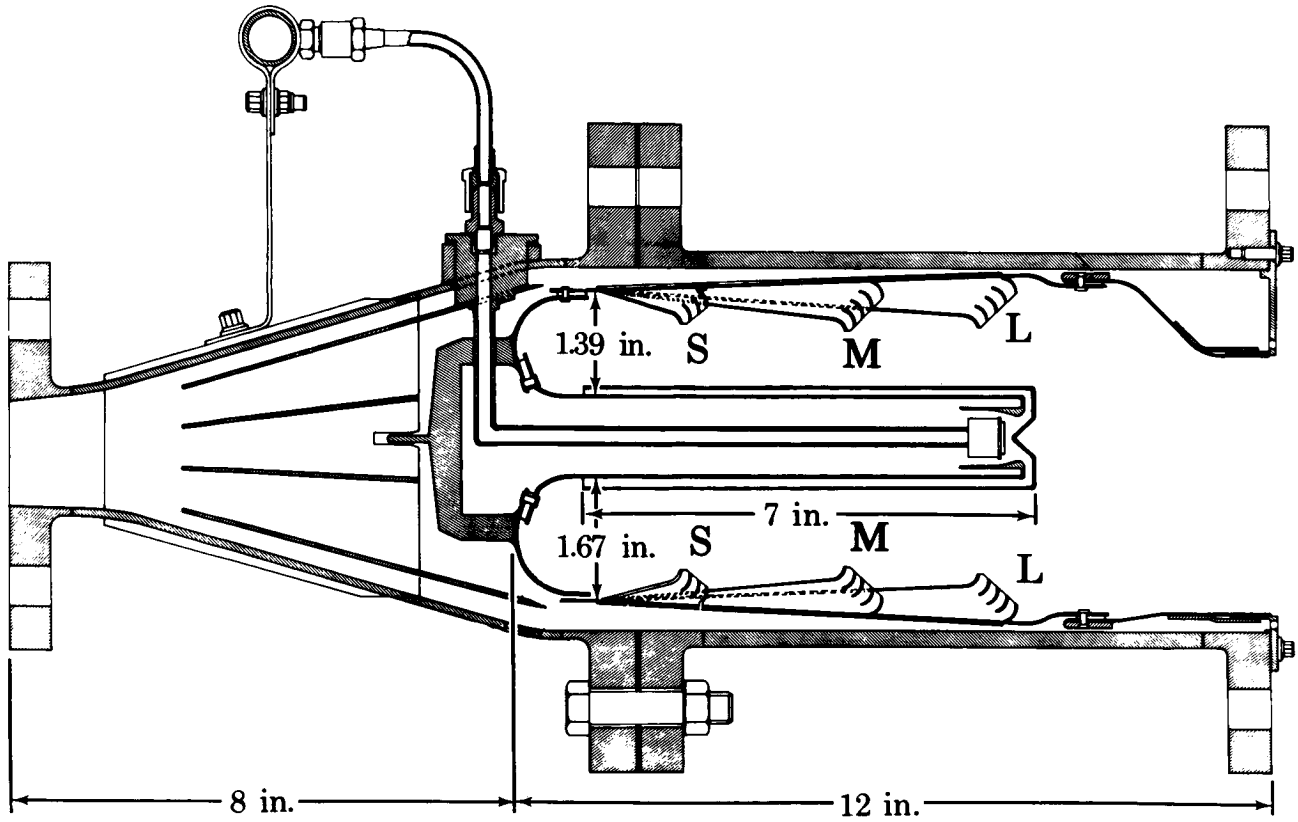

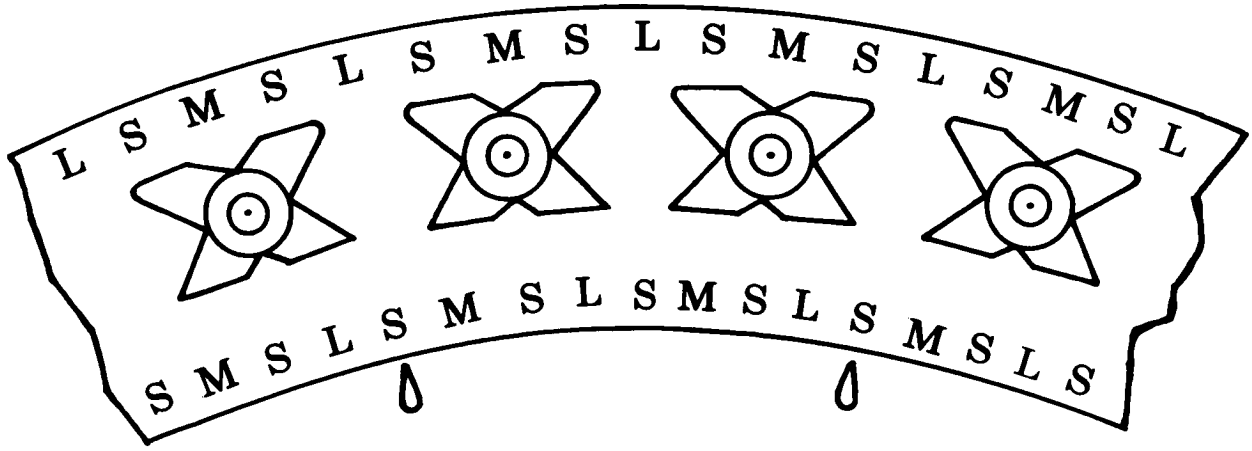

Linear Scoop Discharge Pattern

⊙ Fuel Nozzle Locations

Arrows Indicate Direction of Centertube Scoop Discharge Looking Upstream

Figure 47. Vaporizing Ram Induction Combustor, Model No. 1 FD 13461G

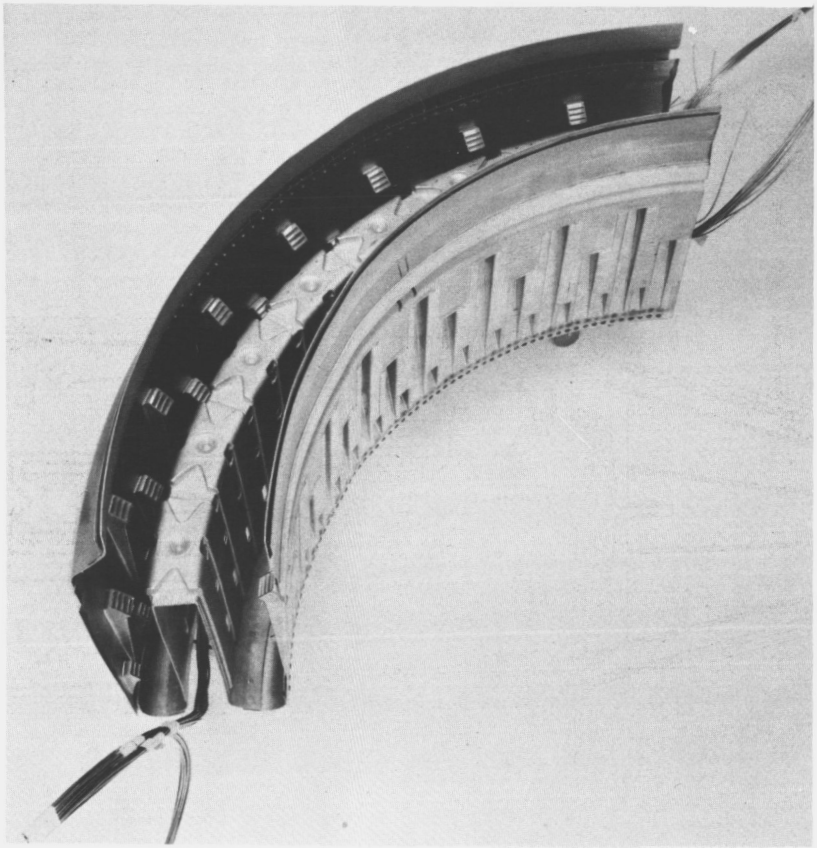

Figure 48. Vaporizer Ram Induction Combustor, Model No. 1 FE 54864

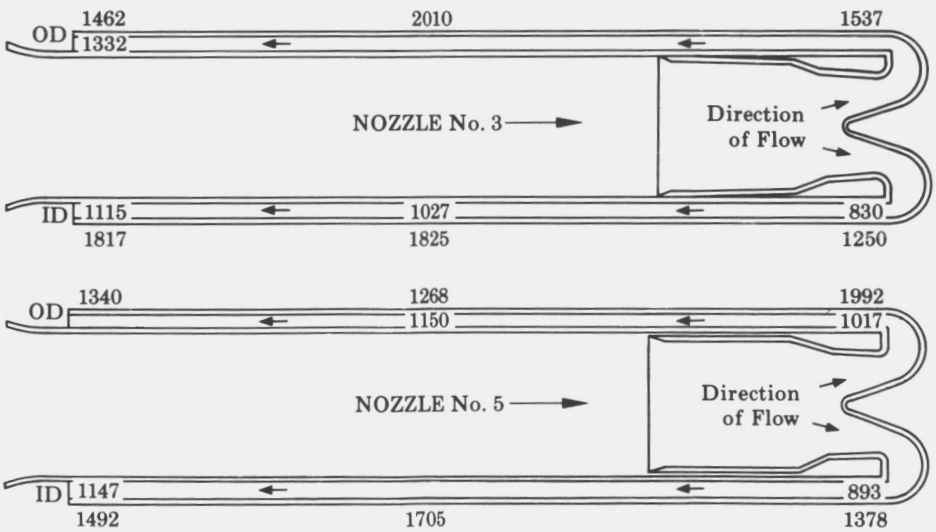

Figure 49. Vaporizer Tube Temperatures, °F Vaporizing Ram Induction Combustor, Model No. 1, Test No. 018 FD 14990A

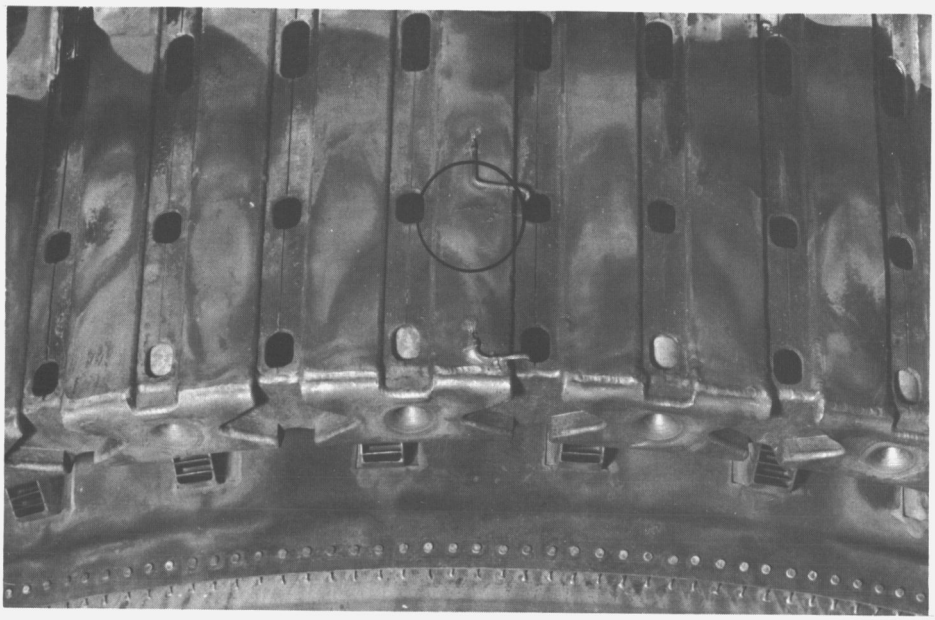

Figure 50. Vaporizing Ram Induction Combustor, Model No. 1, Showing Cracks FD 14993

Figure 51. Vaporizing Centertube OD After Test No. 024, Model No. 2 FE 56483

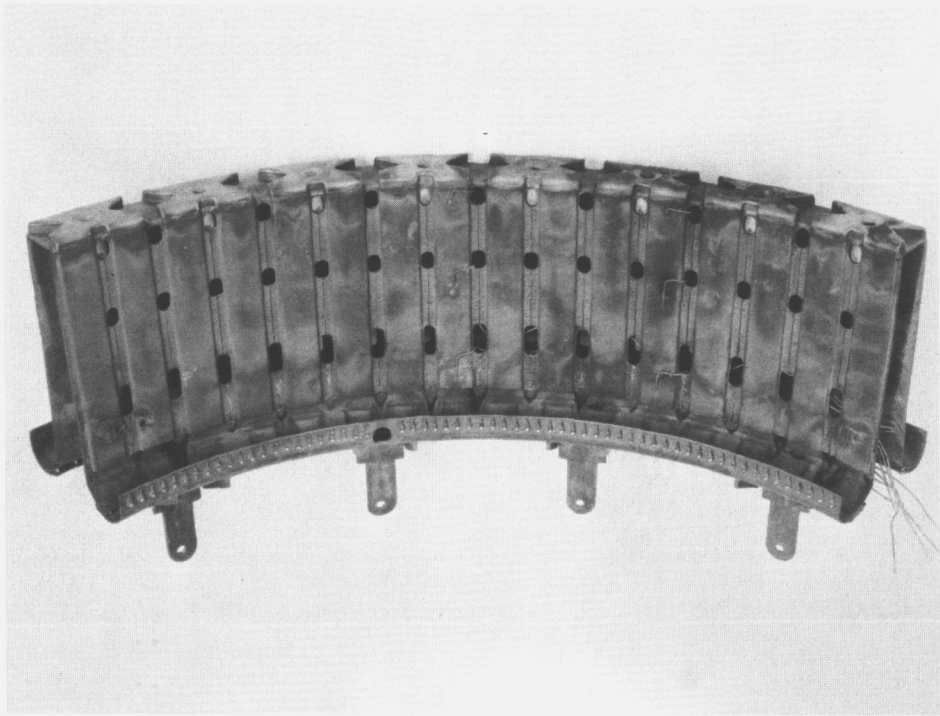

Figure 52. Vaporizing Centertube ID After Test No. 24, Model No. 2 FE 56480

The radial temperature profile for the Model No. 2 (figure 46) was cooler next to the OD liner. However, the cold center section remained.

The Vaporizing Ram Induction Combustor experienced localized liner warpage, as did the Twin Ram Induction Combustor. Inspection indicated possible flame holding behind the second and third rows of scoops.

Before further testing the Vaporizing Ram Induction Combustor was modified to the Model No. 3 configuration (table III). Modifications to the vaporizer assembly included shortening the entire centertube by 2.1 inches, intended to reduce the cold center profile by providing earlier mixing of the OD and ID chamber flows. Also, by reducing the length, and friction loss, of each vaporizer tube, the coolant flow would increase for the same area tube. One 0.25-in. diameter air inlet hole was added at the exit of each vaporizer tube to disperse the fuel-air mixture as it entered the combustion chamber.

The Model No. 3 combustor was tested at 90 psia in test No. 025. Extensive burning of the vaporizer tubes was sustained, as shown in figures 53 and 54. The radial profile continued to have a relatively cool center.

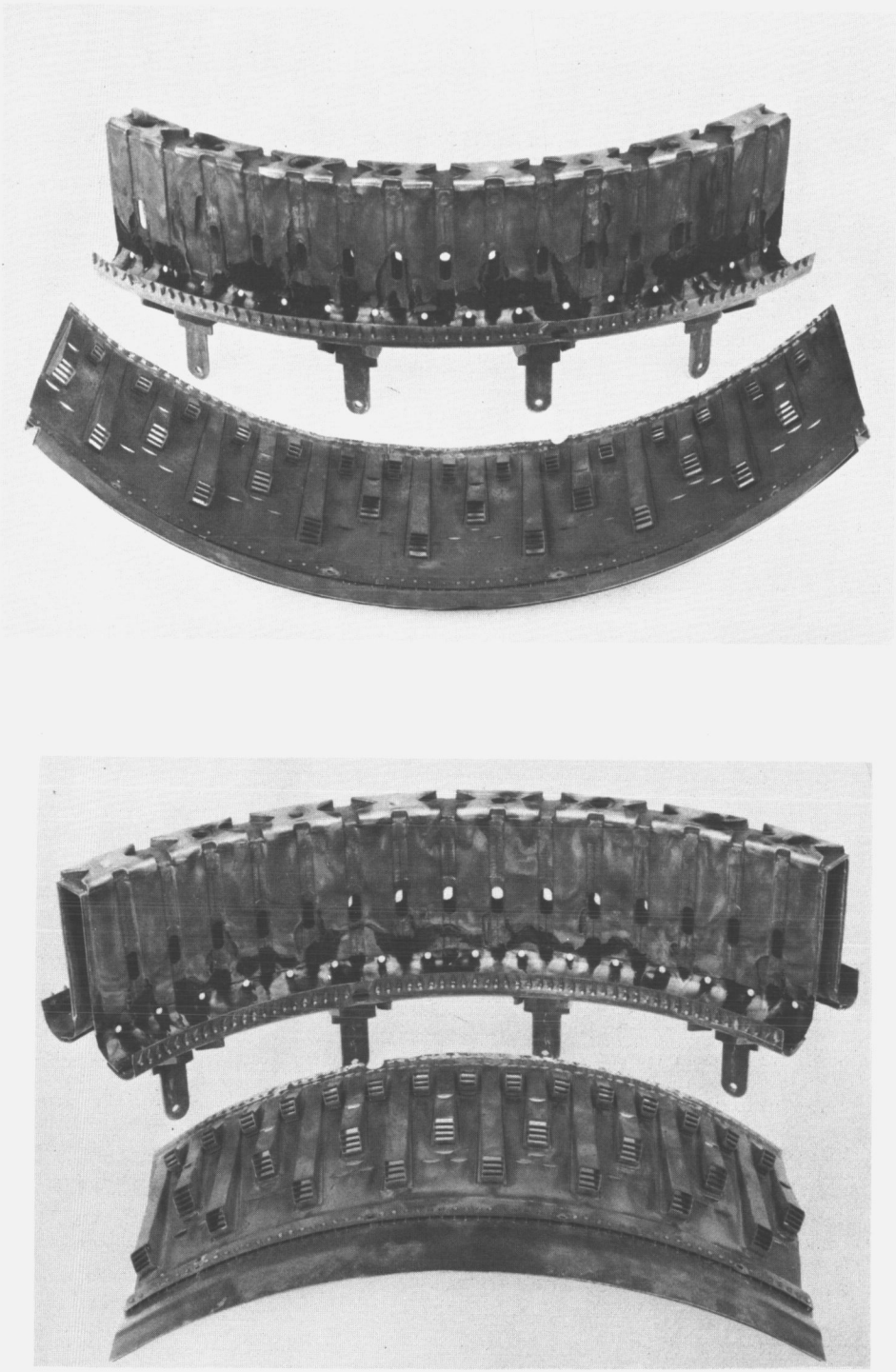

Figure 54. Vaporizing Ram Induction Combustor, Model No. 3, Centertube and Inner Liner Assemblies FE 56910

It was theorized that the vaporizer tube burning was the result of spontaneous reaction occurring within the vaporizer tube passages under high pressure conditions. A survey of the available literature (References 4, 5, 6, 7) on spontaneous ignition indicated this was possible at the existing temperature, pressure, fuel/air ratio, and residence time, but the findings were not conclusive.

The 0.25-inch air inlet holes, positioned at the exit of each vaporizer tube, could also have contributed to the tube burnout. Instead of breaking up and driving the rich fuel/air mixture toward the center of the combustor, the diluting air may have caused local stoichiometric regions at the vaporizer tube exit, with the tube exit lip providing flame holding.

b. Models No. 4 through 6

The modifications made to eliminate vaporizer tube burning included addition of film cooling to reduce the heat input to the walls. The vaporizer tube wall surface area was also reduced by shortening the tubes and decreasing tube width while maintaining the same flow area. These modifications were incorporated in the Model No. 4 combustor, shown in figure 55. The vaporizer tubes were reduced in length from five inches (Model No. 3) to three inches. The outer wall of the vaporizer tube was extended to the combustor dome, and a divider installed to divert the rich fuel/air mixtures sideways at the exit of the tube. Dome slots were positioned directly in line with each vaporizer tube to supply film-cooling air. Approximately 6% of the total airflow was used for this vaporizer tube film-cooling. A heat transfer analysis of the Model No. 4 vaporizing centertube is contained in Appendix B. Figures 56 and 57 show the complete Model No. 4 vaporizing centertube assembly prior to attaching the combustor liners.

The Model No. 4 combustor was tested at atmospheric pressure. The radial temperature profile was improved, but it was still cold in the mid-span and hot near the ID when compared to the design goal.

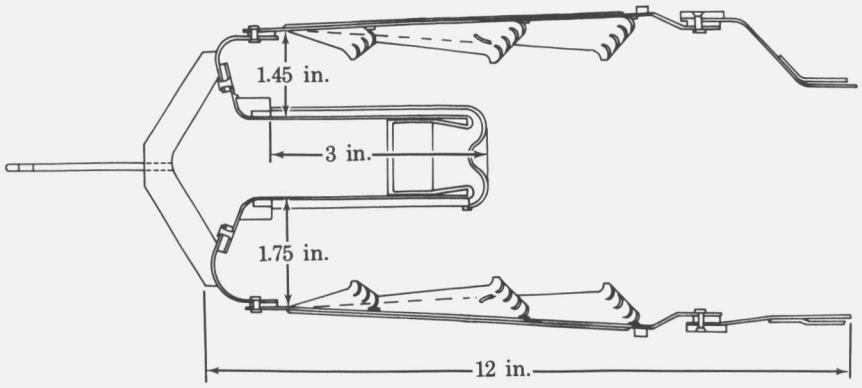

Figure 55. Vaporizing Ram Induction Combustor, Model No. 4 FD 21792A

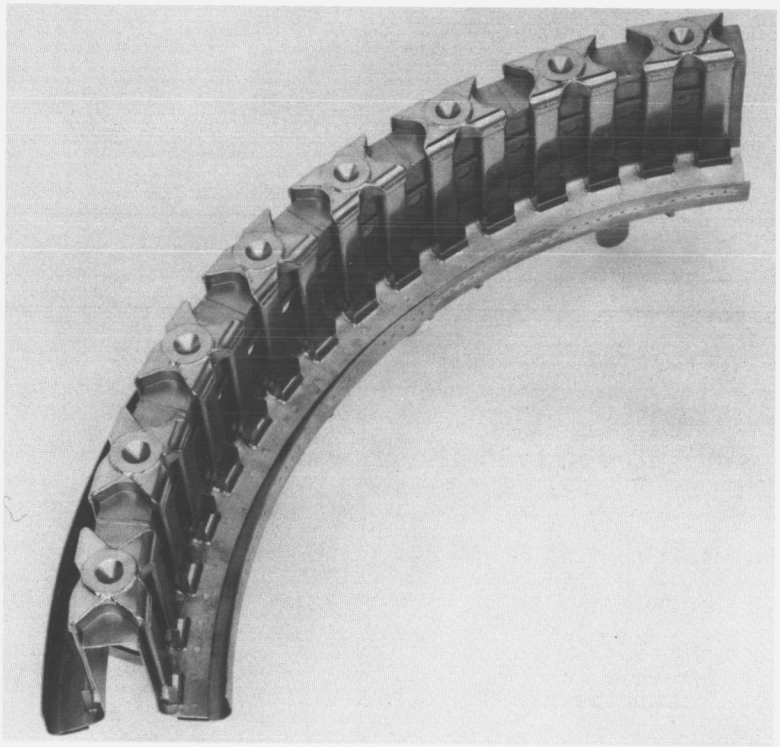

Figure 56. Vaporizing Ram Induction Combustor, Model No. 4, Centertube Assembly FE 63235

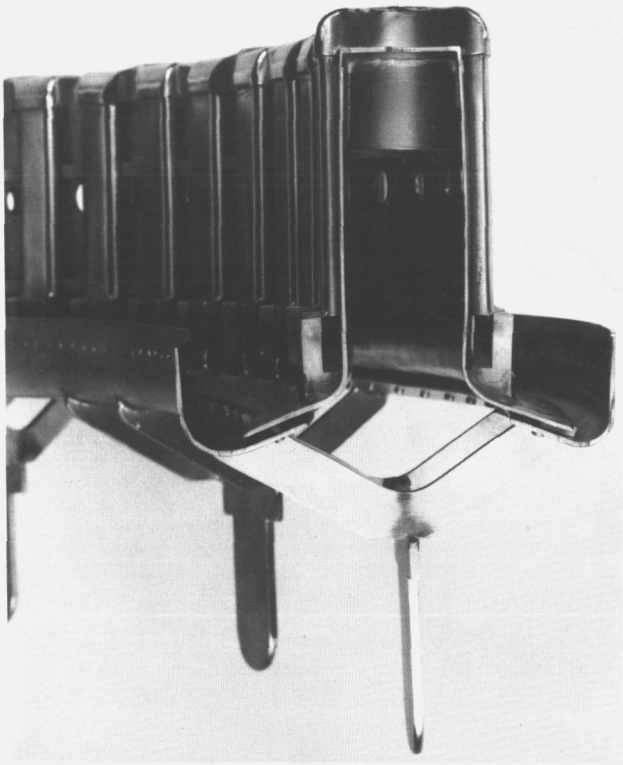

Figure 57. Vaporizing Ram Induction Combustor, Model No. 4, Centertube Assembly FE 63232

Post-test inspection of the combustor revealed no burned or badly distressed areas. However, some areas did show heat patterns that were indicative of potential durability problems. Figures 58 and 59 show the temperature patterns formed on the polished inner liner and vaporizing tube assemblies during test No. 052. These temperature patterns were obtained by color comparison with Hastelloy X material samples previously exposed to known temperature conditions. It was evident that the liners were operating hot behind the second row of ram induction scoops and that the vaporizer assembly was cool. However, discoloration indicated that somewhat higher temperature conditions (about 1300°F maximum) existed on the downstream bulkhead of the vaporizing centertube assembly between nozzle positions (not shown in figure 59).

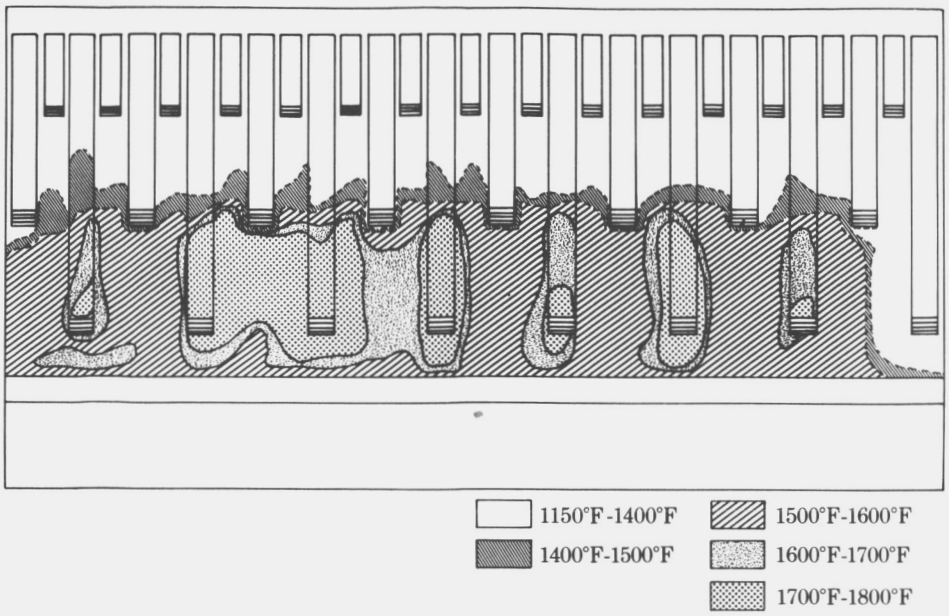

Figure 58. Temperature Coloration Pattern, Vaporizing Ram Induction Combustor, Model No. 4, Inner Liner FD 19120

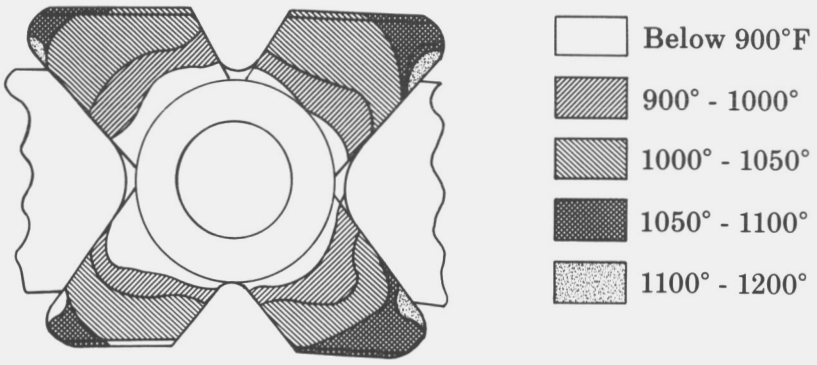

Figure 59. Temperature Coloration Pattern, Model 4, Vaporizing Ram Induction Combustor, Prevaporizing Splitter, Looking Upstream FD 19121

Before high pressure testing the combustor was modified to Model No. 5, table III, by the addition of liner cooling slots, strengthening beams, and heat baffles behind the centertube, as shown in figure 60.

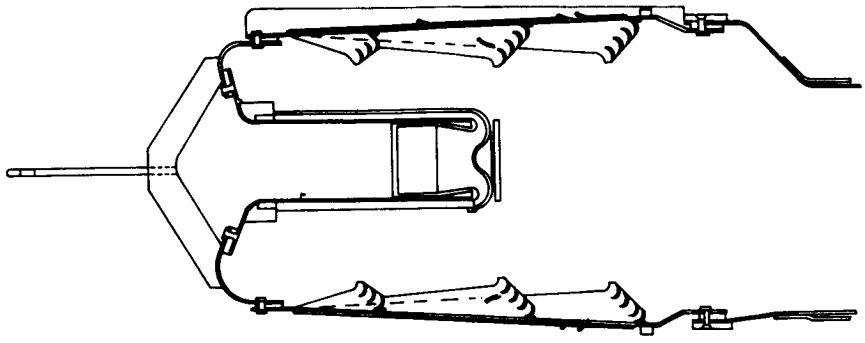

Figure 60. Vaporizing Ram Induction Combustor, Model No. 5 FD 19119

Inspection of Model No. 5 after testing at 75 psia showed moderate coke and soot deposits on the firewall and the outside of the vaporizer tubes near the tube exits. The outer liner showed some temperature distress behind the second row of scoops, with local liner bowing and scoop distortion. The vaporizer passages showed no evidence of hot spots or coking. The combustor exit temperature profile continued cool in the midspan region and hot near both liners.

To improve combustor liner durability and radial exit temperature profile, the combustor was modified to Model No. 6 (table III) by incorporating additional liner cooling. An inner annulus vaporizer tube was instrumented with thermocouples. Figure 61 through 63 present typical measured ID tube temperatures, which indicate that the design analysis was conservative. A maximum measured vaporizer tube temperature of 890°F at the test condition nearest the design condition (figure 63) compares with a maximum predicted tube temperature at the cruise design condition of 1393°F. The decrease in tube temperature with increasing fuel/air ratio was due to increased fuel vaporization and vaporizer tube flow at the higher fuel flows.

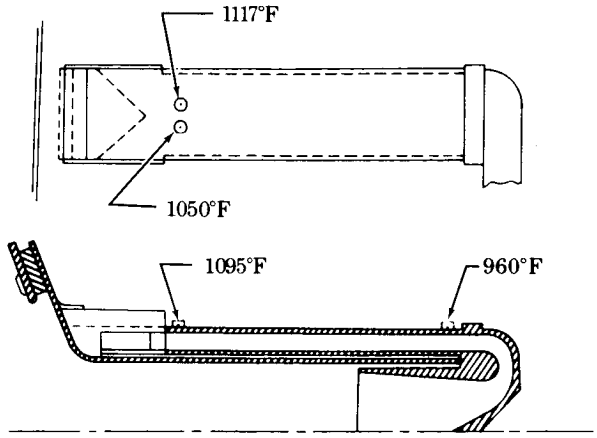

Inlet Total Temperature	1152°F
Inlet Total Pressure	59.18 psia
Reference Velocity	162.03 ft/sec
Overall F/A Ratio	0.0055
Combustor Exit Temperature	1479°F

Figure 61. Wall Temperatures on Instrumented ID Tube, Vaporizing Ram Induction Combustor, Model No. 6, Test No. 083 FD 19875B

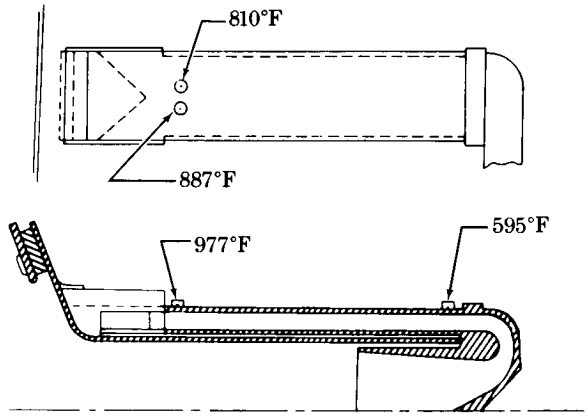

Inlet Total Temperature	1146°F
Inlet Total Pressure	59.40 psia
Reference Velocity	161.79 ft/sec
Overall F/A Ratio	0.0107
Combustor Exit Temperature	1790°F

Figure 62. Wall Temperatures on Instrumented ID Tube, Vaporizing Ram Induction Combustor, Model No. 6, Test No. 084 FD 19874B

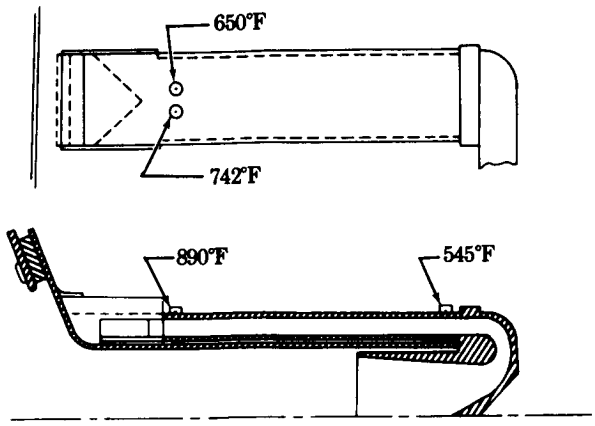

Inlet Total Temperature = 1153°F
Inlet Total Pressure = 59.41 psia
Reference Velocity = 160.34 ft/sec
Overall f/a Ratio = 0.0167
Combustor Exit Temperature = 2109°F

Figure 63. Wall Temperatures on Instrumented ID Tube, Vaporizing Ram Induction Combustor, Model No. 6, Test No. 085 FD 19876A

A typical radial temperature profile for Model No. 6 is shown in figure 46. The added firewall air holes eliminated the carbon deposits, but further increased the temperature profile cold midspan.

c. Model No. 7

Since the two scoop liners used in Twin Ram Induction Combustor Model No. 15 through 19 had excellent durability and provided a circumferential temperature profile close to the ideal, these liners were incorporated in the Model No. 7 Vaporizing Ram Induction Combustor (figure 64). Also, the film cooling slots in line with each vaporizer tube were reduced in area by 62.5% to reduce the cold midspan in the radial temperature profile. Additional minor modifications are listed in table III. Figure 46 shows the radial temperature profile for Model No. 7 compared to the previous models. Again the center midspan was cold, and the ID liner hot, compared to the design goal. The vaporizer tubes showed no evidence of hot spots or coking.

This concluded Vaporizing Ram Induction Combustor testing.

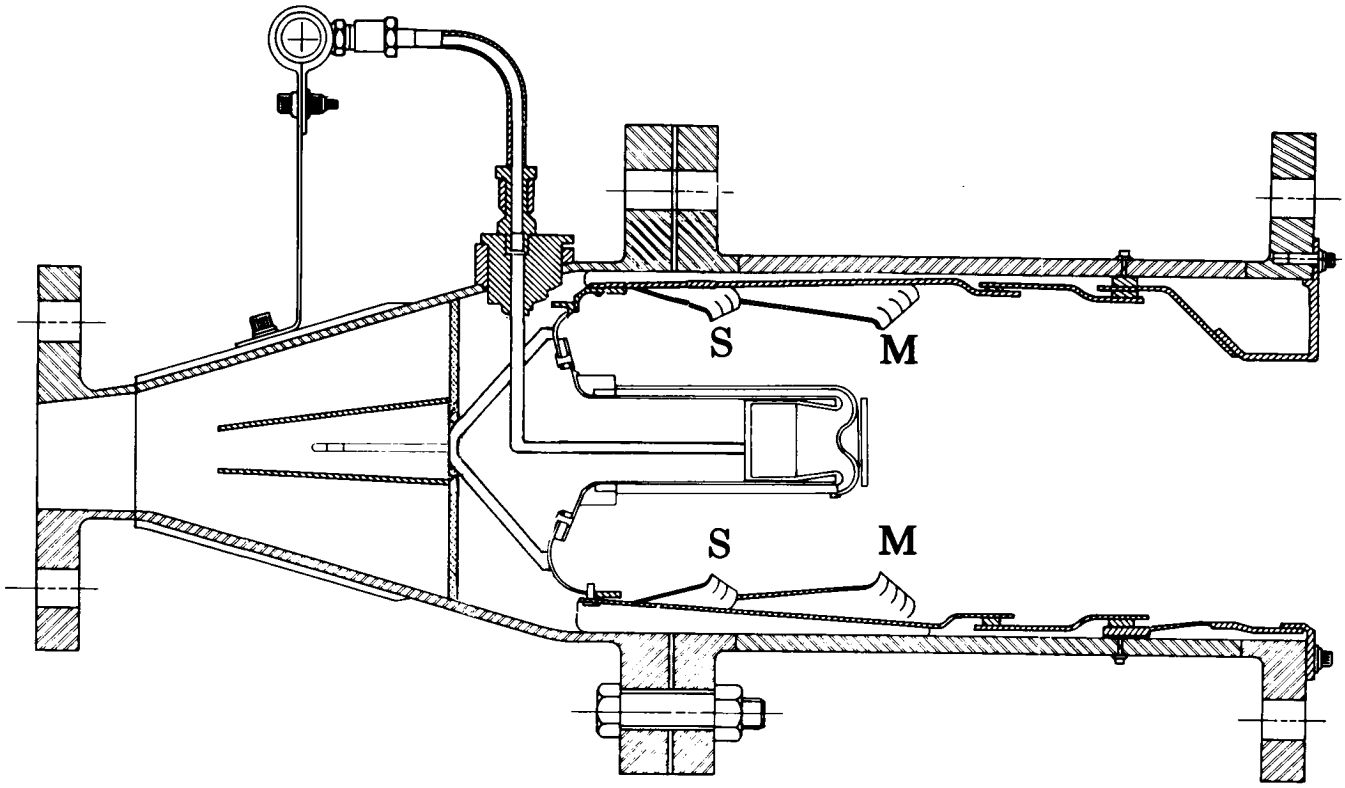

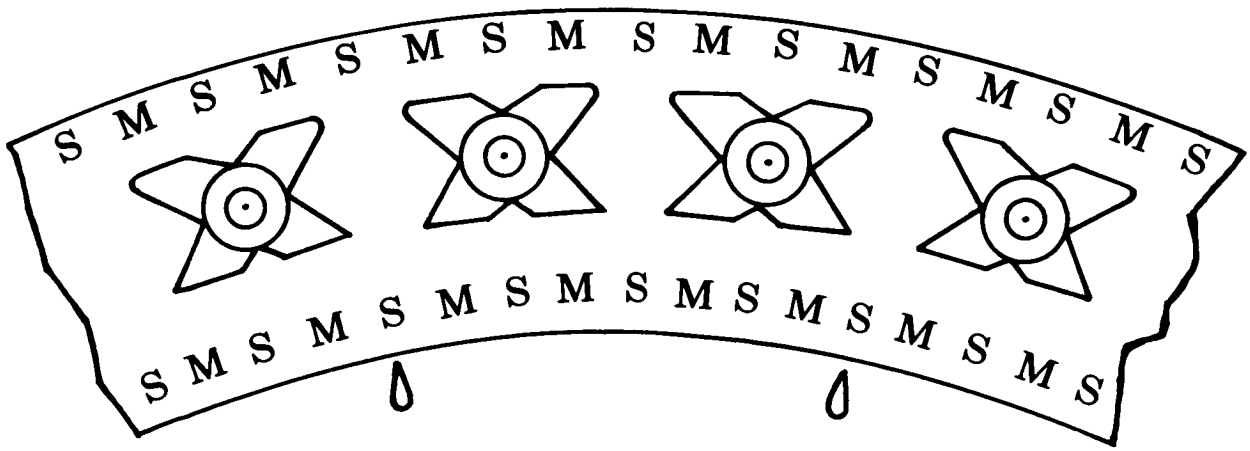

Linear Scoop Discharge Pattern

⊙ Fuel Nozzle Locations

Arrows Indicate Direction of Centertube Scoop Discharge Looking Upstream

Figure 64. Vaporizing Ram Induction Combustor, Model No. 7 FD 21793B

3. Performance of Models No. 6 and 7

Following development of the Model No. 6 Vaporizing Ram Induction Combustor, a performance investigation was conducted similar to that on the Model No. 14 Twin Ram Induction Combustor. Tests were conducted to determine the combustion efficiency, pressure loss, exit temperature pattern, and ignition capability.

a. Combustion Efficiency

Figure 65 presents the results of tests conducted to determine Model No. 6 combustion efficiency over a range of reference velocities (77, 101, and 156 ft/sec) at a combustor inlet temperature of 600°F and an inlet pressure of 60 psia. Performance data were taken at three combustor fuel/air ratios (0.0063, 0.0127, and 0.0201) at each reference velocity. The combustion efficiency was high (above 98%) at design conditions and fell off slightly during increased airflow operation.

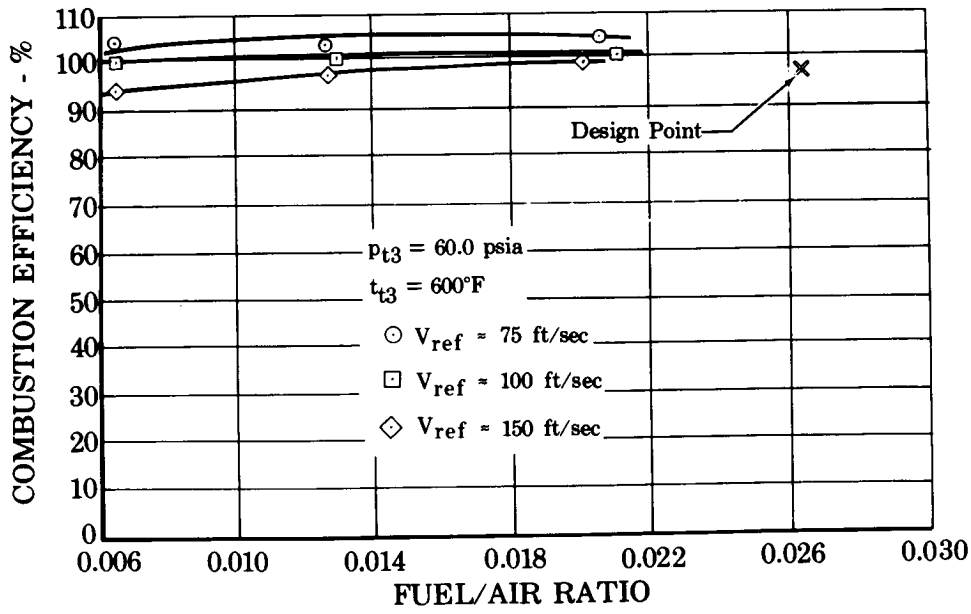

Figure 65. Vaporizing Ram Induction Combustor Model No. 6, Combustion Efficiency vs Fuel/Air Ratio at Takeoff FD 22775

The factors affecting combustion efficiency at low inlet temperatures were:

1. The degree of fuel atomization and dispersion into the vaporizing tubes from the fuel nozzles
2. The level of turbulent mixing of fuel and air within the vaporizing tubes
3. The residence time and mixing level of the fuel/air mixture within the combustor.

Increasing fuel/air ratio by increasing fuel flow at constant reference velocity resulted in increased combustion efficiency. This was attributed to improved nozzle fuel atomization and dispersion augmented by increased mixture turbulence within the tubes due to increased mass flow. This improved efficiency effect was most evident at high reference velocity when vaporizer tube mass flow was highest.

Conversely, when reference velocity was increased at constant fuel/air ratio, combustion efficiency decreased due to less residence time within the vaporizing tubes and the combustion chamber. This effect was most predominant at low fuel/air ratios where fuel nozzle atomization and dispersion were the poorest.

Figure 66 presents the results of tests conducted to determine combustion efficiency at 1150°F inlet temperature and 60 psia inlet pressure with reference velocities of 108, 161, and 187 ft/sec and fuel/air ratios of 0.0055, 0.0111, and 0.0168. At elevated inlet temperature, a greater degree of fuel vaporization occurred within the tubes, although combustion efficiency again was affected by the degree of fuel vaporization and the atomization level of the unvaporized fuel.

The combustion efficiency was highest at reference velocities near the design value of 150 ft/sec. At low reference velocities, with corresponding lower fuel flows, insufficient vaporization apparently resulted from poor initial fuel nozzle atomization. At reference velocities above 165 ft/sec, fuel atomization and vaporization time within the tubes was insufficient to maintain a high combustion efficiency level. This effect was compounded by poor initial nozzle atomization at low fuel/air ratios and by low combustor residence time at high reference velocities.

The combustion efficiency of the Model No. 7 combustor, shown plotted in figure 66 did not vary significantly from that of the Model No. 6 combustor.

In summary, the Vaporizing Ram Induction Combustor demonstrated high combustion efficiency operating near the vaporizing tube design conditions. When operating at conditions considerably away from the design point, combustion efficiency decreased as the probable degree of vaporization declined.

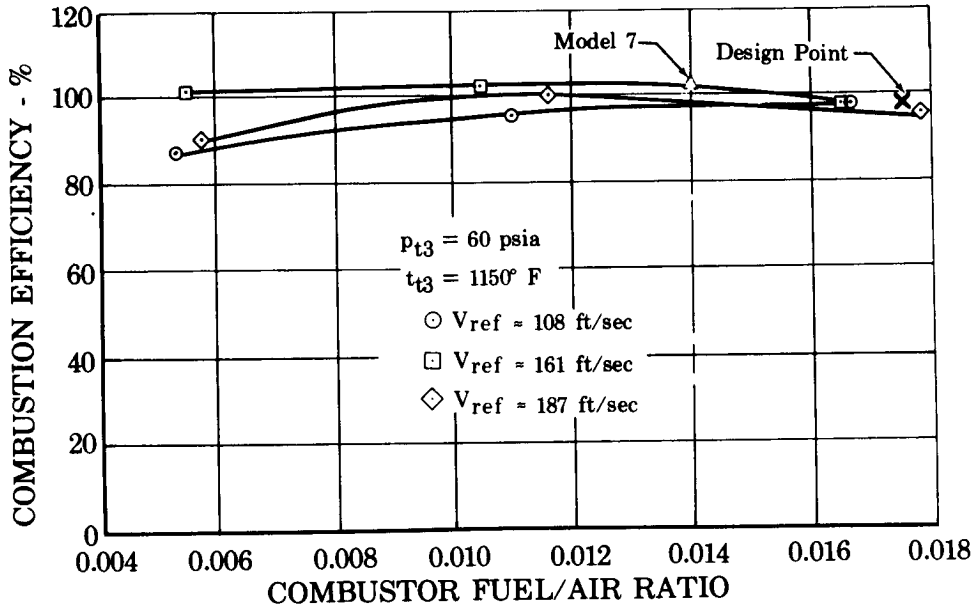

Figure 66. Vaporizing Ram Induction Combustor Model No. 6, Combustion Efficiency vs Fuel/Air Ratio at Cruise FD 22776

b. Combustor System Pressure Loss

Figures 67 and 68 present Model No. 6 combustor system pressure loss as a percentage of inlet total pressure, ($\Delta p/p$), as a function of diffuser inlet Mach number at the takeoff and cruise conditions. Figures 69 through 72 present pressure loss as a percentage of inlet dynamic pressure ($\Delta p/q$) as functions of diffuser inlet Mach number and combustor total temperature ratio at the takeoff and cruise conditions. The $\Delta p/q$ curves appear to vary in trend due to the expanded scale and the sensitivity of this parameter to data scatter.

The isothermal system loss was less than the design goal of 6.0% at 0.281 cruise inlet Mach number and 1150°F inlet temperature. Model No. 7 pressure loss data is also presented in figure 68.

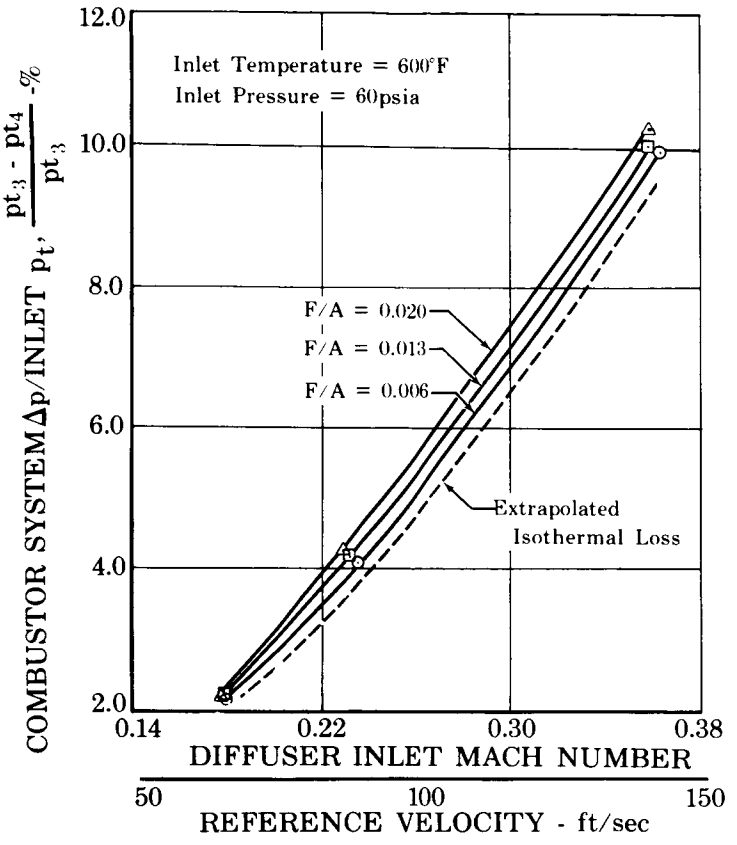

Figure 67. Vaporizing Ram Induction Combustor Pressure Loss at Takeoff FD 22977

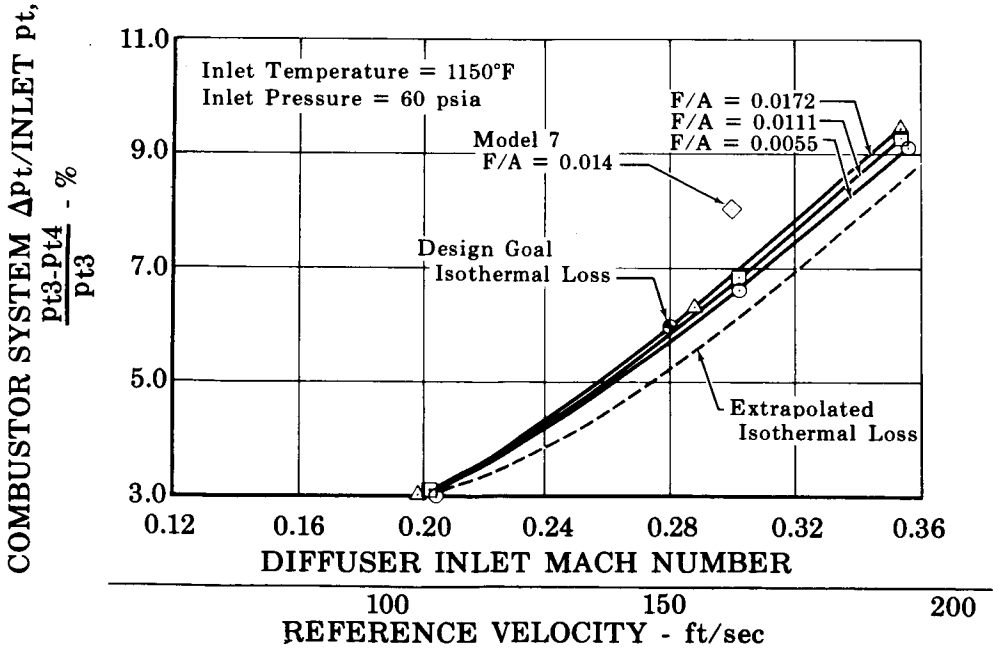

Figure 68. Vaporizing Ram Induction Combustor Pressure Loss at Cruise FD 22777

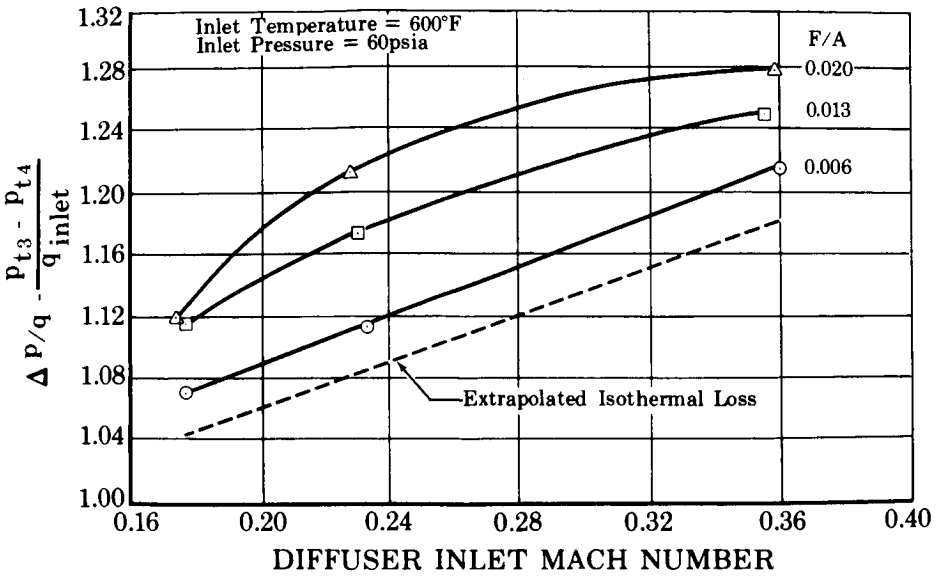

Figure 69. Vaporizing Ram Induction Combustor Pressure Loss Coefficient at Takeoff FD 22786

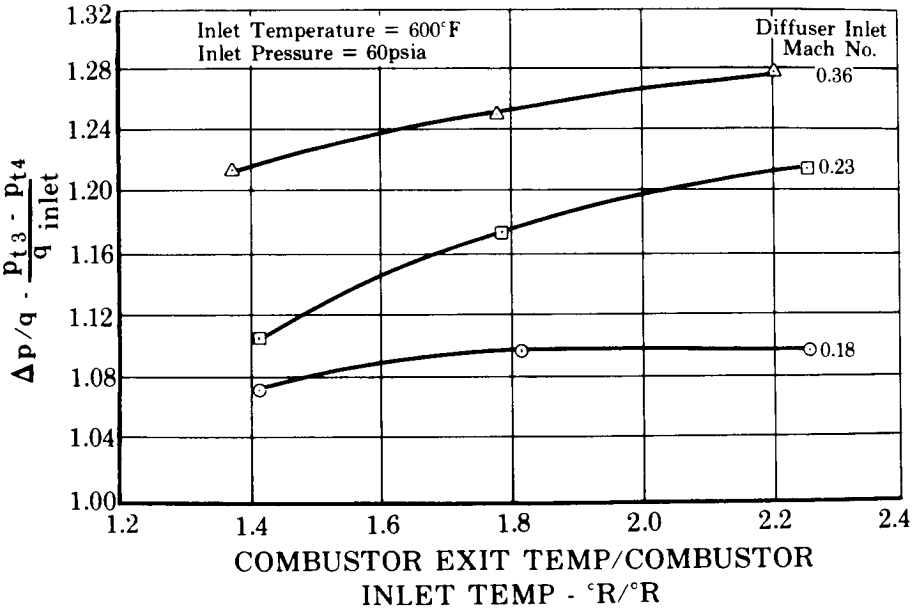

Figure 70. Vaporizing Ram Induction Combustor Pressure Loss Coefficient at Takeoff FD 22787

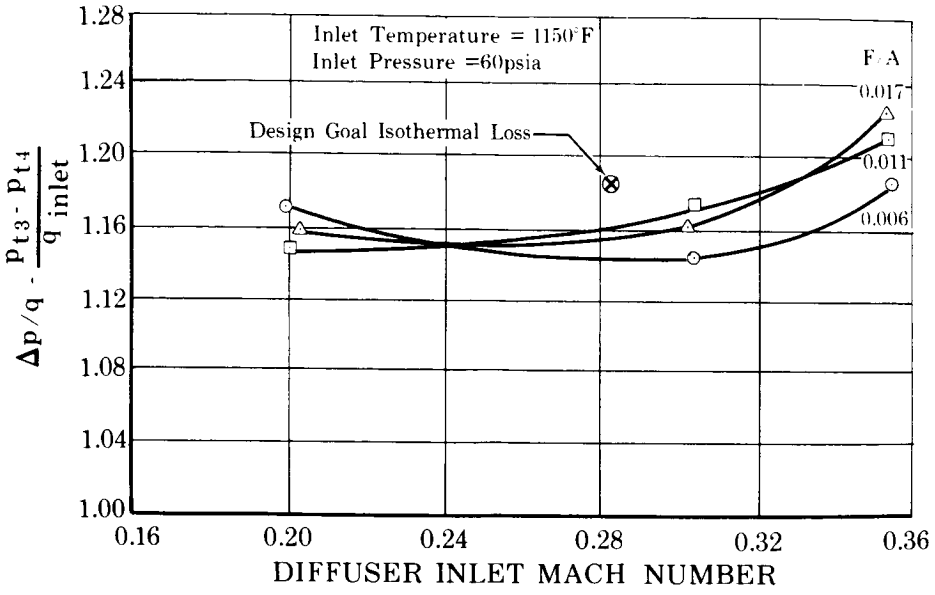

Figure 71. Vaporizing Ram Induction Combustor Pressure Loss Coefficient at Cruise FD 22788

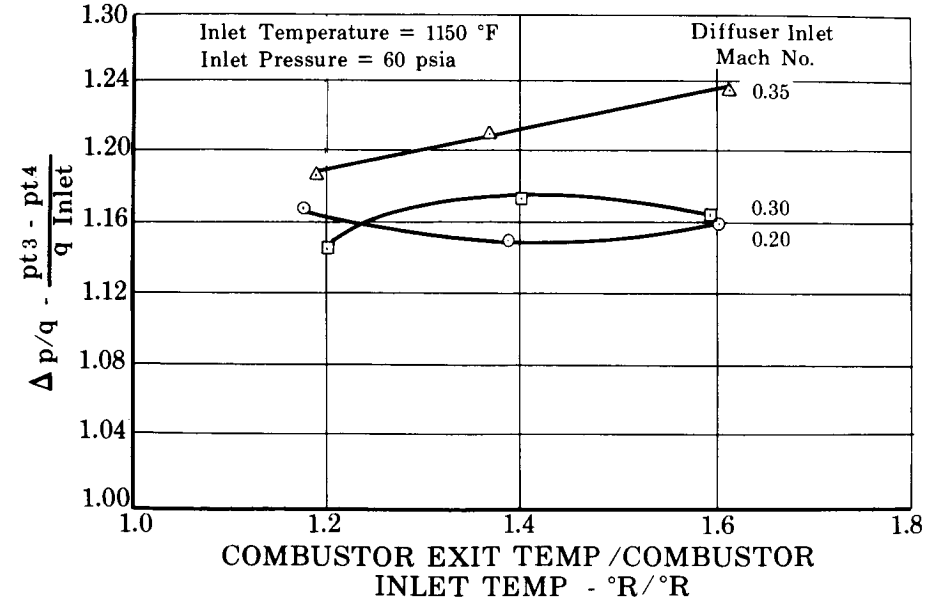

Figure 72. Vaporizing Ram Induction Combustor Pressure Loss Coefficient at Cruise FD 22789

c. Combustor Outlet Temperature Profile

Figures 73 and 74 present Model No. 6 combustor outlet radial temperature profiles at cruise and takeoff test conditions. This combustor demonstrated an exit temperature pattern factor ΔTVR value of 1.29 with D_{max} of 33.5% and $D_{R_{max}}$ of 16.8% at cruise conditions. At takeoff conditions (except average exit temperature was 1930°F), the values were: ΔTVR of 1.33, D_{max} of 45.8% and $D_{R_{max}}$ of 15.4%. The high $D_{R_{max}}$ and D_{max} values were due to a cold midspan in the radial profile.

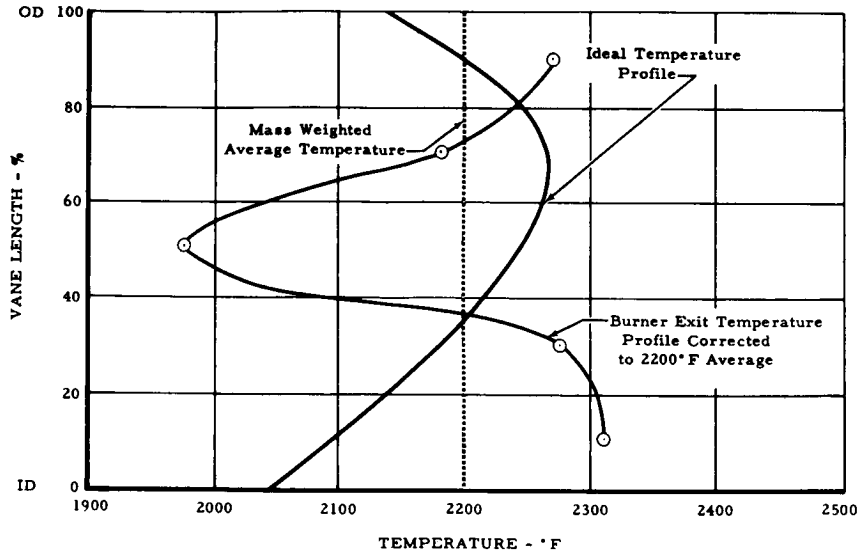

Figure 73. Cruise Radial Temperature Profile for Vaporizing Ram Induction Combustor, Model No. 6 FD 19903

Diffuser Inlet Total Pressure	59.41 psia
Diffuser Inlet Total Temperature	1153.3°F
Diffuser Inlet Mach Number	0.301
Combustor Exit Total Temperature	2109°F

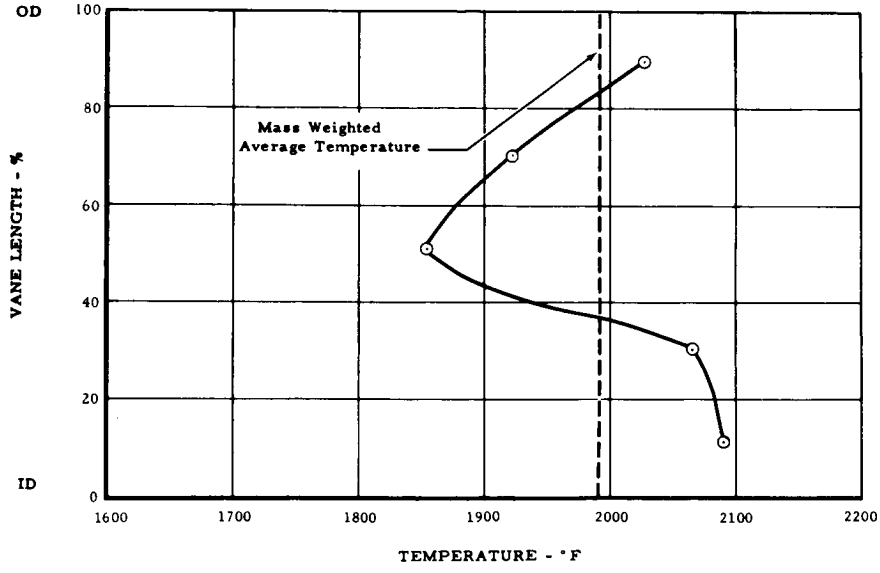

Figure 74. Takeoff Radial Temperature Profile for Vaporizing Ram Induction Combustor, Model No. 6 FD 19862

Diffuser Inlet Total Pressure	59.64 psia
Diffuser Inlet Total Temperature	603.3°F
Diffuser Inlet Mach Number	0.229
Combustor Exit Total Temperature	1930°F

The Model No. 7 combustor radial temperature profile at cruise is shown in figure 75. ΔTVR was 1.37, D_{max} was 49.4% and $D_{R_{max}}$ 32.7%.

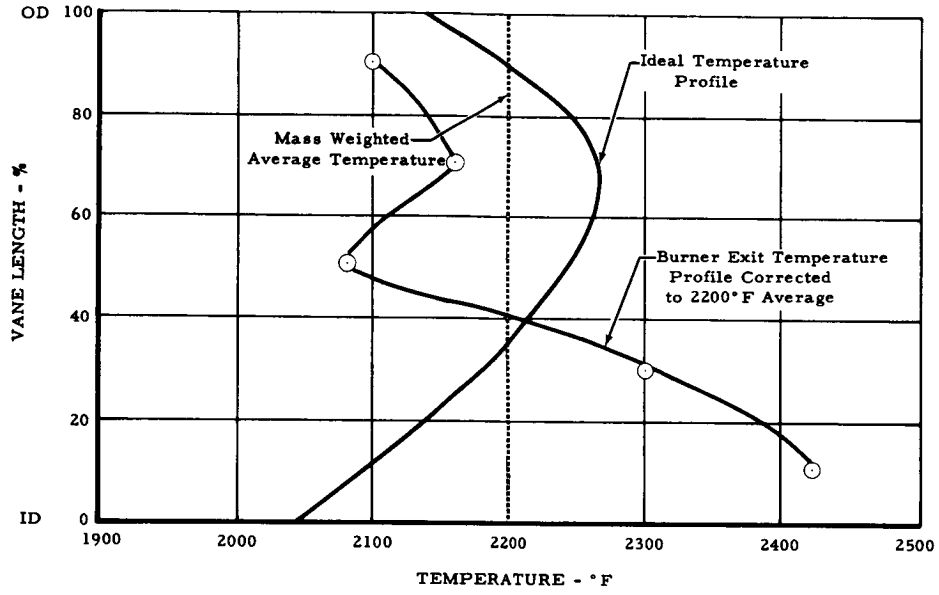

Figure 75. Cruise Radial Temperature Profile for FD 21828 Vaporizing Ram Induction Combustor, Model No. 7

Diffuser Inlet Total Pressure	60.61 psia
Diffuser Inlet Total Temperature	1150.8°F
Diffuser Inlet Mach Number	0.290
Combustor Exit Total Temperature	2010°F

Program effort was ended prior to correction of the radial profile cold midspan. Experience gained through the development of the Twin Ram Induction Combustor indicated that the borders of the exit temperature profile could be controlled by varying the size of the transition cooling gap. However, the additional film cooling required on the vaporizer tubes resulted in a cold midspan temperature profile, but provided good durability at a reduced level of vaporization. It is considered that the Vaporizing Ram Induction Combustor could have achieved the desired temperature profile with moderate additional development.

d. Combustor Durability

Neither the Model 6 nor Model 7 combustors exhibited durability problems over the length of time they were tested. Since endurance tests were not run, no indication of potential combustor life was attained.

e. Ignition

Ignition tests were made with both spark ignition and TEB injection as with the Model No. 14 Twin Ram Induction Combustor. The igniter and TEB injection locations are shown in figure 76.

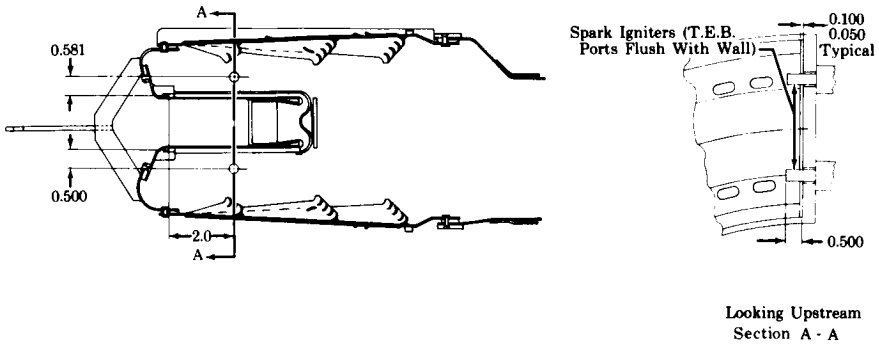

Figure 76. Location of Spark Igniters and TEB Injection Ports on Vaporizer Combustor, Model No. 6 FD 22790

Although insufficient data were available to define complete ignition limits of the Model No. 6 Vaporizing Ram Induction Combustor for any single inlet condition, it was considered that the combustor had potentially good ignition capability for a vaporizing combustor without an auxiliary ignition fuel nozzle.

Limited ignition testing indicated that, at an inlet temperature of 250°F and a reference velocity of 90 ft/sec ± 20 ft/sec, ignition could be obtained at fuel/air ratios above 0.004 at a pressure level of 23 psia, and fuel/air ratios of 0.009 to 0.015 at 14.7 psia. The approximate ignition envelope obtained appeared to limit ignition at the above inlet conditions to pressures above 13 psia.

SECTION V
CONCLUSIONS

A. TWIN RAM INDUCTION COMBUSTOR

The following conclusions were reached concerning the Twin Ram Induction Combustor.

1. The final Model No. 19 combustor demonstrated the following performance compared to the programs goals:

	Goal	Achieved at Cruise Conditions	Achieved at Sea Level Takeoff Conditions
Combustion Efficiency, %	98	100	100
Overall Combustion Total Pressure Loss, %	6.8 (cruise)	6.74	4.66
Maximum Local Excess of Exit Temperature Over Desired Level, °F	100	167	326

2. Visual inspection of the Model No. 19 combustor after testing did not indicate durability problems.

3. The Model No. 19 combustor demonstrated performance and potential durability have shown it to be suitable for developmental operation in the advanced engine for which it was designed.

4. The Twin Ram Induction Combustor may have potential for burning length reduction from the existing 12 inches.

5. Attainment of a more uniform circumferential temperature profile was limited by diffuser flow variation.

6. Satisfactory ignition capability was not demonstrated; however, it is considered that adequate ignition capability could be readily developed.

B. VAPORIZING RAM INDUCTION COMBUSTOR

The following conclusions were reached concerning the Vaporizing Ram Induction Combustor.

1. The Model No. 6 combustor demonstrated the following performance compared to the program goals:

	Goal	Achieved at Cruise Conditions	Achieved at Sea Level Takeoff Conditions
Combustor Efficiency, %	98	98	99
Overall Combustor Total Pressure Loss, %	6.8 (cruise)	6.02	4.16
Maximum Local Excess of Exit Temperature Over Desired Level, °F	100	409	609

2. Visual inspection of the Vaporizing Ram Induction Combustor at the conclusion of testing did not indicate durability problems.

3. Additional development of the Vaporizing Ram Induction Combustor is required to achieve the desired exit temperature profile.

4. Ignition capability was poor compared with conventional combustors, but could be improved with further development.

APPENDIX A
NOMENCLATURE

Symbol	Description	Unit
A	Area	$in.^2$
a	Sonic velocity	ft/sec
A_t	Area of throat	$in.^2$
A_w	Surface area of vaporizer tubes	$in.^2$
b	Width of vaporizer tube	in.
C	Circumference	in.
C_C	Cold circumference	in.
C_d	Coefficient of discharge	
C_H	Hot circumference	in.
C_p	Specific heat at constant pressure	$Btu/(lb_m)(^\circ R)$
C_v	Specific heat at constant volume	$Btu/(lb_m)(^\circ R)$
D	Diameter	in.
D	Hydraulic diameter	in.
D	Difference between local temperature and the ideal profile at the same percent span	
D_{max}	Maximum difference between local temperature and the ideal profile at the same percent span	
D_o	Venturi reference diameter	in.
D_R	Difference between the average temperature profile and the ideal profile at the same percent span	
D_{Rmax}	Maximum difference between the average temperature profile and the ideal profile at the same percent span	
e	Coefficient of linear expansion multiplied by temperature difference	in./in.
F	Gray body view factor	
F/A	Fuel/air ratio	$\frac{lb_m/sec}{lb_m/sec}$
g	Gravitational constant, 32.17	$lb_m\text{-}ft/lb_f\text{-}sec^2$
H	Enthalpy	Btu/hr

Symbol	Description	Unit
h	Convection heat transfer coefficient	$Btu/hr\text{-}ft^2\text{-}^\circ R$
H/C	Hydrogen to carbon mass ratio	lb_m/lb_m
J	Energy-work constant	ft-lb/Btu
K	Thermal coefficient of expansion	$\frac{in./in.}{^\circ R}$
k	Thermal conductivity	$Btu/hr\text{-}ft\text{-}^\circ R$
l	Distance from exit of tube to theoretical starting point of boundary layer	in.
l	Length	in.
l	Length of combustion air slots	in.
L	Radiation beam length	in.
L	Scoop side length	in.
M	Mach number	
m_j	Mass fraction of chemical compound j	
N	Number of combustion air slots	
N_j	Mole fraction of chemical compound j	
N_{pr}	Prandtl number	
p	Pressure	$lb_f/in.^2$
p_{st}	Static pressure	$lb_f/in.^2$
p_t	Total pressure	$lb_f/in.^2$
Q	Heat flux	Btu/hr
q	Heat flux per unit area	$Btu/hr\text{-}ft^2$
q	Dynamic pressure	$lb_f/in.^2$
R	Gas constant	$ft\text{-}lb/(lb_m)\,(^\circ R)$
r	Radius	in.
R_j	Reynolds number evaluated at a characteristic length of (j)	
SLTO	Sea level takeoff	
T	Temperature	$^\circ R$
t	Temperature	$^\circ F$
T_o	Venturi reference temperature	$^\circ R$
T_t	Total temperature	$^\circ R$
V	Velocity	ft/sec

Symbol	Description	Unit
V_b	Axial velocity in combustion chamber at end of forced vortex	ft/sec
V_{ref}	Combustor reference velocity	ft/sec
$\overline{V}$	Velocity of forced vortex at radius r	ft/sec
w	Width	in.
W_{ext}	External work per unit time	ft-lb_f/hr
w	Mass flow rate	lb_m/sec
X	Specific humidity ratio	lb_m(water)/lb_m(dry air)
x	Distance along vaporizing tube starting from entrance of tube	in.
y	Distance from stagnation point to exit of vaporizing tube	in.
α	Radiative absorptivity	
γ	Specific heat ratio	
ΔH	Change of enthalpy per unit time	Btu/hr
ΔKE	Change of kinetic energy per unit time	Btu/hr
ΔPE	Change of potential energy per unit time	Btu/hr
Δp	Differential pressure	$lb_f/in.^2$
ΔTVR	Temperature rise variation ratio	
δ	Boundary layer thickness	in.
ϵ	Emissivity	
η	Efficiency	
ξ	Distance measured from stagnation point toward entrance of vaporizer tube	in.
θ	Angle of arc	Radians or degrees
θ	Angle at which flow impinges on tube	degrees
λ	Defined by equation (19)	(Btu/hr-ft-°R)(ft-hr/lb_m)$^{0.8}$
μ	Dynamic viscosity	lb_m/ft-hr
ρ	Density	lb_m/ft^3
σ	Stefan-Boltzmann's constant	Btu/hr-ft^2-°R^4

Symbol	Description
Subscripts	
a	Air
av	Evaluated at average temperature
c	Convection or combustion
cs	Center shroud
d	Duct
F	Fuel
f	Evaluated at film temperature
g	Hot gases
h	Hole or slot
HB	Heater burner
i	Main combustor inlet
i	Inner
M	Mixture
MB	Main combustor
o	Outer
r	Radiation
st	Static
sat	Saturation temperature
SL	Starting length
t	Total
t	Homogeneous mixture at a particular point
t	Venturi throat
u	Outer skin
w	Surface
w	Wall
w	Water
0	Venturi inlet
1	Heater burner inlet
2	Heater burner outlet
3	Main combustor diffuser inlet
4	Main combustor exit
*	Signifies state at which the Mach number is unity.

APPENDIX B
DESIGN ANALYSIS

A. RIG DESIGN ANALYSIS

This section presents the calculation made to size the venturi throat area and the heater burner effective flow area.

The B-2 stand airflow capacity curve shown in figure B-1 indicated that the required rig airflow of 24 lb/sec could be obtained at rig inlet pressures up to 105 psia. A maximum operating pressure of 100 psia was selected to ensure that test conditions could be met when running under adverse atmospheric conditions. Therefore, no more than 10 psi, or 10% of the inlet pressure, pressure drop was available for the flowmeter, heater burner, plenum chamber, and instrumentation sections to test at the originally specified maximum pressure of 90 psia.

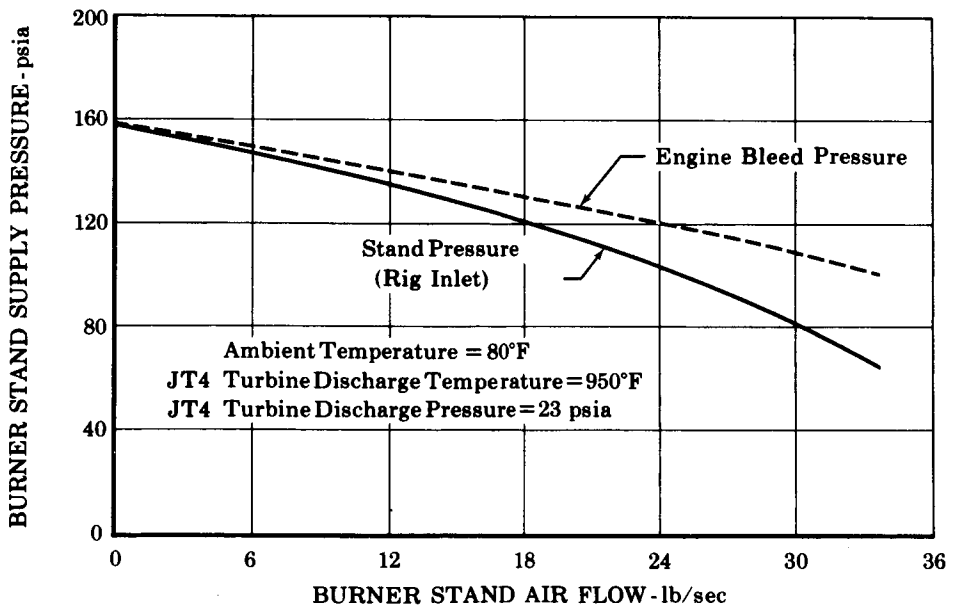

Figure B-1. B-2 Test Stand Slave Engine Compressor Bleed Capacity FD 12598A

To meet this requirement, the rig components were designed for the following pressure losses.

Component	Pressure Loss, %
Combined Plenum Chamber and Instrumentation Section	1.0
Heater Burner	4.0
Venturi Flow Meter	5.0
Total	10.0

The heater burner loss of 4.0% was considered to be the minimum practical value consistent with providing uniform inlet temperature to the test combustor. The heater burner loss was minimized to allow the greatest possible pressure loss for the venturi flow meter. This allowed sizing of the venturi for operation at relatively high Mach number where the high differential between total and static pressures provided greater reading accuracy.

Using these pressure loss values, the inlet pressures of the various sections were computed as follows:

1. Plenum chamber inlet, or heater burner outlet

$$\frac{P_{t2} - P_{t3}}{P_{t2}} = 0.01$$

$$P_{t2} = \frac{P_{t3}}{0.99} = \frac{90}{0.99} = 90.90 \text{ psia.}$$

2. Heater burner inlet, or venturi outlet

$$\frac{P_{t1} - P_{t2}}{P_{t1}} = 0.04,$$

$$P_{t1} = \frac{90.90}{0.96} = 94.69 \text{ psia.}$$

3. Venturi inlet

$$P_{to} = 100 \text{ psia.}$$

The venturi throat was then sized assuming the pressure loss in the rounded entrance was negligible. Based on previous experience, the pressure loss in the venturi diffuser section was assumed to be 20% of the throat velocity head. A heater burner case of 16 inches was selected to allow the use of a J58 main burner can for the heater burner. Therefore, the exit diameter of the venturi diffuser was 16 inches and the mass flow parameter at the diffuser exit was calculated as:

$$\frac{w\sqrt{T_{t1}}}{A_1 P_{t1}} = \frac{24\sqrt{1160}}{\pi/4(16)^2 (94.69)} = 0.0428$$

From the compressible flow functions the Mach number at this point is found to be 0.046, and $p_{st1}/p_{t1} = 0.9985$. The value of velocity head, q, at the venturi exit was negligible.

Therefore:

$$0.20\, q_t = 0.05\, p_{t_t}$$

$$0.20\left(p_{t_t} - p_{st_t}\right) = 0.05\, p_{t_t}$$

$$\frac{p_{st_t}}{p_{t_t}} = 0.75$$

The compressible flow functions then gave

$$M_t = 0.654$$

and

$$A_t/A_* = 1.131$$

Since,

$$M_1 = 0.046$$

$$A_1/A_* = 12.596$$

$$\frac{A_1}{A_t} = \frac{A_1/A_*}{A_t/A_*} = \frac{12.596}{1.131} = 11.137$$

Therefore,

$$D_t^2 = \frac{D_1^2}{11.137} = \frac{256}{11.137} = 22.986 \text{ in.}^2$$

$$D_t = 4.794 \text{ in.}$$

For manufacturing convenience, the venturi throat diameter was made 4.750 inches. The actual measured throat diameter was used for airflow calculation.

The hole area for the heater burner was determined for the 4% pressure loss assuming a pressure loss of one velocity head across the holes, a negligible pressure loss in flow around and within the burner can, and a 0.55 discharge coefficient for the holes. Therefore:

$$(P_t - P_{st})_{\text{in holes}} = 0.04\ P_t$$

or

$$P_{st}/P_t = 0.96 \text{ and Mach number} = 0.242$$

For a Mach number of 0.242, the mass flow parameter was found to be:

$$\frac{w\sqrt{T_t}}{A_{holes}\ P_t} = 0.2147.$$

Solving for the area,

$$A_{holes} = \frac{24\sqrt{1160}}{(0.2147)(94.69)} = 40.208 \text{ in.}^2$$

Using C_d,

$$A_{holes} = \frac{40.208}{0.55} = 73.105 \text{ in.}^2$$

B. TWIN RAM INDUCTION COMBUSTOR DESIGN ANALYSIS

1. Introduction

This section includes the requirements and calculations used to design the liquid fuel injection Twin Ram Induction Combustor Models No. 1 and 5.

a. Design Procedure for the Twin Ram Induction Combustor - Model No. 1

(1) Design Parameters

The diffuser inlet and combustor exit dimensions were obtained from the 600 lb_m/sec STF-219 engine design as of 14 May 1965. The following combustor inlet flow conditions were originally specified by contract for testing:

p_t = 90 psia
t_t = 1150°F
V_{ref} = 150 ft/sec (burner reference velocity)

Additional contract specifications were (1) combustor length of 12 inches from fuel nozzle to turbine inlet guide vane, (2) outer burner case diameter of 40 inches, and (3) use of a 90-degree sector of the combustor for test purposes.

Performance goals for the combustor are listed in Section II of this report.

(2) Design Considerations

The two combustor annuli were designed with equal airflows and velocities, resulting in the inner annulus having a greater radial height than the outer annulus. Airflow within each annulus was divided equally between the inner and outer scoops. The sum of the outer and inner shroud flow was greater than the center shroud flow by the amount of air provided for outlet transition duct cooling. Modifications required to produce the desired outlet radial temperature profile were incorporated during the development program.

Airflow distribution within each combustor annulus was established considering previous experience with ram induction burners. Scoop dimensions were based on this past experience and sizing calculations assuming nonburning flow and uniform static pressure inside the combustor. Figure B-2 shows the design flow area percentage at each point of air admission.

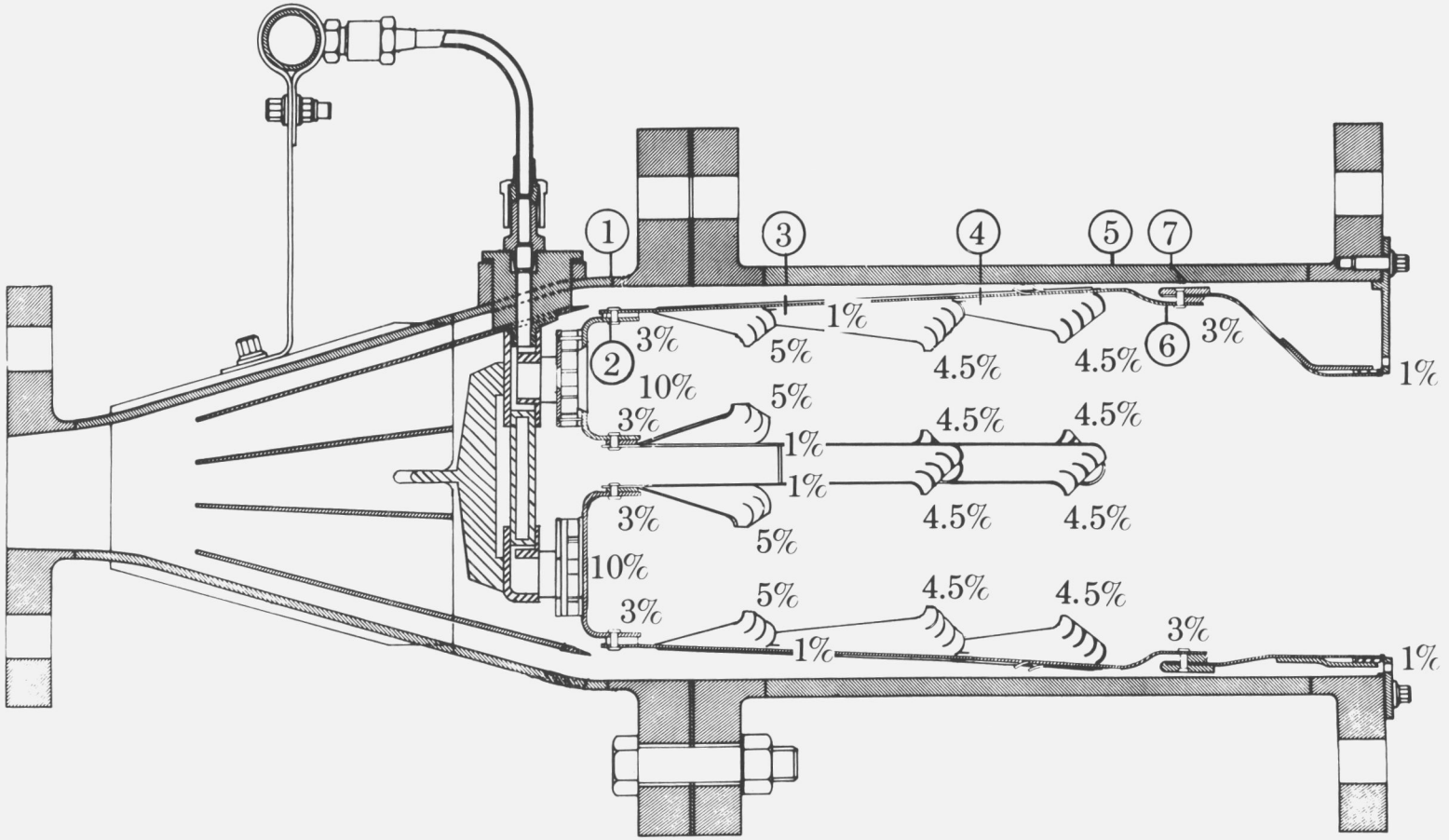

Figure B-2. Airflow Distribution, Twin Ram-Induction Combustor, Model No. 1

FD 12870E

Scoops in the inner and outer liners were identical in size and number. Scoops within each annulus were opposed; the flow from each inner scoop impinged upon flow from a corresponding outer scoop. To provide the opposed flow scoop arrangement, locations of the fuel nozzles relative to the scoop pattern were different in the outer and inner annuli.

All scoops were designed with square exit areas.

The diffuser was designed with 16 struts in the full 360-degree annulus. Maximum strut width corresponded to that of the STF-219 engine.

Each combustor annulus was designed with 32 fuel nozzles in the full 360-degree burner annulus. Thus, a complete engine would have 64 fuel nozzles in the primary combustor.

Individual swirlers were incorporated about each fuel nozzle. Swirler airflow was fed across the combustor firewall by the static pressure differential. The swirler was of the radial in-flow type that incorporated eight internal vanes, which imparted swirl to admitted air to generate a vortex about the fuel spray cone.

Scoops were sized for an exit Mach number of 0.20. This value was determined through consideration of the specified pressure loss of 6.0% and previous experience with ram induction burners. The dynamic pressure head q at Mach 0.20 was 2.8% of total pressure. Thus the specified overall pressure loss of 6.0% was slightly more than twice the scoop discharge q. Previous ram induction combustors had demonstrated satisfactory performance with this level of pressure loss.

The combustor segment was sized to operate with an airflow of 24 lb_m/sec which was the maximum airflow available from B-2 stand at the specified combustor inlet conditions.

(3) Combustor Design Calculations

(a) Diffuser Inlet

The compressor discharge radii were taken from the 600 lb_m/sec STF-219 dimensions.

r_o = 17.867 in.
r_i = 16.247 in.

Therefore,

$$A = \pi \left[r_o^2 - r_i^2 \right]$$

$$A = \pi \left[(17.867)^2 - (16.247)^2 \right] = 173.621 \text{ in.}^2$$

and

$$\frac{w_a \sqrt{T_t}}{A p_t} = \frac{96 \sqrt{1610}}{(173.621)(90)} = 0.24651$$

Using the compressible-flow tables for air, the Mach number was

$$M = 0.281$$

(b) Combustor Case

Using the specified outer combustor case diameter, the reference velocity, and the maximum available test airflow, the diameter of the inner combustor case was found.

$$M = \frac{V_{ref}}{a} = \frac{150}{49.02 \sqrt{1610}} = 0.076$$

$$\frac{w_a \sqrt{T_t}}{A p_t} = 0.0696$$

$$A = \frac{(96) \sqrt{1610}}{(0.0696)(90)} = 615.00 \text{ in.}^2$$

$$r_i = \left[r_o^2 - \frac{A}{\pi} \right]^{1/2} = \left[(20.000)^2 - \frac{615.00}{\pi} \right]^{1/2}$$

$$r_i = 14.330 \text{ in.}, \quad D_i = 28.660 \text{ in.}$$

(c) Diffuser

Diffusion from the compressor exit (at a Mach number of 0.281) to the ID and OD shrouds (at a Mach number of 0.200) was completed in the 8.000-inch diffuser section.

Figure B-3 illustrates the rate of diffusion through the diffuser. The flow was split into five channels at the maximum width of the support strut, located 2.750 inches from the compressor. Flows through the three center channels were equally diffused. Part of the airflow from the center diffuser channels entered the fuel nozzle air swirlers. The remainder was re-accelerated into the OD, ID, and center combustor shrouds.

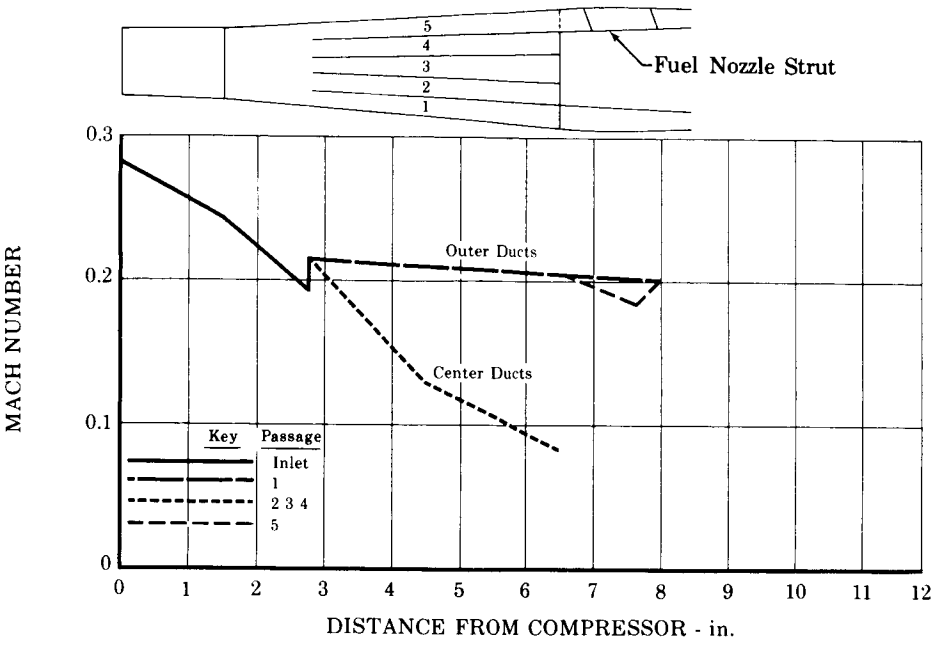

Figure B-3. Diffuser Mach Number vs Length FD 12869 B

(d) Shroud Areas and Location

With 22% of the total mass flow entering the ID and OD shrouds at a Mach number of 0.200, the required areas were calculated as follows:

$$A = \frac{w_a\sqrt{T_t}}{(0.179)p_t} = \frac{(0.22)(96)\sqrt{(1610)}}{(0.179)(90)}$$

$$A = 52.483 \text{ in.}^2$$

The radii required for this area were calculated as follows:

OD Shroud:

$$r_o = 20.000$$

$$r_i = \left[r_o^2 - \frac{A}{\pi}\right]^{1/2} = 19.576 \text{ in.}$$

ID Shroud:

$$r_i = 14.330$$

$$r_o = \left[r_i^2 + \frac{A}{\pi}\right]^{1/2} = 14.902 \text{ in.}$$

The center shroud received 36% of the total mass flow at a Mach number of 0.200. The required area was, therefore,

$$A = \frac{w_a\sqrt{T_t}}{(0.179)p_t} = \frac{(0.36)(96)\sqrt{1610}}{(0.179)(90)}$$

$$A = 85.882 \text{ in.}^2$$

The center shroud was located so that both combustors had equal annular areas.

$$\text{Area between OD shrouds} = \pi\left[(19.576)^2 - (14.902)^2\right] = 506.548 \text{ in.}^2$$

$$\text{Area available for each combustor} = \frac{506.548 - 85.882}{2} = 210.333 \text{ in.}^2$$

The outer radius of the center shroud, therefore, was

$$r_o = \left[(19.576)^2 - \frac{210.333}{\pi}\right]^{1/2} = 17.786 \text{ in.}$$

Similarly, the inner radius of the center shroud was

$$r_i = \left[(14.902)^2 + \frac{210.333}{\pi}\right]^{1/2} = 17.000 \text{ in.}$$

Checking these radii against the previously calculated center shroud area of 85.882 in.^{2} gave

$$A = \pi\left[(17.786)^2 - (17.000)^2\right] = 85.897 \text{ in.}^2$$

which checked to within 0.015 in.^{2}.

(e) Flow in OD Shroud and Cooling Slots

Throughout this discussion, all design calculations shown refer to the OD shroud of the combustor. Similar calculations were made on the ID and center shrouds.

Referring to figure B-4, the following mass flows were found:

$$w_{a_{1+2}} = 0.22(96) = 21.120 \text{ lb}_m/\text{sec}$$

$$w_{a_2} = 0.03(96) = 2.880 \text{ lb}_m/\text{sec}$$

$$w_{a_1} = 0.19(96) = 18.24 \text{ lb}_m/\text{sec}$$

where the subscripts 1 and 2 in this discussion refer to conditions at stations 1 and 2 in figure B-4.

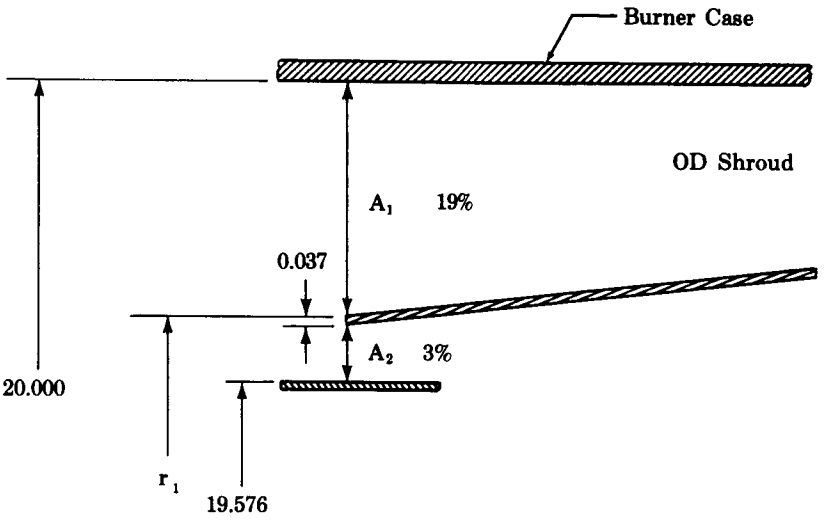

Figure B-4. Flow in OD Shroud FD 12874

For the same Mach number across A_1 and A_2

$$\frac{w_{a_2}\sqrt{T_t}}{A_2 P_t} = \frac{w_{a_1}\sqrt{T_t}}{A_1 P_t} \text{ or } \frac{w_{a_2}}{A_2} = \frac{w_{a_1}}{A_1}$$

and

$$A_1 = \pi\left[(20)^2 - r_1^2\right]$$

$$A_2 = \pi\left[(r_1 - 0.037)^2 - (19.576)^2\right]$$

Combining,

$$\frac{18.24}{(20)^2 - r_1^2} = \frac{2.88}{(r_1 - 0.037)^2 - (19.576)^2}$$

$$r_1^2 = 0.0638 r_1 - 385.506 = 0$$

$$r_1 = 19.665$$

The area of the shroud was, therefore,

$$A_1 = \pi \left[(20.000)^2 - (19.665)^2 \right] = 41.745 \text{ in.}^2$$

The mass flow parameter was found as

$$\frac{w_{a1}\sqrt{T_t}}{A_1 P_t} = \frac{18.240(40.125)}{(41.745)(90)} = 0.1948$$

and

$$M_1 = 0.218$$

Checking, the primary slot area was

$$A_2 = \pi \left[(19.628)^2 - (19.576)^2 \right] = 6.405 \text{ in.}^2$$

The mass flow parameter was, therefore,

$$\frac{w_{a2}\sqrt{T_t}}{A_2 P_t} = \frac{2.88(40.125)}{6.405(90)} = 0.2004$$

and

$$M_2 = 0.224$$

which checked to within 0.006.

The primary slot thickness was, therefore,

$$r_1 - 0.037 - 19.576 = 0.052 \text{ in.}$$

Referring to figure B-2, using a minimum clearance of 0.060 inch at the bypass (section 7), and 1% of the total mass flow for cooling the rear liner,

$$A_7 = \pi\left[(20.000)^2 - (19.940)^2\right] = 7.530$$

and

$$\frac{w_{a_7}\sqrt{T_t}}{A_7 p_t} = \frac{(0.01)(96)\sqrt{1610}}{(7.530)(90)} = 0.05683$$

therefore,

$$M_7 = 0.062.$$

At section 6, for 3% of the total mass flow and a Mach number of 0.200,

$$A_6 = \frac{w_{a_6}\sqrt{T_t}}{(0.17942)p_t} = \frac{(0.03)(96)\sqrt{1610}}{(0.17942)(90)}$$

$$A_6 = 7.156 \text{ in.}^2$$

The radius was

$$r_6 = \left[r^2 - \frac{A_6}{\pi}\right]^{1/2}$$

where

$$r = 19.940 - 0.100 - 0.037 = 19.803 \text{ in.}$$

$$r_6 = \left[(19.803)^2 - \frac{7.156}{\pi}\right]^{1/2} = 19.745 \text{ in.}$$

The gap at section 6 was

$$\text{gap} = 19.803 - 19.745 = 0.058 \text{ in.}$$

To use the same size spacers as those used in the primary cooling slot, the gap at section 6 was reduced to 0.052. The radius r_6 then became 19.751 in.

At section 5, for 4% of the total mass flow and a Mach number of 0.200,

$$A_5 = \frac{w_a\sqrt{T_t}}{(0.17942)p_t} = \frac{(0.04)(96)\sqrt{1610}}{(0.17942)(90)}$$

$$A_5 = 9.542 \text{ in.}^2$$

The radius was

$$r_5 = \left[(20.000)^2 - \frac{9.542}{\pi}\right]^{1/2} = 19.924 \text{ in.}$$

By determining the radii r_5 and r_1, the combustor liner was located relative to the combustor case, as shown in figure B-2.

(f) Flow in Primary Scoops

A scoop Mach number of 0.200 was selected as discussed.

Two primary scoops per nozzle on each wall of each annulus gave a total of 256 primary scoops to admit 20% of the air to the combustor. The total area required for the primary scoops was, therefore,

$$A = \frac{w_a\sqrt{T_t}}{(0.17942)p_t} = \frac{(0.20)(96)\sqrt{1610}}{(0.17942)(90)}$$

$$A = 47.711 \text{ in.}^2$$

For one scoop,

$$\frac{A}{256} = \frac{47.711}{256} = 0.1863 \text{ in.}^2$$

For a square scoop, the dimension of a side was

$$L^2 = 0.1863 \text{ in.}^2$$
$$L = 0.432 \text{ in.}$$

(g) Flow in Secondary Scoops

There were also 256 secondary scoops. Although half of these were long and the other half short, each was designed for the same mass flow and a Mach number of 0.200. Thirty-six percent of the total mass flow was discharged through the secondary scoops. The total area required for the secondary scoops was, therefore,

$$A = \frac{w_a\sqrt{T_t}}{(0.17942)p_t} = \frac{(0.36)(96)\sqrt{1610}}{(0.17942)(90)}$$

$$A = 85.880 \text{ in.}^2$$

For one scoop,

$$\frac{A}{256} = 0.3354 \text{ in.}^2$$

For a square scoop, the dimension of a side was

$$L^2 = 0.3354 \text{ in.}^2$$
$$L = 0.579 \text{ in.}$$

(h) Average Mach Number Through Outer Shroud

The average Mach numbers at sections 3, 4, and 5 were calculated using the total flow area and total mass flow at each section. The parameter

$$\frac{w_a\sqrt{T_t}}{Ap_t}$$

was thus found and the Mach number taken from the compressible flow tables. The results were:

$$M_3 = 0.176$$
$$M_4 = 0.164$$
$$M_5 = 0.200$$

Figure B-5 illustrates the Mach number vs distance from the compressor throughout the entire burner section.

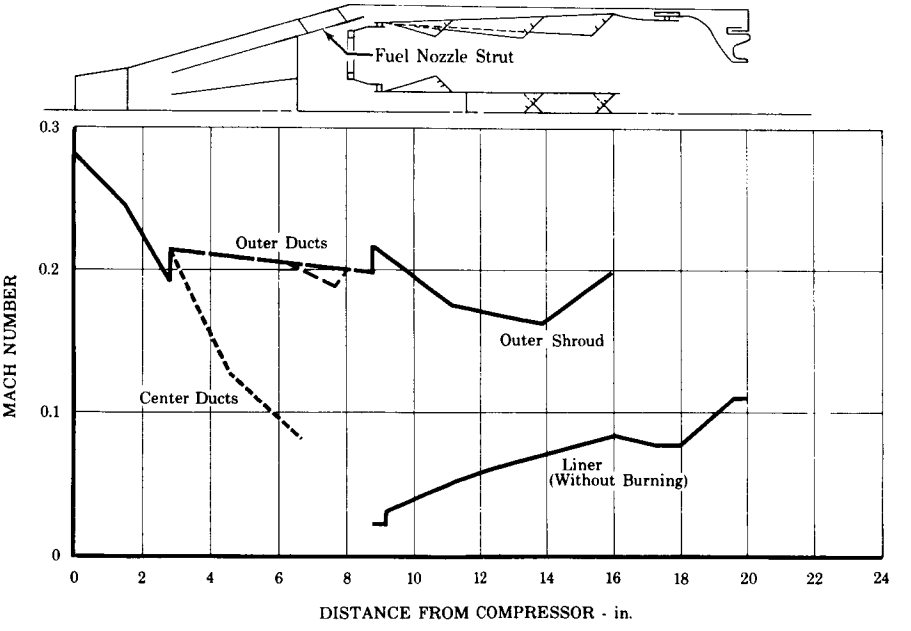

Figure B-5. Combustor Mach Number vs Length FD 12868A

(i) Cold Calculations

All calculations up to this point were made at operating temperatures. In a complete annular combustor, the combustor expands outward radially as it is heated. The material used was Hastelloy X, which has a coefficient of thermal expansion of 8.9×10^{-6} in/in/°F at 1500°F.

1. At the 1% OD shroud bypass (section 7):

   Assuming $\Delta t = 1000°F$

   $$e = (8.9 \times 10^{-6})(1000°F) = 0.0089 \text{ in./in.}$$

   $$r_{7_H} = r_{7_C} + e r_{7_C} = r_{7_C}(1 + e)$$

   $$r_{7_C} = \frac{r_{7_H}}{1 + e}$$

   $$r_{7_C} = \frac{19.940}{1.0089} = 19.764 \text{ in.}$$

2. At section 5:

   $$r_{5_C} = \frac{r_{5_H}}{1 + e} = \frac{19.924}{1.0089} = 19.748 \text{ in.}$$

3. At section 1 for a Δt of 500°F:

   $$r_{1_C} = \frac{r_{1_H}}{1 + e} = \frac{19.665}{1.00445} = 19.577 \text{ in.}$$

The radii at sections 1, 5, and 7 should therefore be reduced to the new radii in constructing a complete annular burner. However, the cylindrical hoop-strength of a full annular burner is lost when only a segment of the burner is used; the burner liners must be rigidly supported from the burner case. This support prevents radial expansion, thus the burner radii need not be adjusted for expansion allowances. Expansion still occurs but in the form of circumferential expansion around a fixed radius. The burner liners tend to expand outward and push against the sector walls. For a Δt of 1000°F,

$$e = (8.9 \times 10^{-6})(1000°F) = 0.0089 \text{ in./in.}$$

The hot circumference of a sector is

$$C_H = \theta_H r$$

Similarly for a cold circumference,

$$C_C = \theta_C r$$

because

$$C_C = \frac{C_H}{1 + e}$$

One may write

$$\theta_C = \frac{\theta_H}{1 + e}$$

$$\theta_C = \frac{90°}{1.0089} = 89.206°$$

Designing the liners with an included angle of 89.206 degrees compensated for expansion in the 90-degree burner case. This angle provided a cold gap of 0.138 in. between each edge of the outer liner sector and the 90-degree sector side walls. The corresponding gap at the edges of the inner liner was 0.099 in.

b. Design Procedure for the Liquid Fuel Injection Twin Ram Induction Combustor, Model No. 5

(1) Modifications

The modifications to the Twin Ram Induction Combustor (Model No. 5) were based on experience gained from Models No. 1 through 4, which had a temperature profile that was relatively cool at the center section.

To correct this condition:

1. The center shroud mass flow was decreased by eliminating the long (third) row of scoops. This allowed an additional 9% of the total mass flow to be divided equally by the OD and ID liners.

2. The OD and ID shroud areas were increased to accept an additional 4.5% of the total mass flow. The flow distribution within each liner was changed to accommodate the additional mass flow.

(2) Combustor Design Calculations

Unless otherwise noted, all design calculations shown refer to the OD liner of the combustor. Similar calculations were made on the ID liner.

The additional 4.5% of air required an increase in shroud area to maintain a Mach number of 0.200. The required area was calculated using the mass flow parameter,

$$\frac{W\sqrt{T_t}}{Ap_t} = 0.17627$$

for M = 0.200.

$$A = \frac{W\sqrt{T_t}}{(0.17627)\,p_t}$$

$$A = \frac{(0.265)(96)\sqrt{1610}}{(0.17627)(90)} = 64.344 \text{ in.}^2$$

The radius required for this area was, therefore,

$$r = \left(r_o^2 - A/\pi\right)^{1/2}$$

$$r = \left[(20)^2 - \frac{64.344}{\pi}\right]^{1/2} = 19.481 \text{ in.}$$

The primary cooling slot was increased to flow 5% of the total mass flow. Because the static pressure across A_1 and A_2 were equal (figure B-6) the Mach number was constant and,

$$\frac{W_2\sqrt{T_t}}{A_2 p_t} = \frac{W_1\sqrt{T_t}}{A_1 p_t}$$

or

$$\frac{W_2}{A_2} = \frac{W_1}{A_1}$$

combining,

$$\frac{0.05}{(r_1 - 0.037)^2 - (19.481)^2} = \frac{0.215}{(20)^2 - r_1^2}$$

$$r_1 = 19.610 \text{ in.}$$

The primary cooling slot thickness was, therefore,

$$19.610 - 0.037 - 19.481 = 0.092 \text{ in.}$$

The Mach number in the OD liner at section 1, figure B-7, was calculated as follows:

$$\frac{W_1\sqrt{T_t}}{A_1 P_t} = \frac{(0.215)(96)\sqrt{1610}}{\pi\left[(20)^2 - (19.610)^2\right](90)} = 0.189611$$

From compressible flow tables

$$M_1 = 0.216.$$

Referring to figure B-7, the transition cooling slot (section 6) was increased to flow 4.5% of the total mass flow, at a Mach number of 0.200. The required flow area was therefore,

$$A_6 = \frac{W_6\sqrt{T_t}}{(0.17627)P_t} = \frac{(0.045)(96)\sqrt{1610}}{(0.17627)(90)} = 10.9264 \text{ in.}^2$$

The radius

$$r_6 = \left[r^2 - \frac{A_6}{\pi}\right]^{1/2}$$

where,

$$r = 19.940 - 0.100 - 0.037 = 19.803 \text{ in.}$$

$$r_6 = \left[(19.803)^2 - \frac{10.9264}{\pi}\right]^{1/2} = 19.715 \text{ in.}$$

The slot thickness at section 6 was

$$19.803 - 19.715 = 0.088 \text{ in.}$$

To use the same size spacers as were used in the primary cooling slot, the slot at section 6 was increased to 0.092 in.

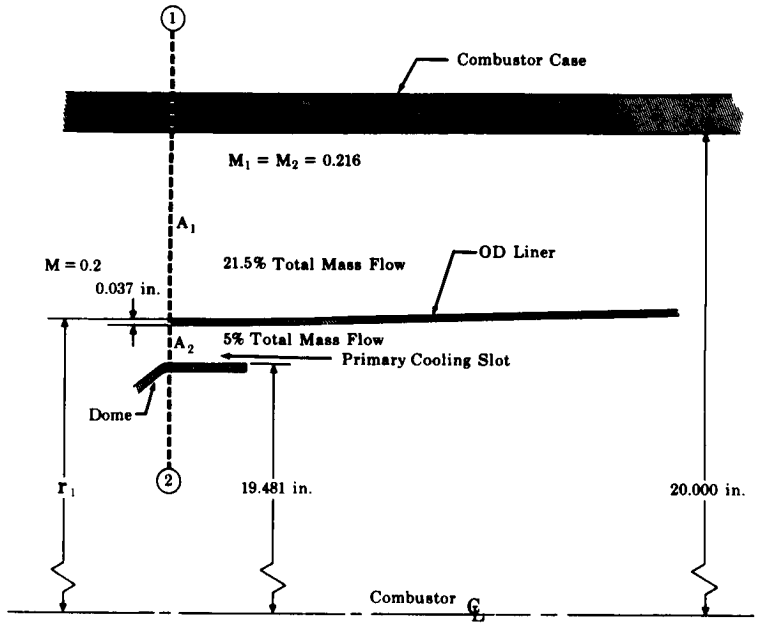

Figure B-6. Primary Cooling Slot Details FD 15134

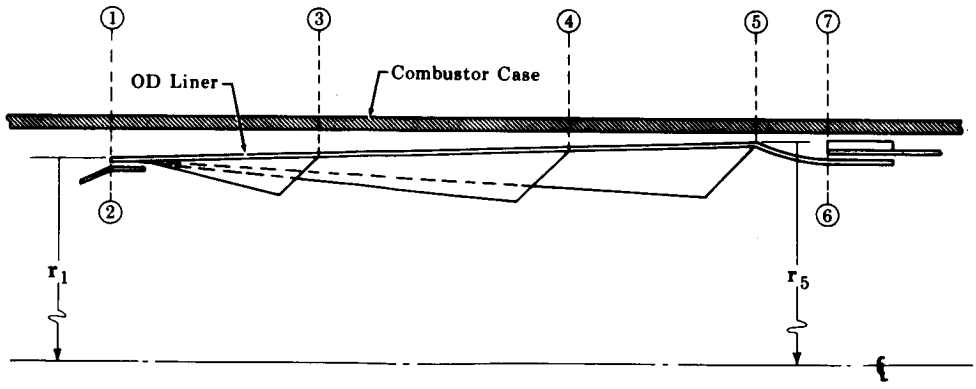

Figure B-7. Positions Along OD Liner FD 15155

The radii at sections 1 and 5 were calculated to establish the OD liner relative to the combustor case. The flow area at section 5 for a Mach number of 0.200 was calculated as follows:

$$A_5 = \frac{W_5\sqrt{T_t}}{(0.17627)p_t} = \frac{(0.055)(96)\sqrt{1610}}{(0.17627)(90)}$$

$$A_5 = 13.3545 \text{ in.}^2$$

The radius was therefore,

$$r_5 = \left[(20)^2 - \frac{13.3545}{\pi}\right]^{1/2} = 19.893 \text{ in.}$$

Similar calculations were conducted on the ID liner.

Thumbnail scoops were positioned on the OD and ID liners to prevent warpage due to overheating behind the second row of scoops. Three thumbnail scoops were positioned behind each second row of scoops, as in the model No. 3. The twenty-four thumbnail scoops passed approximately 2% of the total mass flow. Also, as in models No. 3 and 4, cooling holes of 0.116-in. diameter (8 per nozzle), and deflectors were incorporated around each nozzle to provide dome cooling. The mass flow through the dome cooling holes was 1% of the total mass flow.

Redesign of the center shroud was necessary to prevent excessive area blockage when the third row of scoops was eliminated. The second row of scoops on the center shroud was unchanged. The primary scoop dimensions were changed but the flow area remained the same.

C. VAPORIZING RAM INDUCTION COMBUSTOR DESIGN ANALYSIS

1. Introduction

This section includes the requirements and calculations used to design the Vaporizing Ram Induction Combustor, Models No. 1 and 4.

a. Design Procedure for 90-Degree Vaporizing Ram Induction Combustor, Model No. 1

(1) Design Considerations

The initial designs of the diffuser, outer combustor case, ID shroud, and OD shroud were the same as for the liquid injection Twin Ram Induction Combustor, since the requirements for these components were the same. The percent mass flow through the ID and OD shrouds remained the same as in the Twin Ram Induction Combustor Model No. 1 (44%). The center shroud was enlarged to receive 42% of the mass flow, while the remaining 14% was injected in the front of the OD and ID combustors. Figure B-8 shows the flow area percentage at each point of air admission. This split was chosen to provide the desired combination of ram induction liner air, vaporizing center tube air, and front end dilution air normally admitted around the nozzle swirlers.

(2) Center Shroud

The center shroud received 42% of the total mass flow at a Mach number of 0.150. The required area was therefore

$$A = \frac{W_a\sqrt{T_t}}{(0.13598)p_t} = \frac{(0.42)(96)\sqrt{1610}}{(0.13598)(90)}$$

$$A = 132.198 \text{ in.}^2$$

Fuel lines supplying the nozzles were positioned in the center shroud. Considering 1/4-inch OD tubes supplying 32 fuel nozzles, the area of the fuel lines was therefore,

$$A = 32(\pi/4)(0.25)^2 = 1.571 \text{ in.}^2$$

Figure B-8. Airflow Distribution, Vaporizing Ram-Induction Combustor, Model No. 1

FD 13461D

To maintain a Mach number of 0.150 at the entrance of the center shroud, the required area was increased by the area of the fuel lines.

$$A = 132.198 + 1.571 = 133.769 \text{ in.}^2$$

The center shroud was located so that both combustors had equal annular areas.

$$\text{Area between outer shrouds} = \pi\left[(19.576)^2 - (14.902)^2\right] = 506.548 \text{ in.}^2$$

$$\text{Area available for each burner} = \frac{506.548 - 133.769}{2} = 186.389 \text{ in.}^2$$

The outer and inner radius of the center shroud were, therefore,

$$r_o = \left[(19.576)^2 - \frac{186.389}{\pi}\right]^{1/2} = 17.997 \text{ in.}$$

$$r_i = \left[(14.902)^2 + \frac{186.389}{\pi}\right]^{1/2} = 16.775 \text{ in.}$$

(3) Vaporizer Tubes

Since the inner radius of the center shroud had the minimum circumference, the vaporizer tubes were designed to fit within this dimension.

$$C_i = 2\pi(r_i - 0.037) = 2\pi\left[16.775 - 0.037\right]$$

$$C_i = 105.168 \text{ in.}$$

A minimum clearance of 0.500 inch was maintained between each tube for combustion air holes. Using 128 vaporizer tubes (64 on both walls of the center shroud) the width of each tube was found as

$$b = \frac{C_i - 64\ (0.500)}{64}$$

$$b = 1.143 \text{ in.}$$

To provide sufficient heat transfer area for fuel vaporization, the tubes were made 7 inches long, and to prevent flow area blockage due to warpage, a brace was mounted inside each vaporizer tube, as shown in figure B-9.

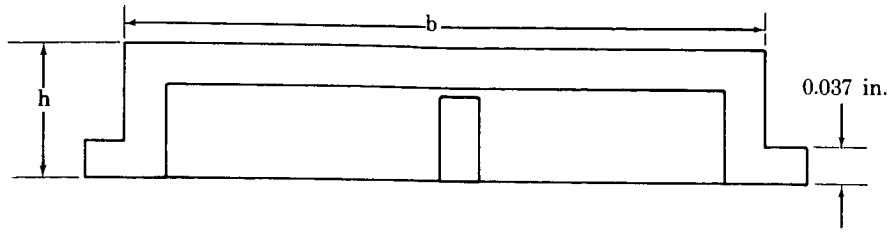

Figure B-9 Vaporizer Tube Cross Section FD 22792

Assuming a one q dump loss through the vaporizer tubes and a 6% overall combustor total pressure loss,

$$p_t - p_{ts} = 0.060\ p_t ,$$

or

$$p_{st}/p_t = 0.940$$

The mass flow parameter for a pressure ratio of 0.940 was

$$\frac{w_a\sqrt{T_t}}{Ap_t} = 0.259$$

For 8% of the total air flow passing through the vaporizer tubes, the total flow area was found:

$$A = \frac{w_a\sqrt{T_t}}{(0.259)(p_t)} = \frac{(0.08)(96)\sqrt{1610}}{(0.259)(90)}$$

$$A = 13.220\ \text{in.}^2$$

Using a C_d of 0.800, the required area was

$$A/0.800 = \frac{13.220}{0.800} = 16.525\ \text{in.}^2$$

Referring to figure B-9,

$$(128)\ (h - 0.037)(b - 0.111) = 16.525,$$

or

$$h = 0.162\ \text{in.}$$

The surface and cross-sectional areas of the vaporizer tubes were, therefore,

$$A_w = 128\left[2h + b\right]7$$

$$A_w = 128\left[1.467\right]7 = 1314.432 \text{ in.}^2$$

$$A = 128(h - 0.037)(b - 0.111)$$

$$A = 128(0.125)(1.032) = 16.512 \text{ in.}^2$$

(4) Combustion Air Slots

The combustion air slots were positioned axially along the center shroud in the same planes as the primary and secondary scoops of the outer and inner liners.

For a 6% overall burner total pressure loss,

$$p_{st_h} = (0.940)\ p_{t_{cs}}$$

where p_{st_h} was the static pressure in the combustion air slots. The total pressure in the combustion air slots was equal to the static pressure in the center shroud. Thus, for the primary air slots, because the Mach number in the center shroud was 0.150, the total pressure in the combustion air slots was

$$p_{t_h} = (0.9844)\ p_{t_{cs}}$$

The pressure ratio in the slots was, therefore,

$$p_{st_h}/p_{t_h} = \frac{0.9400}{0.9844} = 0.95489,$$

from which the mass flow parameter was obtained.

$$\frac{w_a\sqrt{T_t}}{Ap_t} = 0.22702$$

For 16% of the total mass flow, the area was

$$A = \frac{(0.16)(96)\sqrt{1610}}{(0.22702)(0.9844)(90)} = 30.642 \text{ in.}^2$$

Using a C_d of 0.620 the required area was

$$A/C_d = 49.422 \text{ in.}^2$$

For a 0.406-inch slot width and 128 slots, the length of each slot (figure B-10) was determined as

$$A = \left[w(1-w) + \frac{\pi}{4} w^2\right] N,$$

or

$$l = (1 - \pi/4)w + \frac{A}{wN}$$

$$l = (1 - \pi/4)(0.406) + \frac{49.422}{(0.406)(128)}$$

$$l = 0.087 + 0.951 = 1.038 \text{ in.}$$

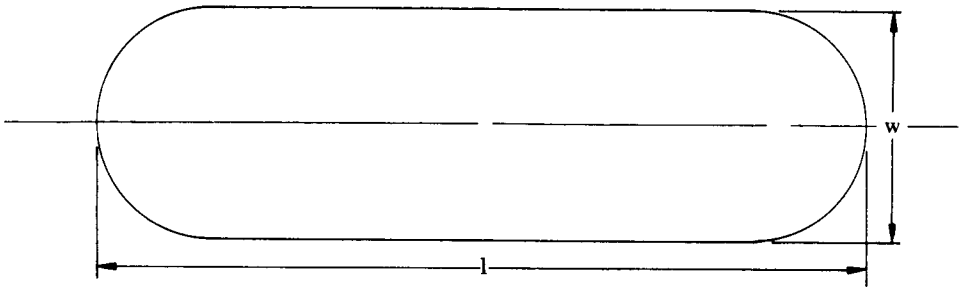

Figure B-10. Combustion Air Slot FD 22766

The secondary slots, which were in the same axial plane with the short secondary scoops, had a lower center shroud Mach number because 16% of the mass flow was directed through the primary slots.

$$\frac{w_a\sqrt{T_t}}{Ap_t} = \frac{(0.26)(96)\sqrt{1610}}{(132.198)(90)} = 0.0841767$$

$$M = 0.092$$

The pressure ratio in the slots was, therefore,

$$p_{st}/p_t = \frac{0.940}{0.99401} = 0.94566$$

from which the mass flow parameter was obtained.

$$\frac{w_a\sqrt{T_t}}{Ap_t} = 0.2479$$

For 9% of the total mass flow, the area was determined as

$$A = \frac{(0.09)(96)\sqrt{1610}}{(0.2479)(0.99401)(90)} = 15.632 \text{ in.}^2$$

Using a C_d of 0.620, the required area was

$$A/C_d = \frac{15.632}{0.620} = 25.212 \text{ in.}^2$$

The length of the slots was, therefore,

$$l = 0.087 + \frac{A}{51.968}$$

$$l = 0.087 + \frac{25.212}{51.968} = 0.572 \text{ in.}$$

The secondary slots, which were in the same axial plane as the long secondary scoops, were also designed for 9% of the total mass flow. The center shroud Mach number was determined from the mass flow parameter.

$$\frac{w_a\sqrt{T_t}}{Ap_t} = \frac{(0.17)(96)\sqrt{1610}}{(132.198)(90)} = 0.05503$$

$$M = 0.060$$

The pressure ratio in the slots was, therefore,

$$p_{st}/p_t = \frac{0.940}{0.99748} = 0.94237,$$

from which the mass flow parameter was obtained.

$$\frac{w_a\sqrt{T_t}}{Ap_t} = 0.25502,$$

or

$$A = \frac{(0.09)(96)\sqrt{1610}}{(0.25502)(0.99748)(90)} = 15.143 \text{ in.}^2$$

Using a C_d of 0.620, the required area was

$$A/C_d = \frac{15.143}{0.620} = 24.424 \text{ in.}^2$$

The length of the slots was, therefore,

$$l = 0.087 + \frac{A}{51.968}$$

$$l = 0.087 + \frac{24.424}{51.968} = 0.557 \text{ in.}$$

(5) Combustor Dome Slots

As discussed previously, 7% of the mass flow was injected in the front of each combustor. An axial distance of 0.250 inch from the front of the combustor provided a center shroud Mach number of 0.14. For a 6% overall combustor total pressure loss, the pressure ratio in the dome slots was

$$P_{st}/P_t = \frac{0.9400\ P_T}{0.9864\ P_T} = 0.9529,$$

from which the mass flow parameter was obtained.

$$\frac{w_a\sqrt{T_t}}{Ap_t} = 0.23189$$

Solving for the dome slot area,

$$A = \frac{(0.07)(96)\sqrt{1610}}{(0.23189)(0.9864)(90)} = 13.097\ \text{in.}^2$$

At an axial distance of 0.250 inch from the OD and ID combustors, the radii to the combustor domes were 18.220 inches for the outer combustor and 16.485 inches for the inner combustor. The width of the dome slots was therefore determined as:

Outer combustor

$$\text{Dome Slot Width} = \frac{A}{2\pi r_o} = \frac{13.097}{2\pi(18.220)} = 0.114\ \text{in.}$$

Inner combustor

$$\text{Dome Slot Width} = \frac{A}{2\pi r_i} = \frac{13.097}{2\pi(16.485)} = 0.126\ \text{in.}$$

b. Heat Transfer Analysis of the Vaporizer Tubes for the Model No. 1 Vaporizing Ram-Induction Combustor

(1) Introduction

The heat transfer problem associated with the vaporizer tube was a combination of forced convection and radiation. Heat input to the tube wall was due to radiation and forced convection from the combustion gases. Heat was rejected from the tube walls by forced convection to

the fuel-air mixture in the vaporizer tube and by radiation to the inner wall of the center shroud. Figure B-11 shows the ideal temperatures of the combustion gases based on fuel/air ratios at different sections in the combustion chamber.

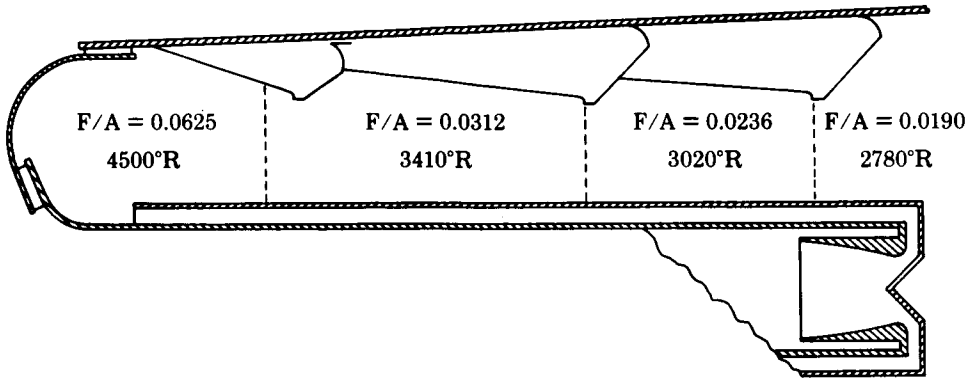

Figure B-11. Combustion Gas Temperature Gradient Through Vaporizing Ram Induction Combustor FD 13955

(2) Assumptions

The following physical assumptions were used in developing the analysis.

1. Steady-state, one-dimensional flow existed
2. Forced vortex flow existed in the burner dome
3. The combustion products were treated as a nonluminous radiating gas
4. The absorbtivity due to the CO_2 and H_2O in the products of combustion was equal to the emissivity
5. The heat balance equation was written for a local point on the vaporizer tube wall and considered one-dimensional heat flow
6. The back side of the tube wall was at the fluid (JP-5 - air) temperature
7. Flat plate heat transfer coefficients calculated for the top of the tube applied also to the sides
8. A thin film of fuel adhered to the mixing manifold wall and nucleate boiling occurred

9. Temperature mixing was complete at the entrance to the vaporizer tube

10. The gas side heat transfer coefficient in the separated flow region (mixing manifold wall) was equal to the gas side heat transfer coefficient at the entrance section of the vaporizer tube.

(3) External Flow Conditions

The external flow conditions on the vaporizer tube are shown in figure B-12. A forced vortex was assumed in the dome region of the combustor.

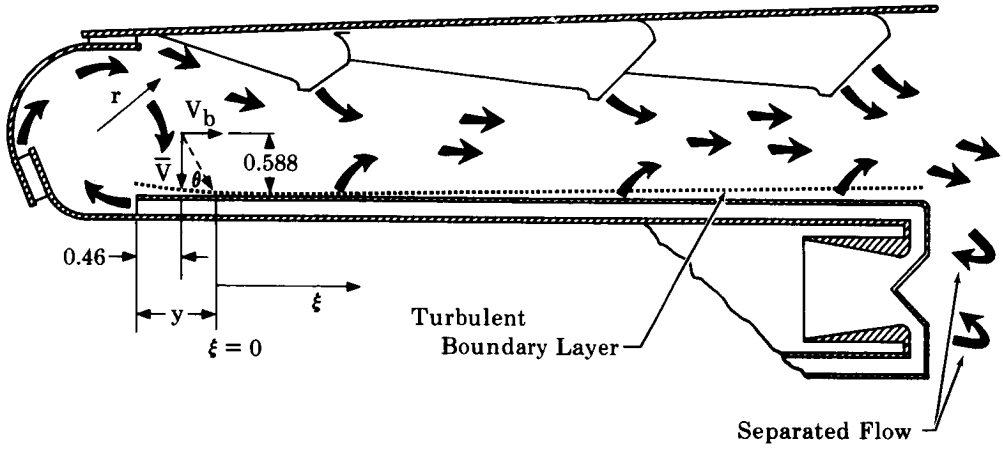

Figure B-12. External Flow Conditions FD 13954

The driving velocities were due to the injection flows from the shroud primary slot, vaporizer tubes, and combustor dome slot. Using the mass flow parameter relation, the driving velocities from the shroud and dome slots were calculated. For the shroud primary slot:

$$\frac{W\sqrt{T_t}}{Ap_t} = \frac{(0.03)(96)\sqrt{1610}}{(6.40)(90)} = 0.2005 \text{ lb}_m \sqrt{^\circ R}/\text{lb}_f \text{ sec}$$

From the compressible-flow tables for air the Mach number and static temperature were found and the velocity calculated as:

$$V = M(49.02)\sqrt{\frac{\gamma_1}{\gamma}\ (T_s)}$$

$$V = (0.229)(49.02)\sqrt{\frac{1.35}{1.40}\ (1600)}$$

$$V = 441 \text{ ft/sec}$$

Similarly, for the burner dome slot

$$V = 504 \text{ ft/sec}$$

Before the driving velocity from the vaporizer tubes could be calculated the properties of the fluid inside the tube had to be known. The fuel was assumed completely vaporized at the exit of the tube. This assumption will later be verified. The gas constant for the mixture was found as follows.

$$R_M = m_a R_a + m_F R_F$$

$$R_M = (0.821)(53.35) = (0.179)(9.15)$$

$$R_M = 45.84 \text{ lb}_f \text{ ft/lb}_m \text{ °R}$$

At this point the exit mixture temperature was assumed at 1340°R. The specific heat of the mixture was

$$C_{p_M} = m_a C_{p_a} + m_F C_{p_F}$$

where C_p for JP-5 is almost constant in the vapor region at 90 psia. (See figure B-13.)

$$C_{p_F} = \frac{\Delta H}{\Delta t} = 0.70 \text{ Btu/lb}_m \text{ °R}$$

$$C_{p_M} = (0.821)(0.258) + (0.179)(0.70)$$

$$C_{p_M} = 0.337 \text{ Btu/lb}_m \text{ °R}$$

NASA CR-54560
PWA FR-2433

DEVELOPMENT OF A SHORT-LENGTH TURBOJET COMBUSTOR

by

D. L. Kitts

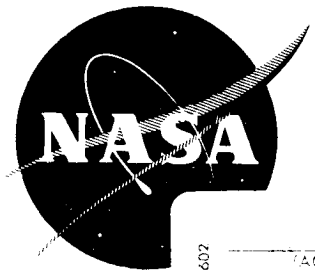

Prepared for

NATIONAL AERONAUTICS AND SPACE ADMINISTRATION

Contract NAS3-7905

Pratt & Whitney Aircraft DIVISION OF UNITED AIRCRAFT CORPORATION
FLORIDA RESEARCH AND DEVELOPMENT CENTER
BOX 2691, WEST PALM BEACH, FLORIDA 33402

Requests for copies of this report should be referred to

National Aeronautics and Space Administration
Office of Scientific and Technical Information
Attention: AFSS-A
Washington, D.C. 20546